Sequential Proteolysis by γ-Secretase and Its Implications for Alzheimer's Disease

Sequential proteolysis by γ-secretase

and its implications for Alzheimer's disease

A dissertation presented

by

Marty Alyse Fernandez

to

The Division of Medical Sciences

in partial fulfillment of the requirements

for the degree of

Doctor of Philosophy

in the subject of

Biological Chemistry and Molecular Pharmacology

Harvard University

Cambridge, Massachusetts

May 2015

Dissertation Advisor: Dr. Michael S. Wolfe Marty Alyse Fernandez

Sequential proteolysis by γ-secretase and its implications for Alzheimer's disease

Abstract

The production and aggregation of the amyloid β-peptide (Aβ) is thought to play a central role in Alzheimer's disease (AD) pathogenesis. The presenilin (PS)-containing γ-secretase complex cleaves the amyloid β-protein precursor C-terminal fragment (APP CTFβ) to generate Aβs of 38-49 residues. Evidence suggests that these Aβs are the result of successive γ-secretase cleavages, which are thought to start at the ε sites to generate Aβ48 or Aβ49, followed by C-terminal trimming mostly every three residues to produce secreted Aβs. Specifically, two product lines have been proposed: the Aβ49-46-43-40 line and the Aβ48-45-42-38 line. An increased proportion of aggregation-prone Aβ42 compared to Aβ40 is believed to be important in AD pathogenesis. Despite the apparent relevance of the production of the Aβ C-terminus in AD, questions surround the mechanisms by which γ-secretase generates the Aβ spectrum and how familial AD-causing (FAD) mutations alter Aβ production.

This dissertation first examined the C-terminal trimming function of γ-secretase and how PS FAD mutations alter this activity. We found that synthetic Aβ49, Aβ48, Aβ46, and Aβ45 are trimmed to Aβ40 and Aβ42 by γ-secretase *in vitro*. Moreover, our results were consistent with the two-pathway model in which Aβ49 is primarily converted to Aβ40 and Aβ48 to Aβ42, but also demonstrated a small degree of crossover between the pathways. Most importantly, we

found that PS1 FAD mutations dramatically reduce the efficiency of trimming of ε-cleaved Aβs, particularly the trimming of Aβ49 to Aβ40.

We also investigated substrate determinants for ε site endoproteolysis and C-terminal trimming of APP CTFβ by γ-secretase. The deletion of residues around the ε sites indicated that upstream sequences, and not depth within the transmembrane domain, are the determinants of ε site specificity. We also show that instability of the APP CTFβ transmembrane helix near the ε site increases endoproteolysis, and that instability near the carboxypeptidase cleavage sites facilitates C-terminal trimming by γ-secretase.

Last, the potential role of Aβ45-49 in AD pathogenesis was considered. We did not detect these Aβ species in AD brains by immunoprecipitation and western blot. However, we developed cellular systems to investigate their toxicity and obtained preliminary data suggesting that these Aβs may be neurotoxic.

TABLE OF CONTENTS

TABLE OF FIGURES AND TABLES

Acknowledgements

I would first like to thank Dr. Wolfe for allowing me to work on these projects and for being a patient, enthusiastic, and generous mentor and teacher. I am very lucky to have found a lab to join with a PI who is motivated not only by an endless interest in science, but also by a genuine desire to help people. Dr. Wolfe was always available for advice on problems large and small, and if I ever went into a meeting feeling anxious or discouraged by experimental troubles or negative results, I would always leave more excited than before to pursue a solution or new idea that had come up. In my mind, this is a sign of a great mentor. I also thank my labmates, who have been both friends and teachers to me. It has been a wonderful experience working with people who are always willing to help and who are happy to share their extensive knowledge and expertise. I could not have asked for a better group of people to have worked with and to have celebrated publications, new jobs, weddings, and birthdays with throughout the years. I also thank my colleagues in the CND for being an extension of my lab, always willing to help and great friends. They were also kind (or, should I say unkind?!) enough to select me as the involuntary president of the CND "Beer Camp," during which we shared many a fun evening. I thank all of the students I had the opportunity to mentor for all of their hard work in the lab, their refreshing enthusiasm that was heart-warming to see on days that I was discouraged by failed experiments, and for allowing me to learn about teaching and managing students. I also thank my advisory committee. As a nervous student embarking on my PhD, I never thought I would say that committee meetings were fun, but my advisors were able to accomplish just that with their sage advice and thought-provoking conversations. I also thank my classmates in the

BBS program for often teaching me as much as the class lecturers and for always being willing to lend a hand.

Most importantly, I thank my family. I am indebted to my parents for their endless love, support, and encouragement. They instilled in me the importance of learning and doing well in school, and taught by example the value of working hard. I thank my brother for being my first and most loyal friend, my friends and extended family for making my life rich and fun, and my friends in Boston for making this city a home. I also thank my husband for being a source of endless support and patience and my best friend. I would be lost without him, especially his ability to make me laugh and be happy no matter what stress is going on. We started out as two kids at the University of Florida, and I can hardly believe where life has taken the two of us.

Dedication

I dedicate this thesis to my maternal grandfather, Abraham Klapper, and my paternal grandmother, Dalia Fernandez. They didn't develop Alzheimer's Disease, but likely vascular dementia. They worked hard their whole lives, making a living as a grocer and a carpenter and postman. They raised families, and my grandfather served overseas in the US army during WWII. Although I was young when my grandmother died, I remember eagerly going to visit her, then asking my mother why she was pointing at me, asking who I was, and saying that she was waiting for my father to get home from school. My grandfather often thought I was my mother when she was younger (although he thought my mom was also there, just that there were two of her from different times in his life there together at the same time). I learned firsthand the importance of preserving memory and cognition in old age when I saw my grandparents affected

in this way, their minds alternately confusing them by bringing up old memories as if they were the happening in the present, and failing them by not recalling who the people around them were despite the memories and love they had shared. All of this, made even more painful knowing that this was happening to them at the time in their lives when they should enjoy the fruits their lifetime of hard work and their remaining time with their children, grandchildren, and friends. Although working on enzymes and cells may seem far-removed from the human side of disease, thoughts of my grandparents and people and families affected by dementia and Alzheimer's disease were never far from my mind.

Chapter 1:

Introduction

Alzheimer's disease

Alzheimer's disease (AD) was first described by psychiatrist and neuropathologist Alois Alzheimer at a 1906 meeting in Tübingen, Germany, where he presented the case of a patient in her 50s experiencing progressive memory impairment, cognitive dysfunction, and behavioral changes that culminated in her death (Selkoe, 2001). The patient's name was Auguste Deter, and upon autopsy of her brain, Alzheimer documented the deposition of extracellular plaques and intracellular fibrillar tangles. Many decades later, AD was recognized as a common ailment in the elderly and not limited to rare presenile cases like Auguste Deter; the identification of the specific clinical and pathological features of AD, rooted in Alzheimer's seminal observations, has led to the recognition this disorder as a progressive and fatal disease and not an inevitable result of aging (Wippold et al., 2008). Individuals with AD initially experience transient memory or behavioral impairments which inexorably progress to a loss of memory and cognitive function, confusion, language breakdown, and eventual loss of the ability to care for oneself, to respond to the environment, and to control motor functions (Selkoe, 2001; Alzheimers Association, 2015a). The physical insults of AD are ultimately fatal within an average of eight years after diagnosis (Alzheimers Association, 2015a).

The most common neurodegenerative disease, AD is the sixth-leading cause of death in America and affects an estimated 35 million individuals worldwide (Alzheimer's Association, 2015b; Querfurth and LaFerla, 2010). The nature of AD can also lead to profound emotional impacts on caregivers and family members. Age is the leading risk factor for developing the disorder, and AD looms as a major public health concern presenting unprecedented human and financial costs as the aged population of the United States and other nations increases

(Brookmeyer, 2007). There are currently no disease-modifying treatments available for AD (Selkoe, 2013), and current clinical diagnosis generally occurs after irreversible neurodegenerative processes have been underway for some time, even years, and thus after the opportunity to intervene may have passed (Selkoe, 2013; Sperling et al., 2011).

Amyloid-β and AD

In addition to the loss of synapses and degeneration of neurons in the hippocampus and cerebral cortex, AD is pathologically characterized by the presence of the two hallmark proteinaceous structures in the brain that were first described by Alzheimer himself over a century ago: neurofibrillary tangles (NFTs) and neuritic plaques (Selkoe, 2001). NFTs are intraneuronal deposits primarily composed of hyperphosphorylated forms of the protein tau (Grundke-Iqbal et al., 1986; Kosik et al., 1986). Tau is a normally soluble protein, primarily localized to axons, that binds to microtubules, promoting assembly and stability of this important cytoskeletal network in neurons (Weingarten, 1975; Wolfe, 2012a). Neuritic plaques are extracellular aggregates of the amyloid β-peptide (Aβ) containing cores of amyloid fibrils as well as non-fibrillar forms of Aβ (Glenner and Wong, 1984; Masters et al., 1985). Plaques are intimately associated with significant cytopathology, with degenerating neurites within and closely surrounding the deposits, and are also surrounded by activated microglia and reactive astrocytes (Selkoe, 2001).

Aβ is generated through proteolytic processing of the amyloid β-protein precursor (APP), a ubiquitously expressed type I transmembrane protein (Selkoe, 1998). APP can be processed through an amyloidogenic pathway (Figure 1.1), in which it is first cleaved by the membrane-anchored protease β-secretase, releasing the soluble ectodomain, known as APPsβ, and leaving a

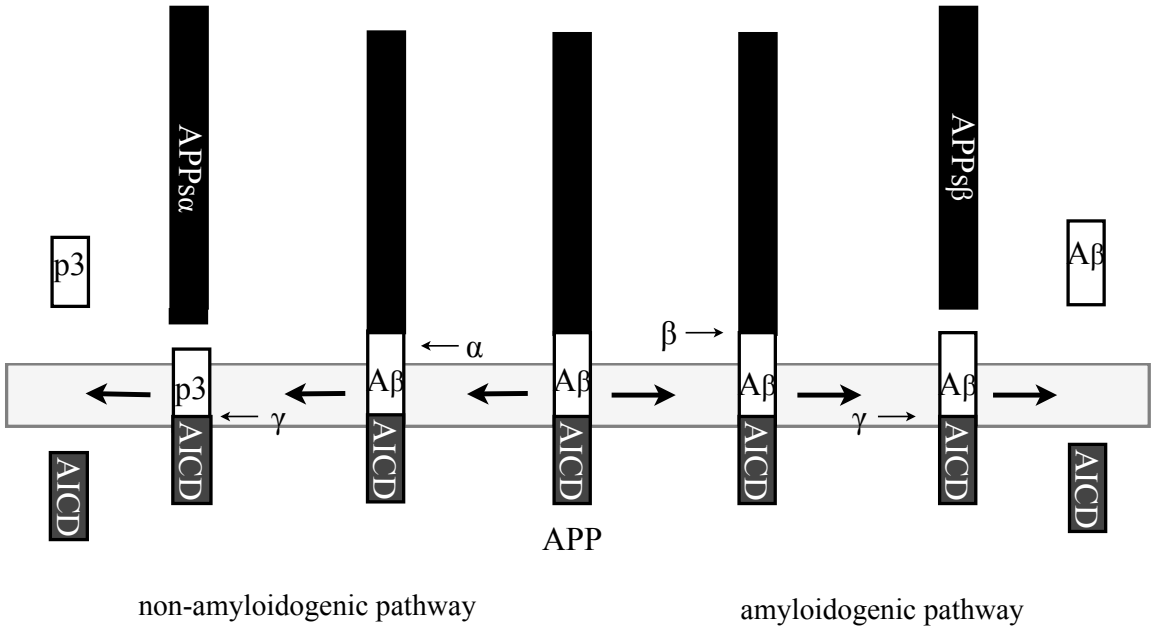

Figure 1.1. Proteolytic processing of APP by α-, β-, and γ-secretases. Cleavage of APP by α-secretase followed by γ-secretase produces the nonamyloidogenic p3 peptide, while cleavage by β-secretase followed by γ- secretase produces Aβ. The horizontal, light grey rectangle represents the membrane.

99-residue C-terminal stub, known as APP CTFβ, in the membrane (Vassar et al., 1999). CTFβ then undergoes scission within its transmembrane domain by the membrane-embedded γ-secretase complex (Wolfe, 2008), liberating the APP intracellular domain (AICD) and the secreted Aβ peptide from the membrane. In an alternative, non-amyloidogenic, pathway (Figure 1.1), APP is first cleaved 17 residues into the Aβ sequence by α-secretase, generating APPsα and the membrane-anchored APP CTFα. Cleavage by α-secretase thereby precludes the generation of Aβ, as subsequent intramembrane cleavage of CTFα by γ-secretase instead produces the non-amyloidogenic p3 peptide (Selkoe, 1998).

Evidence suggests that Aβ is not only the primary proteinaceous component of the characteristic plaques of the AD brain, but that aberrant production and aggregation of Aβ is actually the initiator of AD pathogenesis, triggering a complex cascade leading to synaptic and neuronal injury and loss, ultimately resulting in the manifestation of clinical AD (Hardy and Selkoe, 2002). Support for this model primarily comes from genetic evidence. APP has been localized to chromosome 21, and it is recognized that trisomy 21 (Down syndrome) leads to Aβ overproduction and early-onset AD neuropathology, as does a duplicated APP gene locus (Prasher et al., 1998; Rovelet-Lecrux et al., 2006). In addition, dominantly-inherited mutations that cause familial forms of AD (FAD), in which symptoms begin devastatingly early--in midlife--have provided valuable clues about the role of Aβ in the pathogenesis of AD, as they are all found in either APP or the γ-secretase component presenilin (PS), and all lead to aberrant Aβ production (Hardy and Selkoe, 2002). FAD mutations in APP have been identified that lead to general Aβ overproduction or increase Aβ's propensity to aggregate (Selkoe, 2001; Tanzi and Bertram, 2005). In addition, over 100 FAD mutations have been identified in PS that, along with

several FAD mutations in APP, result in an increase in the relative production of 42-residue Aβ (Aβ42) compared to 40-residue Aβ (Aβ40) (Bentahir et al., 2006; Citron et al., 1997; Duff et al., 1996; Scheuner et al., 1996; Selkoe, 2001). Aβ40 is the major species produced by γ-secretase, while Aβ42, the result of γ-secretase cleavage occurring two residues closer to the C-terminal end of the CTFβ transmembrane domain, is a minor isoform accounting for less than 10% of the Aβ produced (Selkoe, 2001). However, the longer Aβ42, with its two additional hydrophobic transmembrane residues, is more prone to aggregation than Aβ40 (Jarrett et al., 1993), is initially deposited in the brain, and, despite its relatively low abundance, predominates in neuritic plaques (Iwatsubo et al., 1994). There are two possible isoforms of PS, PS1 and PS2, and the majority of the PS FAD mutations are found in PS1 (Tanzi and Bertram, 2005). The recent discovery of a mutation within APP that is protective against AD has also provided evidence of a causative role of Aβ in AD pathogenesis, as this mutation apparently lowers Aβ production by reducing β-secretase cleavage of APP (Jonsson et. al, 2012).

Apart from the age of onset, most FAD is phenotypically indistinguishable from the more common, sporadic forms of AD with late-onset (LOAD), with virtually identical tau and amyloid pathology and clinical symptoms (Selkoe, 2001). Thus, it is believed that FAD cases can provide insight into the pathogenesis of LOAD, and that accumulation and aggregation of Aβ is therefore the pathogenic initiator in these sporadic cases as well. While the causes of Aβ accumulation in sporadic AD are not fully understood, the apolipoprotein ε4 allele has been identified as the strongest risk factor to date for development of LOAD (Tanzi and Bertram, 2005). This natural genetic variant, which results in accelerated Aβ deposition, is thought to reduce the clearance of Aβ from the brain (Castellano et al, 2011). Therefore diminished Aβ clearance, rather than

aberrant Aβ production, may be to blame for Aβ elevation in some cases of LOAD. The identification of further genetic and environmental factors that may cause Aβ accumulation in LOAD is an area of intense investigation (Selkoe, 2011).

Despite the evidence for a central role of the dyshomeostasis and self-association of Aβ in AD pathogenesis, the mechanisms by which Aβ exerts its synaptotoxic and neurotoxic effects remain poorly understood. This is partly because the identity of the Aβ assembly mediating this toxicity is unclear. The earliest studies of Aβ toxicity focused on Aβ fibrils, as the amyloid plaques that characterize AD are primarily composed of fibrillar Aβ. While these pioneering studies showed that aggregated Aβ is neurotoxic and that aggregation was essential for this toxicity (Busciglio et al., 1992; Lorenzo and Yankner, 1994; Howlett et al., 1995; Pike et al., 1991), it was assumed that Aβ fibrils mediated these effects, as this was the readily detected form of Aβ in the aggregated preparations. However, there is a weak correlation between fibrillar amyloid plaque burden and the severity of dementia (Terry et al, 1991; Walsh and Selkoe, 2007). The level of soluble Aβ in the brain, however, is a strong correlate of the severity of synapse loss and cognitive decline (McLean et al., 1999; Näslund et al., 2000; Walsh and Selkoe, 2007). Thus, the focus of Aβ toxicity studies has shifted to soluble Aβ assemblies, and these studies suggest that soluble forms of Aβ, ranging from low-*n* oligomers to protofibrils, may be the main toxic agents, rather than the fibrillar Aβ in plaques. Protofibrils and globular intermediates known as Aβ-derived diffusible ligands (ADDLs), prepared *in vitro* from synthetic Aβ, are neurotoxic and impede long-term potentiation (LTP) (Hartley et al., 1999; Lambert et al., 1998; O'Nuallain et al., 2010). Cell-derived Aβ oligomers, but not monomers, inhibit hippocampal LTP and memory in rats (Walsh et al., 2002) and trigger synapse and dendritic spine loss in rat

hippocampal slices (Shankar et al., 2007). In particular, Aβ dimers isolated from human AD brains impair LTP and reduce dendritic spine density in rodent hippocampal slices, and induce memory deficits in rats (Shankar et al., 2008). While Aβ fibrils may be a relatively inert species, the presence of plaques may indicate the accumulation of a large burden of harmful soluble Aβ assemblies in the brain, and plaques may serve as a reservoir of toxic oligomeric Aβ species (Selkoe, 2011).

In addition to questions surrounding toxic Aβ assemblies, the pathways between Aβ and tau pathology are not understood. As stated above, human genetics have pointed to a central role for Aβ in initiating AD pathogenesis: FAD mutations cause changes in Aβ, suggesting that altered Aβ production is sufficient to precipitate AD, including the NFT pathology invariably observed in AD. Moreover, mutations in tau do not cause AD or Aβ plaque formation, but instead cause fronto-temporal dementia, suggesting that Aβ is not affected by changes in tau (Wolfe, 2012a). Work in AD mouse models also indicates that Aβ influences tau pathology. Co-expression of mutant APP with mutant tau in mice or injection of Aβ into the brains of tau transgenic mice results in accelerated tau hyperphosphorylation and increased tangle formation compared to mice that express mutant tau alone, without Aβ injection or APP co-expression. (Götz et al., 2001; Lewis et al., 2001). However, this is not to suggest that tau is not important in AD. Rather, evidence suggests that tau is in fact a downstream mediator of Aβ toxicity. For example, hippocampal neurons from tau knockout mice are not susceptible to Aβ-induced degeneration observed in wildtype neurons (Rapoport et al., 2002), and knockout of tau in APP transgenic mice reduces memory deficits and early mortality compared to tau-expressing mice (Roberson et al., 2007). In addition, NFTs correlate tightly with severity of cognitive decline,

and the spreading of tau pathology from the entorinal cortex correlates with the progression of clinical symptoms (Braak and Braak, 1995).

The pathogenic changes in tau that occur in AD have been widely studied. As mentioned above, the tau present in tangles is hyperphosphorylated. This phosphorylation occurs at specific sites and is mediated by several kinases including glycogen synthase kinase 3β, microtubule affinity-regulating kinase, and cyclin-dependent kinase 5 (Ittner and Götz, 2011; Wolfe, 2012a). Hyperphosphorylated tau detaches from microtubules and accumulates in somatodendritic compartments; therefore, the functions it serves in stabilizing microtubules may be compromised, and this loss of function may contribute to disease. This mislocalized, hyperphosphorylated tau eventually aggregates and forms NFTs, which are thought to exert their own toxic effects. In addition, soluble oligomers of hyperphosphorylated tau may also play a role in neuronal dysfunction (Ittner and Götz, 2011; Wolfe, 2012a).

Although tau is primarily sorted into axons, a small fraction has a dendritic function. Tau interacts with the tyrosine kinase Fyn, and this interaction targets Fyn to dendrites, where it phosphorylates the NMDA receptor subunit NR2B. Phosphorylated NMDA receptors associate with postsynaptic density protein 95, and this interaction is involved in excitotoxic signaling (Ittner et al, 2010). Excitotoxicity has been implicated in Aβ toxicity, and the localization of tau to soma or tau knockout reduces Fyn localization in dendrites and lessens seizure activity and memory impairment in AD mice (Ittner et al., 2010). In addition, Fyn overexpression worsens synaptic deficits and premature mortality in AD mice, while knockout of Fyn reduces these effects (Chin et al, 2004).

Despite these studies on the effects that Aβ can have on axonal and dendritic tau, the mechanisms by which extracellular Aβ elicits these intracellular changes in tau are still unclear. Several membrane receptors have been implicated as Aβ targets such as nicotinic receptors (Wang et al., 2000), NMDA receptors (De Felice et al., 2007), insulin receptors (De Felice et al., 2009), and prion protein (Laurén et al, 2009). It has also been proposed that, instead of binding a specific protein receptor, Aβ assemblies interact with and disrupt the neuronal lipid bilayer. This membrane interaction could then exert downstream effects on resident transmembrane proteins. (Jin et al., 2011; Marchesi, 2005; Selkoe, 2011). In this regard, Aβ oligomers have been shown to bind GM1 ganglioside of neuronal membranes (Hong et al., 2014).

The confusion and open questions still surrounding the neurotoxic mechanism of Aβ is partly due to the limitations of AD mouse models, which have failed to reproduce key features of AD. Most significantly, mouse models of pathogenic Aβ production do not develop tau pathology, and there is a paucity of neuronal loss in these mice (Selkoe, 2011; Yanker and Lu, 2009). AD mouse models only develop a fuller spectrum of AD pathology, including changes in tau and substantial neuronal loss, with the introduction of a human tau transgene harboring a mutation that promotes tau aggregation but which is not linked to AD (Chin, 2011). However, more promising paradigms have since emerged that may enable investigation of the mechanism of Aβ-mediated tau pathology. Rats, which have the six isoforms of tau that are present in humans (Hanes et al. 2009), as opposed to mice, which only harbor three, have proven to be a valuable model. Treatment of rat neurons expressing endogenous tau with Aβ oligomers results in changes in tau, including hyperphosphorylation, release from microtubules, and sorting into dendrites and also leads to neuritic degeneration (Jin et al., 2011; Zempel et al., 2010). In

addition, a rat model expressing APP and PS1 transgenes with FAD mutations exhibits key features of AD: age-dependent accumulation of Aβ, including oligomers; tau pathology, including hyperphosphorylation and silver-positive, sarkosyl-insoluble deposits; gliosis; neuron death; and cognitive impairment (Cohen et al., 2013). Non-human primates can develop amyloid and tau pathology as they age (Oikawa et al., 2010), and in a recent study the injection of Aβ oligomers into the brains of macaques elicited accelerated synapse loss, astrocyte and microglial activation, and formation of phospho-tau and NFTs (Forny-Germano et al., 2014). In addition, human cell lines have recently emerged as powerful models of AD. First, induced pluripotent stem cells, derived from the fibroblasts of AD subjects, can be directed to neuronal fates and analyzed for changes in Aβ and tau compared to controls. Studies performed in cells derived from Down syndrome and FAD patients report alterations in Aβ as well as in total tau and phospho-tau levels (Muratore et al., 2014; Shi et al., 2012). In addition, a novel, 3-dimensional system of differentiated human neuroprogenitor cells overexpressing FAD mutant APP and PS1 has recently been reported (Choi et al., 2014). This is the closest mimic of Aβ and tau pathology in a culture system to date, as both amyloid plaques and NFTs were formed. Although the changes in Aβ production caused by the FAD mutations were sufficient to induce NFT pathology in these human cells, the Aβ species that precipitated this effect was not examined. This model will be a valuable tool for further investigation into the mechanisms by which Aβ drives tau tangle formation.

PS, γ-secretase, and intramembrane proteolysis

γ-secretase is an intramembrane-cleaving aspartyl protease complex with PS as the catalytic component (Wolfe et. al, 1999). The other components of the γ-secretase complex are

nicastrin, presenilin enhancer 2 (Pen-2), and anterior pharynx defective 1 (Aph1) (Figure 1.2), and these three proteins and PS are necessary and sufficient for γ-secretase activity (Edbauer et al., 2003; Kimberly et al., 2003; Tagasuki et al., 2003). PS is autoproteolytically cleaved into a C-terminal and N-terminal fragment (CTF and NTF) when it associates with the other three components of the γ-secretase complex (Wolfe, 2009); PS becomes catalytically active when it undergoes autoproteolysis, as this event results in the scission of a hydrophobic loop that is thought to be an inhibitory pro-domain (Fukumori et al., 2010; Wolfe et al., 1999). The PS NTF and CTF remain associated, and each contributes one of the essential catalytic aspartate residues, suggesting that the active site of γ-secretase is at the PS CTF-NTF interface (Wolfe, 2009). Aph1 initially associates with nicastrin within the ER, and PS joins this subcomplex as a holoprotein (LaVoie et al., 2003); this association of PS with nicastrin and Aph1 stabilizes the PS holoprotein, which is otherwise rapidly degraded (Steiner et al., 1998; Ratovitski et al., 1997; Thinakaran et al., 1997). Pen2 then joins this trio, triggering PS autoproteolysis (Tagasuki et al., 2003). A 1:1:1:1 stoichiometry of each γ-secretase component within active γ-secretase complexes has been demonstrated (Sato et al., 2007). There are three possible isoforms of Aph1: Aph1A (which has two possible splicing variants) and Aph1B (Shirotani et al., 2004); along with PS1 and PS2, six different γ-secretase complexes can be formed. All six of these γ-secretase complexes are active, although PS1-containing complexes are more active in processing CTFβ than those containing PS2 (Acx et al., 2014; Shirotani et al., 2004) and are responsible for the majority of Aβ generated in the central nervous system (De Strooper et al., 1998).

γ-secretase cleaves the stubs of type I transmembrane proteins generated after ectodomain shedding. This antecedent cleavage, which occurs close to the membrane to generate a very

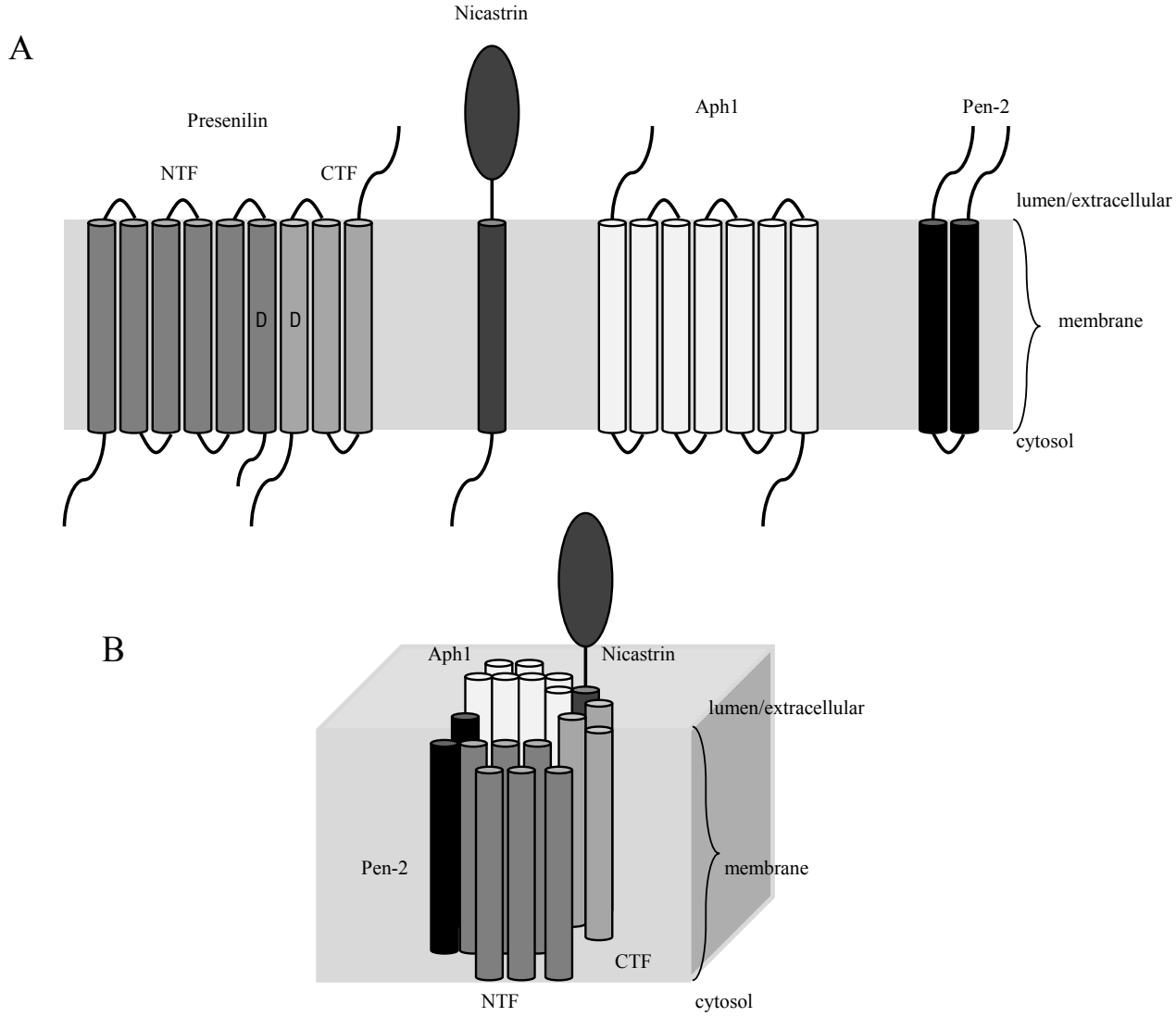

Figure 1.2. The components of the γ-secretase complex. γ-secretase is composed of PS, Aph1, nicastrin, and Pen-2. (A) PS, the catalytic component, is autoproteolytically cleaved into a CTF and an NTF. The catalytic aspartates within transmembrane domains 6 and 7 are indicated. Nicastrin is a type I transmembrane protein with a large, highly glycosylated ectodomain, Aph1 has 7 transmembrane domains, and Pen-2 has two transmembrane domains. (B) The general arrangement of PS, nicastrin, Aph1, and Pen-2 within the γ-secretase complex. Adapted from Wolfe, 2008.

short residual ectodomain, is a requirement for γ-secretase processing (Hemming et al., 2008). γ-secretase exhibits broad substrate specificity, cleaving the transmembrane stubs of over 60 type I membrane proteins (Haapasalo and Kovacs, 2011), and there is no apparent motif or consensus sequence for γ-secretase cleavage (Hemming et al., 2008). In some cases, most notably with the Notch receptor, the intracellular domain that is released from a membrane protein by γ-secretase cleavage has a clear role in signaling; other γ-secretase substrates do not appear to have a specific function. Due to its apparently loose substrate requirements and the unclear roles of many of its substrates, γ-secretase has been proposed to serve a general degradative function by clearing protein stubs from the membrane (Kopan and Ilagan, 2004).

The specific biochemical roles of the PS cofactors within the γ-secretase complex have been widely studied. Pen2 triggers PS autoproteolysis and activation (Ahn et al., 2010; Takasugi et al., 2003). Nicastrin is thought to play a role in substrate recognition: it has been proposed that the nicastrin ectodomain binds to the free N-termini of ectodomain-shed substrates, thus serving as a receptor that excludes substrates with intact ectodomains (Shah et al., 2005). A recent high resolution crystal structure of nicastrin revealed structural homology to an aminopeptidase and provided the most firm support of this model to date (Xie et al., 2014). The specific functions of Aph1 within the complex have remained the most enigmatic. This 7-pass transmembrane protein is traditionally thought to serve as a scaffold during the assembly and maturation of the complex (Wolfe, 2009). However, recent studies demonstrate that the presence of Aph1A versus Aph1B within γ-secretase complexes changes the Aβ profile generated (Serneels et al, 2009; Acx et al., 2014). This suggests that Aph1 can affect PS1 conformation, and differences in the conformation of PS within Aph1A- and Aph1B-containing complexes have

indeed been measured by fluorescence lifetime imaging microscopy (Serneels et al., 2009). Aph1 also interacts with γ-secretase substrates, suggesting a potential role in substrate recognition (Chen et al., 2010).

γ-secretase belongs to a larger group of intramembrane cleaving proteases (I-CLiPs). Signal peptide peptidase is an aspartyl protease I-CLiP cousin of γ-secretase. However, unlike γ-secretase, SPP is a single unit and does not function as a complex. SPP cleaves certain signal peptides once they are released from membrane pre-proteins by signal peptidase cleavage, and also plays a role in immune surveillance (Beel and Sanders, 2008; Weihofen et al., 2002; Wolfe, 2009). Site-2 protease is a metalloprotease involved in sterol biosynthesis, cleaving sterol regulatory element binding proteins after they are cleaved by site-1 protease (Beel and Sanders, 2008; Rawson et al., 1997; Wolfe, 2009). Last, rhomboid is a serine protease involved in diverse functions including epidermal growth factor signaling in Drosophila (Urban et al., 2002); unlike the other I-CLiPs, rhomboid does not require prior cleavage of substrates (Beel and Sanders, 2008; Wolfe, 2009).

I-CLiPs have the same key residues and catalytic chemistry as water-soluble proteases, but the process of intramembrane proteolysis has several unique features. First, these proteases must create an environment within the hydrophobic membrane to carry out a hydrolytic reaction. Therefore, the hydrophilic residues and catalytic water within the active site must be sequestered in the interior of the protease and away from the membrane environment (Beel and Sanders, 2008; Wolfe, 2009). Substrates are thought to initially dock at a site on the outer surface of the protease, followed by lateral entry to bring the substrate into the internal enzyme active site (Esler et al, 2002; Kornilova et al., 2005; Wolfe 2009). In addition, the single pass

transmembrane substrates of I-CLiPs are typically folded into α helices, a conformation that should render peptide bonds poorly accessible to proteolysis because of steric hindrance from the amino acid side chains (Beel and Sanders, 2008; Wolfe, 2009). Therefore, the helices should require at least partial unfolding or bending to make peptide bonds susceptible to cleavage. Rhomboid protease (Urban and Freeman, 2003), site-2 protease (Ye et al., 2000), and signal peptide peptidase (Lemberg and Martoglio, 2002) have an apparent requirement for helix-destabilizing residues in their substrates. Such a requirement has thus far not been demonstrated for γ-secretase, as no consensus helix-destabilizing motif has been identified within the TMDs of γ-secretase substrates (Hemming et al., 2008, Wolfe, 2009).

Electron microscopy studies of the structure of γ-secretase originally yielded low-resolution structures revealing basic features of the complex, such as a central cavity, a groove that may be the docking site for substrates, and possible sites for water entry (Osenkowski et al., 2009). A recent, higher resolution structure at 4.5 Å reveals a large nicastrin ectodomain and a horseshoe arrangement of the transmembrane domains, with the open pocket being a potential site for substrate entry (Lu et al., 2014).

Sequential proteolysis by γ-secretase

As explained above, cleavage of CTFβ by γ-secretase to produce the C-terminus of Aβ is variable and results in the production of secreted Aβ species of heterogenous lengths. The secreted Aβs include not only the major species Aβ40 and Aβ42, but also Aβ43 and Aβ38. That the longer Aβ42 aggregates much more rapidly than Aβ40 into potentially neurotoxic oligomers and that mutations that cause FAD lead to an increase in the Aβ42/40 ratio strongly suggest the

importance of the C-terminus of Aβ in AD pathogenesis; therefore, a central issue in AD research is how the heterogenous C-termini of Aβ come about.

Cleavage of CTFβ by γ-secretase was originally thought to occur at the so-called γ sites in the middle of the transmembrane domain of APP to generate secreted Aβ40 and Aβ42, as these were the main Aβ species that had been detected; it was widely assumed that the primary AICD fragments that are generated by γ-secretase would correspond to cleavage events occurring at Aβ residues 40 and 42, and therefore would have N-termini starting at position 41 and 43 of Aβ. However, instead of having N-termini beginning at the expected sites, the major AICD species generated by γ-secretase was found to have an N-terminus beginning at amino acid 50 (AICD50-99), and a minor species was found to have an N-terminus starting at position 49 (AICD49-99) (Gu et al., 2001; Sastre et al., 2001; Weidemann et al., 2001). Thus, cleavage at the sites which produce the AICD N-terminus, which were named the ε sites, occurs close to the membrane-cytoplasm border of CTFβ and is distinct from proteolysis at the γ sites in the middle of the CTFβ transmembrane domain (Figure 1.3). This finding raised more questions, as the residues in the middle of these two sites were unaccounted for (Figure 1.3), and it was unclear if proteolysis at these sites were completely independent cleavage events or if they were linked in some way.

Insight into a potential connection between these cleavage sites originally came from studies examining the relationships between the Aβ and AICD species generated by γ-secretase. While wildtype PS primarily generates Aβ40 and AICD50-99, certain FAD mutations in PS and APP that increase the relative production of AICD49-99 also increased the relative proportion of Aβ42 generated (Sato et al., 2003). This suggested that proteolysis at these two sites may not

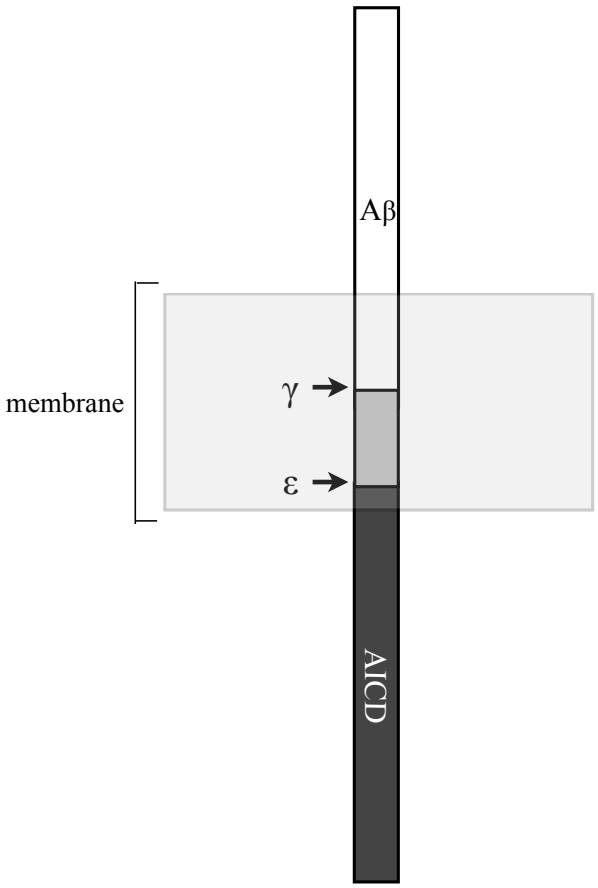

Figure 1.3. Dual γ-secretase cleavage sites within APP CTFβ. Secreted Aβ species Aβ40 and Aβ42 have C-termini corresponding to the γ sites of CTFβ near the middle of the transmembrane domain. The AICD species that are generated by γ-secretase cleavage, however, have N-termini corresponding to the ε sites of CTFβ near the membrane-cytoplasm border.

be independent events, since a shift in the position of cleavage at the ε site correlated with a shift in position of cleavage at the γ site.

Evidence has accumulated in recent years that demonstrates that these cleavage events occur sequentially, with γ-secretase first cleaving at the ε sites and then at the γ sites. First, analysis of intracellular Aβ revealed the presence of longer forms of Aβ, including Aβ48 and Aβ49, the species that would result from cleavage at the ε sites, as well as Aβ45 and Aβ46, which result from cleavage between the ε and γ sites at the so-called ζ sites (Figure 1.4A) (Qi-Takahara et al., 2005; Zhao et al., 2004); longer AICDs with N-termini that extend beyond the ε site have never been detected, which supports the idea that ζ and γ site cleavage don't occur prior to or independent of ε cleavage (Qi-Takahara et al., 2005) In addition, Funamoto et al. expressed Aβ49 in cells and found that this ε-cleaved product was indeed a substrate for γ-secretase and underwent γ site cleavage, leading to the secretion of Aβ40 and Aβ42 (Funamoto et al., 2004). In addition, installing three tryptophans, which prevents cleavage by γ-secretase, at the γ, ε, and ζ sites showed that ε cleavage could occur without γ cleavage, but that γ cleavage could not occur without ε and ζ cleavage (Sato et al., 2005).

Ihara and colleagues have unified these findings into a sequential model of CTFβ cleavage: an initial endoproteolytic cut at the ε sites releases AICD and generates Aβ48 or Aβ49, which remain in the membrane and undergo C-terminal trimming mostly every three residues, first at the ζ sites, then at the γ sites, to produce shorter, secreted forms of Aβ (Qi-Takahara et al., 2005) (Figure 1.4A). Cleavage at the final γ sites apparently relieves the hydrophobicity of the Aβ peptide enough that these products are then released from the membrane and secreted from cells.

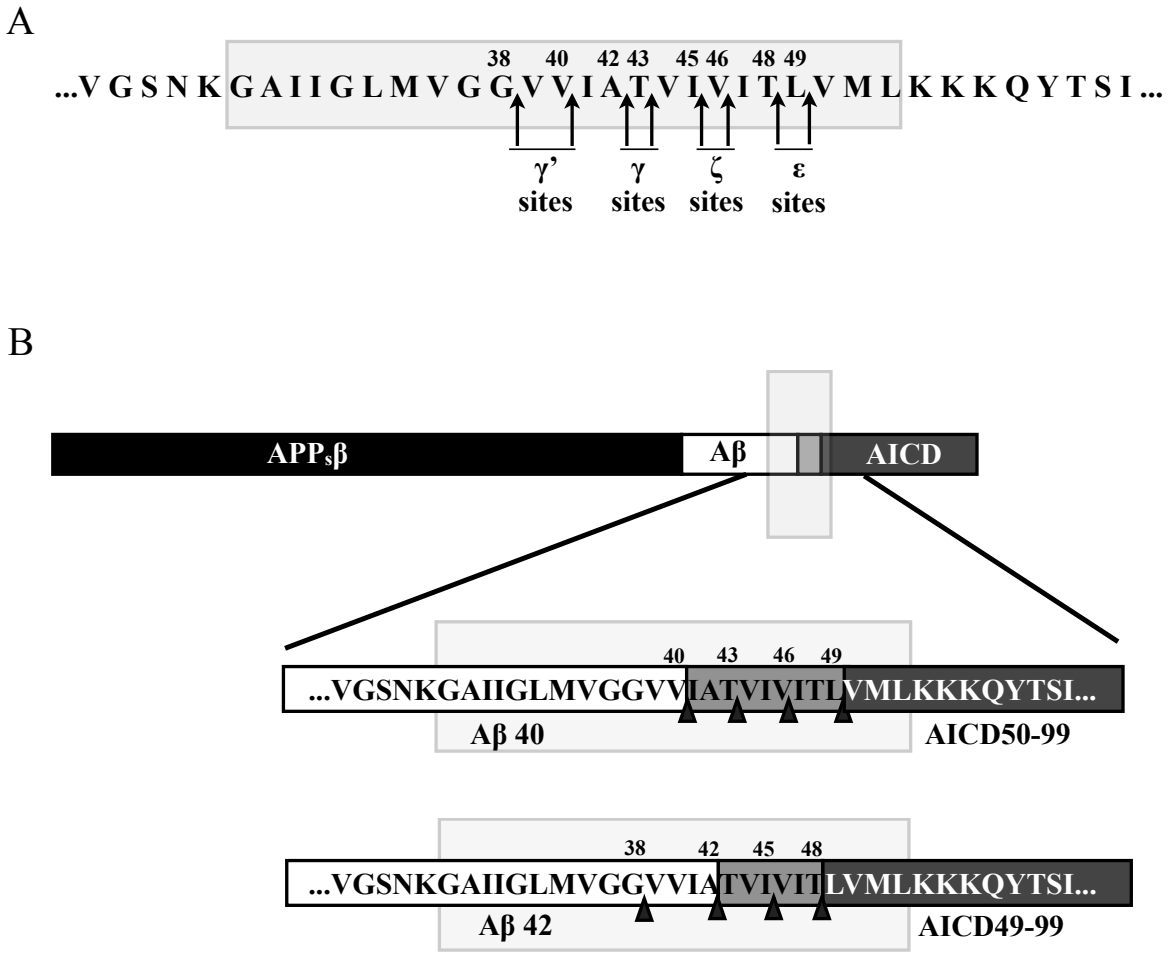

Figure 1.4. γ-secretase processing of the APP CTFβ transmembrane domain. (A) The transmembrane domain of APP (within the grey rectangle) is cleaved sequentially by γ-secretase at the ε, ζ, and γ sites. These cleavage events result in Aβs with the indicated C-termini. (B) The Aβ40 (top) and Aβ42 (bottom) generating pathways. ε cleavage that produces AICD50-99 and Aβ49 leads to Aβ40, while ε cleavage that produces AICD49-99 and Aβ48 leads to Aβ42. The tri and tetrapeptides detected by Takami et al. (2009) are indicated by arrowheads.

Specifically, Ihara and co-workers propose that Aβ49 is primarily processed to Aβ46, Aβ43, and Aβ40 and that Aβ48 is primarily trimmed to Aβ45, Aβ42, and Aβ38 (Figure 1.4B). The tripeptide and tetrapeptide products that would be expected to be generated from these trimming events have been detected in cell-free γ-secretase assays by mass spectrometry (Takami et al. 2009).

While not as well characterized as APP, the γ-secretase substrates Notch and CD44 also exhibit dual cleavage sites analogous to the ε and γ sites of APP, and a recent study suggests that endoproteolysis of PS also occurs in a stepwise manner (Fukumori et al., 2010; Lammich et al., 2002; Okochi et al., 2002).

FAD PS1 mutations

Over 100 dominantly-inherited FAD mutations in PS have been identified, and as explained above, they increase the Aβ42/Aβ40 ratio. Some of these mutations also cause a reduction in the overall proteolytic activity of γ-secretase (Bentahir et al., 2006; Chávez-Gutiérrez et al., 2012; Quintero-Monzon et al., 2011); while these mutants may produce lower levels of total Aβ than the WT enzyme, they still generate an increased proportion of Aβ42 compared to Aβ40 (Bentahir et al., 2006). It is generally thought that FAD PS mutations cause AD by increasing the ratio of aggregation-prone Aβ42 produced relative to Aβ40, as this increase in Aβ42/Aβ40 leads to the formation of toxic oligomeric Aβ assemblies regardless of total Aβ levels (Kuperstein et al., 2010).

This idea has been met with controversy, however, as an alternative hypothesis focusing on the reduction of activity of these PS1 mutants has arisen. This hypothesis suggests that these mutations cause FAD not by altering Aβ levels, but through a loss of presenilin function (Shen

and Kelleher, 2007). However, this model is problematic for a variety of reasons. First, it ignores the fact that mutations in APP that alter Aβ production are also associated with FAD (Bertram and Tanzi, 2005). In addition, some FAD mutant PS1 complexes have been shown to have activity equal to that of WT PS1 complexes (Chávez-Gutiérrez et al., 2012; Quintero-Monzon et al., 2011). Moreover, complete loss of function mutations in PS1, nicastrin, and Pen2 have been identified; heterozygous carriers of these mutations have an inherited skin disorder linked to deficits in Notch signaling, but not neurodegeneration (Wang et al., 2010). In addition, even mutations that result in a severe loss of proteolytic activity still result in an increase in the Aβ42/Aβ40 ratio and amyloid plaque deposition in mice, suggesting that even these mutations retain some function, namely the ability to generate Aβ42 (Heilig et al., 2010; Heilig et al., 2013; Xia et al., 2015). While it has been suggested that the FAD PS interacts with and exerts dominant negative effects on the WT copy of PS to elicit these changes in Aβ (Heilig et al., 2013; Kelleher and Shen, 2010), there is no evidence for an interaction of two PS molecules within active γ-secretase complexes (Sato et al., 2007). Thus, no FAD PS1 mutations have been shown to result in complete loss of function, and even so, they are dominantly inherited alongside a WT copy of PS1 and two PS2 alleles. In this regard, mice with only a single copy of WT PS1 and the remaining three PS alleles deleted are healthy (Herreman et al., 1999). While conditional knockout of all four PS genes in adult mice results in progressive neurodegeneration, synaptic loss, and memory deficits (Saura et al., 2007), this situation does not reflect the genetics of AD.

With the recent identification of the longer membrane-associated forms of Aβ generated by ε and ζ site cleavage and the understanding that the crucial Aβ C-terminus is actually generated by endoproteolysis and subsequent C-terminal trimming by γ-secretase, the effects of FAD

mutations on the γ-secretase trimming function and the entire spectrum of Aβ products has been of great interest. We and others have examined both the overall endoproteolytic activity and the spectrum of Aβs generated by a handful of FAD mutant PS1 complexes; while only some of the FAD mutations examined reduce endoproteolytic function, they all result in the accumulation of long Aβs of 42-49 residues (Chávez-Gutiérrez et al., 2012 Quintero-Monzon et al., 2011), suggesting that the C-terminal trimming function of γ-secretase is reduced by these mutations. In addition, the particular trimming steps that convert Aβ42 to Aβ38 and Aβ43 to Aβ40 have been examined in great detail and have been shown to be impaired by FAD mutations (Chávez-Gutiérrez et al., 2012; Okochi et al., 2013). It is clear that further exploration of the effects of PS1 FAD mutations on the trimming function of γ-secretase is warranted.

Modulators and selective inhibitors of γ-secretase

The current clinically available treatments for AD provide only temporary symptomatic relief and do nothing to modify AD pathogenesis and stop neuron death. AD therapies that will address the molecular events that initiate AD pathogenesis are urgently needed, and decreasing the production of Aβ, and in particular Aβ42, has been vigorously pursued as an approach to AD therapy. γ-secretase has thus emerged as an attractive target. However, since γ-secretase cleaves many important substrates, simply inhibiting γ-secretase activity is not an option. In particular, collateral inhibition of Notch cleavage results in unacceptable toxicity and may be the reason behind the recent failure of the stage 3 clinical trial of the inhibitor semagacestat (De Strooper 2014). Therefore, a major effort in discovering drugs which can allosterically target γ-secretase cleavage to inhibit Aβ production while maintaining Notch cleavage has emerged. One class of such compounds are Notch-sparing inhibitors, which inhibit γ-secretase cleavage of APP CTFβ

with more potency than Notch proteolysis (Wolfe, 2012b). However, the failure of the Notch-sparing inhibitor avegacestat during a phase 2 clinical trial has called this strategy into question (Coric et al., 2012). Notch related side effects were reported, and subsequent investigation revealed that the drug was not as selective for inhibiting the processing of APP vis-à-vis Notch as originally thought (Chávez-Gutiérrez et al., 2012; Crump et al., 2012). More troubling, both treatment with avegasestat and semagasestat caused cognitive worsening in patients, which may be attributable to the elevation of APP CTFs (Mitani et al., 2012). These data suggest that inhibition of APP CTF cleavage by γ-secretase is not a viable option, and programs to develop these compounds have since halted. An alternative approach that has been considered involves the use of compounds that selectively target specific isoforms of PS and Aph1. For example, PS1-selective inhibitors that spare PS2 function have been reported (Zhao et al., 2008). Although knockout of PS1 inhibits notch signaling and produces lethal phenotypes in mice (Shen et al., 1997; Wong et al., 1997), the use of a PS1 inhibitor in adult mice reduces Aβ production and plaque deposition without Notch side effects (Best et al., 2007; Borgegård et al., 2012), suggesting that PS2 may be sufficient to fulfill the role of Notch cleavage in the periphery of adult mice when PS1 is inhibited. PS2 inhibition may also be possible, as knockout of PS2 in mice, unlike that of PS1, is not lethal, and results in relatively mild phenotypes (Herreman et al., 1999); however, PS2 complexes only generate a minor portion of the Aβ in the central nervous system (De Strooper et al., 1998; Frånberg et al., 2011). In addition, selectively targeting Aph1 isoforms may be an option. While Aph1A is not dispensable, Aph1B deletion is tolerated and does not cause Notch toxicity in mice (Serneels et al. 2004, Serneels et al., 2009). Importantly, Aph1B-containing γ-secretase complexes have been shown to generate an increased proportion

of longer Aβ peptides (Acx et al., 2014; Serneels et al., 2009), and deletion of Aph1B reduces plaque burden and behavioral deficits in AD transgenic mice (Serneels et al., 2009). However, Aph1B was subsequently shown to play an important role in neuregulin processing (Dejaegere et al., 2008), raising concerns for this strategy as well. One last strategy that has been pursued involves the use of molecules, collectively known as γ-secretase modulators, that shift Aβ production towards shorter, more-soluble forms (Wolfe, 2012b). The site of cleavage of Notch may be similarly affected, but this change does not affect the release of the Notch intracellular domain and subsequent Notch signaling. Moreover, APP CTF cleavage is not inhibited by these compounds, thus avoiding any potential side effects that may be caused by their elevation (Mitani et al., 2012).

Concluding remarks

Despite the progress made in our understanding of AD pathogenesis, key questions remain unanswered. The mechanisms by which Aβ elicits changes in tau and exerts toxicity are still not understood, and the effects of FAD mutations in PS on pathogenesis are still under debate. Moreover, the C-terminal trimming function of γ-secretase and the Aβ species that are generated as a result of sequential cleavage have only recently been appreciated. Validation of C-terminal trimming by γ-secretase and examination of the effects of FAD mutations in PS on this particular proteolytic function are needed. In addition, examining substrate determinants of both endoproteolysis and C-terminal trimming by γ-secretase will be necessary to gain a fuller understanding of how γ-secretase cleaves and trims CTFβ to generate specific Aβ peptides. Last, a potential pathogenic role of the long membrane-associated Aβ species generated by ε and ζ site cleavage should be considered.

References

Acx H, Chávez-Gutiérrez L, Serneels L, Lismont S, Benurwar M, Elad N, De Strooper B. Signature amyloid β profiles are produced by different γ-secretase complexes. J Biol Chem. 2014 Feb 14;289(7):4346-55.

Ahn K, Shelton CC, Tian Y, Zhang X, Gilchrist ML, Sisodia SS, Li YM. Activation and intrinsic gamma-secretase activity of presenilin 1. Proc Natl Acad Sci U S A. 2010 Dec 14;107(50): 21435-40.

Alzheimer's Association. 2015 Alzheimer's Disease Facts and Figures. http://www.alz.org

Alzheimer's Association. Seven Stages of Alzheimer's. http://www.alz.org

Beel AJ, Sanders CR. Substrate specificity of gamma-secretase and other intramembrane proteases. Cell Mol Life Sci. 2008 May;65(9):1311-34.

Bentahir M, Nyabi O, Verhamme J, Tolia A, Horré K, Wiltfang J, Esselmann H, De Strooper B. Presenilin clinical mutations can affect gamma-secretase activity by different mechanisms.J Neurochem. 2006 Feb;96(3):732-42.

Best JD, Smith DW, Reilly MA, O'Donnell R, Lewis HD, Ellis S, Wilkie N, Rosahl TW, Laroque PA, Boussiquet-Leroux C, Churcher I, Atack JR, Harrison T, Shearman MS. The novel gamma secretase inhibitor N-[cis-4-[(4-chlorophenyl)sulfonyl]-4-(2,5-difluorophenyl)cyclohexyl]-1,1,1-trifluoromethanesulfonamide (MRK-560) reduces amyloid plaque deposition without evidence of notch-related pathology in the Tg2576 mouse. J Pharmacol Exp Ther. 2007 Feb;320(2):552-8.

Borgegård T, Gustavsson S, Nilsson C, Parpal S, Klintenberg R, Berg AL, Rosqvist S, Serneels L, Svensson S, Olsson F, Jin S, Yan H, Wanngren J, Jureus A, Ridderstad-Wollberg A, Wollberg P, Stockling K, Karlström H, Malmberg A, Lund J, Arvidsson PI, De Strooper B, Lendahl U, Lundkvist J. Alzheimer's disease: presenilin 2-sparing γ-secretase inhibition is a tolerable Aβ peptide-lowering strategy. J Neurosci. 2012 Nov 28;32(48):17297-305.

Braak H, Braak E. Staging of Alzheimer's disease-related neurofibrillary changes. Neurobiol Aging. 1995 May-Jun;16(3):271-8.

Busciglio J, Lorenzo A, Yankner BA. Methodological variables in the assessment of beta amyloid neurotoxicity. Neurobiol Aging. 1992 Sep-Oct;13(5):609-12.

Castellano JM, Kim J, Stewart FR, Jiang H, DeMattos RB, Patterson BW, Fagan AM, Morris JC, Mawuenyega KG, Cruchaga C, Goate AM, Bales KR, Paul SM, Bateman RJ, Holtzman DM. Human apoE isoforms differentially regulate brain amyloid-β peptide clearance. Sci Transl Med. 2011 Jun 29;3(89):89ra57.

Citron M, Westaway D, Xia W, Carlson G, Diehl T, Levesque G, Johnson-Wood K, Lee M, Seubert P, Davis A, Kholodenko D, Motter R, Sherrington R, Perry B, Yao H, Strome R, Lieberburg I, Rommens J, Kim S, Schenk D, Fraser P, St George Hyslop P, Selkoe DJ. Mutant presenilins of Alzheimer's disease increase production of 42-residue amyloid beta-protein in both transfected cells and transgenic mice. Nat Med. 1997 Jan;3(1):67-72.

Chávez-Gutiérrez L, Bammens L, Benilova I, Vandersteen A, Benurwar M, Borgers M, Lismont S, Zhou L, Van Cleynenbreugel S, Esselmann H, Wiltfang J, Serneels L, Karran E, Gijsen H, Schymkowitz J, Rousseau F, Broersen K, De Strooper B. The mechanism of γ-Secretase dysfunction in familial Alzheimer disease. EMBO J. 2012 May 16;31(10):2261-74.

Chen AC, Guo LY, Ostaszewski BL, Selkoe DJ, LaVoie MJ. Aph-1 associates directly with full-length and C-terminal fragments of gamma-secretase substrates. J Biol Chem. 2010 Apr 9;285(15):11378-91.

Chin J, Palop JJ, Yu GQ, Kojima N, Masliah E, Mucke L. Fyn kinase modulates synaptotoxicity, but not aberrant sprouting, in human amyloid precursor protein transgenic mice. J Neurosci. 2004 May 12;24(19):4692-7.

Chin J. Selecting a mouse model of Alzheimer's disease. Methods Mol Biol. 2011;670:169-89.

Choi SH, Kim YH, Hebisch M, Sliwinski C, Lee S, D'Avanzo C, Chen H, Hooli B, Asselin C, Muffat J, Klee JB, Zhang C, Wainger BJ, Peitz M, Kovacs DM, Woolf CJ, Wagner SL, Tanzi RE, Kim DY. A three-dimensional human neural cell culture model of Alzheimer's disease. Nature. 2014 Nov 13;515(7526):274-8.

Cohen RM, Rezai-Zadeh K, Weitz TM, Rentsendorj A, Gate D, Spivak I, Bholat Y, Vasilevko V, Glabe CG, Breunig JJ, Rakic P, Davtyan H, Agadjanyan MG, Kepe V, Barrio JR, Bannykh S, Szekely CA, Pechnick RN, Town T. A transgenic Alzheimer rat with plaques, tau pathology, behavioral impairment, oligomeric aβ, and frank neuronal loss. J Neurosci. 2013 Apr 10;33(15): 6245-56.

Coric V, van Dyck CH, Salloway S, Andreasen N, Brody M, Richter RW, Soininen H, Thein S, Shiovitz T, Pilcher G, Colby S, Rollin L, Dockens R, Pachai C, Portelius E, Andreasson U, Blennow K, Soares H, Albright C, Feldman HH, Berman RM. Safety and tolerability of the γ-secretase inhibitor avagacestat in a phase 2 study of mild to moderate Alzheimer disease. Arch Neurol. 2012 Nov;69(11):1430-40.

Crump CJ, Castro SV, Wang F, Pozdnyakov N, Ballard TE, Sisodia SS, Bales KR, Johnson DS, Li YM. BMS-708,163 targets presenilin and lacks notch-sparing activity. Biochemistry. 2012 Sep 18;51(37):7209-11.

De Strooper B. Lessons from a failed γ-secretase Alzheimer trial. Cell. 2014 Nov 6;159(4): 721-6.

De Felice FG, Velasco PT, Lambert MP, Viola K, Fernandez SJ, Ferreira ST, Klein WL. Abeta oligomers induce neuronal oxidative stress through an N-methyl-D-aspartate receptor-dependent mechanism that is blocked by the Alzheimer drug memantine. J Biol Chem. 2007 Apr 13;282(15):11590-601.

De Felice FG, Vieira MN, Bomfim TR, Decker H, Velasco PT, Lambert MP, Viola KL, Zhao WQ, Ferreira ST, Klein WL. Protection of synapses against Alzheimer's-linked toxins: insulin signaling prevents the pathogenic binding of Abeta oligomers. Proc Natl Acad Sci U S A. 2009 Feb 10;106(6):1971-6.

Dejaegere T, Serneels L, Schäfer MK, Van Biervliet J, Horré K, Depboylu C, Alvarez-Fischer D, Herreman A, Willem M, Haass C, Höglinger GU, D'Hooge R, De Strooper B. Deficiency of Aph1B/C-gamma-secretase disturbs Nrg1 cleavage and sensorimotor gating that can be reversed with antipsychotic treatment. Proc Natl Acad Sci U S A. 2008 Jul 15;105(28):9775-80.

De Strooper B, Saftig P, Craessaerts K, Vanderstichele H, Guhde G, Annaert W, Von Figura K, Van Leuven F. Deficiency of presenilin-1 inhibits the normal cleavage of amyloid precursor protein. Nature. 1998 Jan 22;391(6665):387-90.

De Strooper B, Annaert W, Cupers P, Saftig P, Craessaerts K, Mumm JS, Schroeter EH, Schrijvers V, Wolfe MS, Ray WJ, Goate A, Kopan R. A presenilin-1-dependent gamma-secretase-like protease mediates release of Notch intracellular domain. Nature. 1999 Apr 8;398(6727):518-22.

Duff K, Eckman C, Zehr C, Yu X, Prada CM, Perez-tur J, Hutton M, Buee L, Harigaya Y, Yager D, Morgan D, Gordon MN, Holcomb L, Refolo L, Zenk B, Hardy J, Younkin S.Increased amyloid-beta42(43) in brains of mice expressing mutant presenilin 1.Nature. 1996 Oct 24;383(6602):710-3.

Edbauer D, Winkler E, Regula JT, Pesold B, Steiner H, Haass C. Reconstitution of gamma-secretase activity. Nat Cell Biol. 2003 May;5(5):486-8.

Esler WP, Kimberly WT, Ostaszewski BL, Ye W, Diehl TS, Selkoe DJ, Wolfe MS. Activity-dependent isolation of the presenilin- gamma -secretase complex reveals nicastrin and a gamma substrate. Proc Natl Acad Sci U S A. 2002 Mar 5;99(5):2720-5.

Forny-Germano L, Lyra e Silva NM, Batista AF, Brito-Moreira J, Gralle M, Boehnke SE, Coe BC, Lablans A, Marques SA, Martinez AM, Klein WL, Houzel JC, Ferreira ST, Munoz DP, De Felice FG. Alzheimer's disease-like pathology induced by amyloid-β oligomers in nonhuman primates. J Neurosci. 2014 Oct 8;34(41):13629-43.

Frånberg J, Svensson AI, Winblad B, Karlström H, Frykman S. Minor contribution of presenilin 2 for γ-secretase activity in mouse embryonic fibroblasts and adult mouse brain. Biochem Biophys Res Commun. 2011 Jan 7;404(1):564-8.

Fukumori A, Fluhrer R, Steiner H, Haass C. Three-amino acid spacing of presenilin endoproteolysis suggests a general stepwise cleavage of gamma-secretase-mediated intramembrane proteolysis. J Neurosci. 2010 Jun 9;30(23):7853-62.

Funamoto S, Morishima-Kawashima M, Tanimura Y, Hirotani N, Saido TC, Ihara Y. Biochemistry. 2004 Oct 26;43(42):13532-40.Truncated carboxyl-terminal fragments of beta-amyloid precursor protein are processed to amyloid beta-proteins 40 and 42.Biochemistry. 2004 Oct 26;43(42):13532-40.

Glenner GG, Wong CW. Alzheimer's disease: initial report of the purification and characterization of a novel cerebrovascular amyloid protein. Biochem Biophys Res Commun. 1984 May 16;120(3):885-90.

Götz J, Chen F, van Dorpe J, Nitsch RM. Formation of neurofibrillary tangles in P301l tau transgenic mice induced by Abeta 42 fibrils. Science. 2001 Aug 24;293(5534):1491-5.

Grundke-Iqbal I, Iqbal K, Tung YC, Quinlan M, Wisniewski HM, Binder LI. Abnormal phosphorylation of the microtubule-associated protein tau (tau) in Alzheimer cytoskeletal pathology. Proc Natl Acad Sci U S A. 1986 Jul;83(13):4913-7.

Gu Y, Misonou H, Sato T, Dohmae N, Takio K, Ihara Y.Distinct intramembrane cleavage of the beta-amyloid precursor protein family resembling gamma-secretase-like cleavage of Notch. J Biol Chem. 2001 Sep 21;276(38):35235-8. Epub 2001 Aug 1.

Haapasalo A, Kovacs DM. The many substrates of presenilin/γ-secretase.J Alzheimers Dis. 2011;25(1):3-28.

Haass C, Selkoe DJ. Cellular processing of beta-amyloid precursor protein and the genesis of amyloid beta-peptide. Cell. 1993 Dec 17;75(6):1039-42.

Hanes J, Zilka N, Bartkova M, Caletkova M, Dobrota D, Novak M. Rat tau proteome consists of six tau isoforms: implication for animal models of human tauopathies. J Neurochem. 2009 Mar; 108(5):1167-76.

Hardy J, Selkoe DJ.̲The amyloid hypothesis of Alzheimer's disease: progress and problems on the road to therapeutics. Science. 2002 Jul 19;297(5580):353-6.

Hartley DM, Walsh DM, Ye CP, Diehl T, Vasquez S, Vassilev PM, Teplow DB, Selkoe DJ. Protofibrillar intermediates of amyloid beta-protein induce acute electrophysiological changes and progressive neurotoxicity in cortical neurons. J Neurosci. 1999 Oct 15;19(20):8876-84.

Heilig EA, Xia W, Shen J, Kelleher RJ 3rd. A presenilin-1 mutation identified in familial Alzheimer disease with cotton wool plaques causes a nearly complete loss of gamma-secretase activity. J Biol Chem. 2010 Jul 16;285(29):22350-9.

Heilig EA, Gutti U, Tai T, Shen J, Kelleher RJ 3rd. Trans-dominant negative effects of pathogenic PSEN1 mutations on γ-secretase activity and Aβ production. J Neurosci. 2013 Jul 10;33(28):11606-17.

Hemming ML, Elias JE, Gygi SP, Selkoe DJ. Proteomic profiling of gamma-secretase substrates and mapping of substrate requirements. PLoS Biol. 2008 Oct 21;6(10):e257.

Herreman A, Hartmann D, Annaert W, Saftig P, Craessaerts K, Serneels L, Umans L, Schrijvers V, Checler F, Vanderstichele H, Baekelandt V, Dressel R, Cupers P, Huylebroeck D, Zwijsen A, Van Leuven F, De Strooper B. Presenilin 2 deficiency causes a mild pulmonary phenotype and no changes in amyloid precursor protein processing but enhances the embryonic lethal phenotype of presenilin 1 deficiency. Proc Natl Acad Sci U S A. 1999 Oct 12;96(21):11872-7.

Hong S, Ostaszewski BL, Yang T, O'Malley TT, Jin M, Yanagisawa K, Li S, Bartels T, Selkoe DJ. Soluble Aβ oligomers are rapidly sequestered from brain ISF in vivo and bind GM1 ganglioside on cellular membranes. Neuron. 2014 Apr 16;82(2):308-19.

Howlett DR, Jennings KH, Lee DC, Clark MS, Brown F, Wetzel R, Wood SJ, Camilleri P, Roberts GW. Aggregation state and neurotoxic properties of Alzheimer beta-amyloid peptide. Neurodegeneration. 1995 Mar;4(1):23-32.

Ittner LM, Ke YD, Delerue F, Bi M, Gladbach A, van Eersel J, Wölfing H, Chieng BC, Christie MJ, Napier IA, Eckert A, Staufenbiel M, Hardeman E, Götz J. Dendritic function of tau mediates amyloid-beta toxicity in Alzheimer's disease mouse models. Cell. 2010 Aug 6;142(3):387-97.

Ittner LM, Götz J. Amyloid-β and tau--a toxic pas de deux in Alzheimer's disease. Nat Rev Neurosci. 2011 Feb;12(2):65-72.

Iwatsubo T, Odaka A, Suzuki N, Mizusawa H, Nukina N, Ihara Y. Visualization of A beta 42(43) and A beta 40 in senile plaques with end-specific A beta monoclonals: evidence that an initially deposited species is A beta 42(43).Neuron. 1994 Jul;13(1):45-53.

Jarrett JT, Berger EP, Lansbury PT Jr. The carboxy terminus of the beta amyloid protein is critical for the seeding of amyloid formation: implications for the pathogenesis of Alzheimer's disease. Biochemistry. 1993 May 11;32(18):4693-7.

Jonsson T, Atwal JK, Steinberg S, Snaedal J, Jonsson PV, Bjornsson S, Stefansson H, Sulem P, Gudbjartsson D, Maloney J, Hoyte K, Gustafson A, Liu Y, Lu Y, Bhangale T, Graham RR, Huttenlocher J, Bjornsdottir G, Andreassen OA, Jönsson EG, Palotie A, Behrens TW, Magnusson OT, Kong A, Thorsteinsdottir U, Watts RJ, Stefansson K. A mutation in APP protects against Alzheimer's disease and age-related cognitive decline. Nature. 2012 Aug 2;488(7409):96-9.

Jin M, Shepardson N, Yang T, Chen G, Walsh D, Selkoe DJ. Soluble amyloid beta-protein dimers isolated from Alzheimer cortex directly induce Tau hyperphosphorylation and neuritic degeneration. Proc Natl Acad Sci U S A. 2011 Apr 5;108(14):5819-24.

Kelleher RJ 3rd, Shen J. Genetics. Gamma-secretase and human disease. Science. 2010 Nov 19;330(6007):1055-6.

Kimberly WT, LaVoie MJ, Ostaszewski BL, Ye W, Wolfe MS, Selkoe DJ. Gamma-secretase is a membrane protein complex comprised of presenilin, nicastrin, Aph-1, and Pen-2.Proc Natl Acad Sci U S A. 2003 May 27;100(11):6382-7.

Kopan R, Ilagan MX. Gamma-secretase: proteasome of the membrane? Nat Rev Mol Cell Biol. 2004 Jun;5(6):499-504.

Kornilova AY, Bihel F, Das C, Wolfe MS. The initial substrate-binding site of gamma-secretase is located on presenilin near the active site. Proc Natl Acad Sci U S A. 2005 Mar 1;102(9): 3230-5.

Kosik KS, Joachim CL, Selkoe DJ. Microtubule-associated protein tau (tau) is a major antigenic component of paired helical filaments in Alzheimer disease. Proc Natl Acad Sci U S A. 1986 Jun; 83(11):4044-8.

Kuperstein I, Broersen K, Benilova I, Rozenski J, Jonckheere W, Debulpaep M, Vandersteen A, Segers-Nolten I, Van Der Werf K, Subramaniam V, Braeken D, Callewaert G, Bartic C, D'Hooge R, Martins IC, Rousseau F, Schymkowitz J, De Strooper B. Neurotoxicity of Alzheimer's disease Aβ peptides is induced by small changes in the Aβ42 to Aβ40 ratio. EMBO J. 2010 Oct 6;29(19): 3408-20.

Lambert MP, Barlow AK, Chromy BA, Edwards C, Freed R, Liosatos M, Morgan TE, Rozovsky I, Trommer B, Viola KL, Wals P, Zhang C, Finch CE, Krafft GA, Klein WL.Diffusible, nonfibrillar ligands derived from Abeta1-42 are potent central nervous system neurotoxins. Proc Natl Acad Sci U S A. 1998 May 26;95(11):6448-53.

Lammich S, Okochi M, Takeda M, Kaether C, Capell A, Zimmer AK, Edbauer D, Walter J, Steiner H, Haass C. Presenilin-dependent intramembrane proteolysis of CD44 leads to the liberation of its intracellular domain and the secretion of an Abeta-like peptide. J Biol Chem. 2002 Nov 22;277(47):44754-9.

Laurén J, Gimbel DA, Nygaard HB, Gilbert JW, Strittmatter SM. Cellular prion protein mediates impairment of synaptic plasticity by amyloid-beta oligomers. Nature. 2009 Feb 26;457(7233): 1128-32.

LaVoie MJ, Fraering PC, Ostaszewski BL, Ye W, Kimberly WT, Wolfe MS, Selkoe DJ. Assembly of the gamma-secretase complex involves early formation of an intermediate subcomplex of Aph-1 and nicastrin. J Biol Chem. 2003 Sep 26;278(39):37213-22.

Lemberg MK, Martoglio B. Requirements for signal peptide peptidase-catalyzed intramembrane proteolysis.Mol Cell. 2002 Oct;10(4):735-44.

Lewis J, Dickson DW, Lin WL, Chisholm L, Corral A, Jones G, Yen SH, Sahara N, Skipper L, Yager D, Eckman C, Hardy J, Hutton M, McGowan E. Enhanced neurofibrillary degeneration in transgenic mice expressing mutant tau and APP. Science. 2001 Aug 24;293(5534):1487-91.

Lorenzo A, Yankner BA. Beta-amyloid neurotoxicity requires fibril formation and is inhibited by congo red. Proc Natl Acad Sci U S A. 1994 Dec 6;91(25):12243-7.

Lu P, Bai XC, Ma D, Xie T, Yan C, Sun L, Yang G, Zhao Y, Zhou R, Scheres SH, Shi Y. Three-dimensional structure of human γ-secretase. Nature. 2014 Aug 14;512(7513):166-70.

Masters CL, Simms G, Weinman NA, Multhaup G, McDonald BL, Beyreuther K. Amyloid plaque core protein in Alzheimer disease and Down syndrome. Proc Natl Acad Sci U S A. 1985 Jun; 82 (12):4245-9.

McLean CA, Cherny RA, Fraser FW, Fuller SJ, Smith MJ, Beyreuther K, Bush AI, Masters CL. Soluble pool of Abeta amyloid as a determinant of severity of neurodegeneration in Alzheimer's disease. Ann Neurol. 1999 Dec;46(6):860-6.

Mitani Y, Yarimizu J, Saita K, Uchino H, Akashiba H, Shitaka Y, Ni K, Matsuoka N. Differential effects between γ-secretase inhibitors and modulators on cognitive function in amyloid precursor protein-transgenic and nontransgenic mice. J Neurosci. 2012 Feb 8;32(6):2037-50.

Muratore CR, Rice HC, Srikanth P, Callahan DG, Shin T, Benjamin LN, Walsh DM, Selkoe DJ, Young-Pearse TL. The familial Alzheimer's disease APPV717I mutation alters APP processing and Tau expression in iPSC-derived neurons. Hum Mol Genet. 2014 Jul 1;23(13):3523-36.

Näslund J, Haroutunian V, Mohs R, Davis KL, Davies P, Greengard P, Buxbaum JD. Correlation between elevated levels of amyloid beta-peptide in the brain and cognitive decline. JAMA. 2000 Mar 22-29;283(12):1571-7.

Oikawa N, Kimura N, Yanagisawa K. Alzheimer-type tau pathology in advanced aged nonhuman primate brains harboring substantial amyloid deposition. Brain Res. 2010 Feb 22;1315:137-49.

Okochi M, Steiner H, Fukumori A, Tanii H, Tomita T, Tanaka T, Iwatsubo T, Kudo T, Takeda M, Haass C. Presenilins mediate a dual intramembranous gamma-secretase cleavage of Notch-1. EMBO J. 2002 Oct 15;21(20):5408-16.

Okochi M, Tagami S, Yanagida K, Takami M, Kodama TS, Mori K, Nakayama T, Ihara Y, Takeda M.γ-secretase modulators and presenilin 1 mutants act differently on presenilin/γ-secretase function to cleave Aβ42 and Aβ43. Cell Rep. 2013 Jan 31;3(1):42-51.

O'Nuallain B, Freir DB, Nicoll AJ, Risse E, Ferguson N, Herron CE, Collinge J, Walsh DM. Amyloid beta-protein dimers rapidly form stable synaptotoxic protofibrils. J Neurosci. 2010 Oct 27;30(43):14411-9.

Osenkowski P, Li H, Ye W, Li D, Aeschbach L, Fraering PC, Wolfe MS, Selkoe DJ, Li H. Cryoelectron microscopy structure of purified gamma-secretase at 12 A resolution. J Mol Biol. 2009 Jan 16;385(2):642-52.

Pike CJ, Walencewicz AJ, Glabe CG, Cotman CW. In vitro aging of beta-amyloid protein causes peptide aggregation and neurotoxicity. Brain Res. 1991 Nov 1;563(1-2):311-4.

Prasher VP, Farrer MJ, Kessling AM, Fisher EM, West RJ, Barber PC, Butler AC. Molecular mapping of Alzheimer-type dementia in Down's syndrome. Ann Neurol. 1998 Mar;43(3):380-3.

Querfurth HW, LaFerla FM. Alzheimer's disease. N Engl J Med. 2010 Jan 28;362(4):329-44.

Qi-Takahara Y, Morishima-Kawashima M, Tanimura Y, Dolios G, Hirotani N, Horikoshi Y, Kametani F, Maeda M, Saido TC, Wang R, Ihara Y. Longer forms of amyloid beta protein: implications for the mechanism of intramembrane cleavage by gamma-secretase.J Neurosci. 2005 Jan 12;25(2):436-45.

Quintero-Monzon O, Martin MM, Fernandez MA, Cappello CA, Krzysiak AJ, Osenkowski P, Wolfe MS. Dissociation between the processivity and total activity of γ-secretase: implications for the mechanism of Alzheimer's disease-causing presenilin mutations. Biochemistry. 2011 Oct 25;50(42):9023-35.

Rapoport M, Dawson HN, Binder LI, Vitek MP, Ferreira A. Tau is essential to beta -amyloid-induced neurotoxicity. Proc Natl Acad Sci U S A. 2002 Apr 30;99(9):6364-9.

Ratovitski T, Slunt HH, Thinakaran G, Price DL, Sisodia SS, Borchelt DR. Endoproteolytic processing and stabilization of wild-type and mutant presenilin. J Biol Chem. 1997 Sep 26;272(39):24536-41.

Rawson RB, Zelenski NG, Nijhawan D, Ye J, Sakai J, Hasan MT, Chang TY, Brown MS, Goldstein JL. Complementation cloning of S2P, a gene encoding a putative metalloprotease required for intramembrane cleavage of SREBPs. Mol Cell. 1997 Dec;1(1):47-57.

Roberson ED, Scearce-Levie K, Palop JJ, Yan F, Cheng IH, Wu T, Gerstein H, Yu GQ, Mucke L. Reducing endogenous tau ameliorates amyloid beta-induced deficits in an Alzheimer's disease mouse model. Science. 2007 May 4;316(5825):750-4.

Rovelet-Lecrux A, Hannequin D, Raux G, Le Meur N, Laquerrière A, Vital A, Dumanchin C, Feuillette S, Brice A, Vercelletto M, Dubas F, Frebourg T, Campion D. APP locus duplication causes autosomal dominant early-onset Alzheimer disease with cerebral amyloid angiopathy. Nat Genet. 2006 Jan;38(1):24-6.

Sastre M, Steiner H, Fuchs K, Capell A, Multhaup G, Condron MM, Teplow DB, Haass C.Presenilin-dependent gamma-secretase processing of beta-amyloid precursor protein at a site corresponding to the S3 cleavage of Notch.EMBO Rep. 2001 Sep;2(9):835-41. Epub 2001 Aug 23.

Sato T, Dohmae N, Qi Y, Kakuda N, Misonou H, Mitsumori R, Maruyama H, Koo EH, Haass C, Takio K, Morishima-Kawashima M, Ishiura S, Ihara Y.Potential link between amyloid beta-protein 42 and C-terminal fragment gamma 49-99 of beta-amyloid precursor protein. J Biol Chem. 2003 Jul 4;278(27):24294-301.

Sato T, Tanimura Y, Hirotani N, Saido TC, Morishima-Kawashima M, Ihara Y. Blocking the cleavage at midportion between gamma- and epsilon-sites remarkably suppresses the generation of amyloid beta-protein. FEBS Lett. 2005 May 23;579(13):2907-12.

Sato T, Diehl TS, Narayanan S, Funamoto S, Ihara Y, De Strooper B, Steiner H, Haass C, Wolfe MS. Active gamma-secretase complexes contain only one of each component. J Biol Chem. 2007 Nov 23;282(47):33985-93.

Saura CA, Choi SY, Beglopoulos V, Malkani S, Zhang D, Shankaranarayana Rao BS, Chattarji S, Kelleher RJ 3rd, Kandel ER, Duff K, Kirkwood A, Shen J. Loss of presenilin function causes impairments of memory and synaptic plasticity followed by age-dependent neurodegeneration. Neuron. 2004 Apr 8;42(1):23-36.

Scheuner D, Eckman C, Jensen M, Song X, Citron M, Suzuki N, Bird TD, Hardy J, Hutton M, Kukull W, Larson E, Levy-Lahad E, Viitanen M, Peskind E, Poorkaj P, Schellenberg G, Tanzi R, Wasco W, Lannfelt L, Selkoe D, Younkin S. Secreted amyloid beta-protein similar to that in the senile plaques of Alzheimer's disease is increased in vivo by the presenilin 1 and 2 and APP mutations linked to familial Alzheimer's disease. Nat Med. 1996 Aug;2(8):864-70.

Selkoe DJ. The cell biology of beta-amyloid precursor protein and presenilin in Alzheimer's disease. Trends Cell Biol. 1998 Nov;8(11):447-53.

Selkoe DJ. Alzheimer's disease: genes, proteins, and therapy. Physiol Rev. 2001 Apr;81(2): 741-66.

Selkoe DJ. Resolving controversies on the path to Alzheimer's therapeutics. Nat Med. 2011 Sep 7;17(9):1060-5.

Selkoe DJ. The therapeutics of Alzheimer's disease: Where we stand and where we are heading. Ann Neurol. 2013 Sep;74(3):328-36.

Serneels L, Dejaegere T, Craessaerts K, Horré K, Jorissen E, Tousseyn T, Hébert S, Coolen M, Martens G, Zwijsen A, Annaert W, Hartmann D, De Strooper B. Differential contribution of the three Aph1 genes to gamma-secretase activity in vivo. Proc Natl Acad Sci U S A. 2005 Feb 1;102(5):1719-24.

Serneels L, Van Biervliet J, Craessaerts K, Dejaegere T, Horré K, Van Houtvin T, Esselmann H, Paul S, Schäfer MK, Berezovska O, Hyman BT, Sprangers B, Sciot R, Moons L, Jucker M, Yang Z, May PC, Karran E, Wiltfang J, D'Hooge R, De Strooper B. gamma-Secretase heterogeneity in the Aph1 subunit: relevance for Alzheimer's disease. Science. 2009 May 1;324(5927):639-42.

Shah S, Lee SF, Tabuchi K, Hao YH, Yu C, LaPlant Q, Ball H, Dann CE 3rd, Südhof T, Yu G. Nicastrin functions as a gamma-secretase-substrate receptor. Cell. 2005 Aug 12;122(3):435-47.

Shankar GM, Bloodgood BL, Townsend M, Walsh DM, Selkoe DJ, Sabatini BL. Natural oligomers of the Alzheimer amyloid-beta protein induce reversible synapse loss by modulating an NMDA-type glutamate receptor-dependent signaling pathway. J Neurosci. 2007 Mar 14;27(11):2866-75.

Shankar GM, Li S, Mehta TH, Garcia-Munoz A, Shepardson NE, Smith I, Brett FM, Farrell MA, Rowan MJ, Lemere CA, Regan CM, Walsh DM, Sabatini BL, Selkoe DJ. Amyloid-beta protein dimers isolated directly from Alzheimer's brains impair synaptic plasticity and memory. Nat Med. 2008 Aug;14(8):837-42.

Shen J, Bronson RT, Chen DF, Xia W, Selkoe DJ, Tonegawa S. Skeletal and CNS defects in Presenilin-1-deficient mice. Cell. 1997 May 16;89(4):629-39.

Shen J, Kelleher RJ 3rd. The presenilin hypothesis of Alzheimer's disease: evidence for a loss-of-function pathogenic mechanism. Proc Natl Acad Sci U S A. 2007 Jan 9;104(2):403-9.

Shi Y, Kirwan P, Smith J, MacLean G, Orkin SH, Livesey FJ. A human stem cell model of early Alzheimer's disease pathology in Down syndrome. Sci Transl Med. 2012 Mar 7; 4(124):124ra29.

Shirotani K, Edbauer D, Prokop S, Haass C, Steiner H. Identification of distinct gamma-secretase complexes with different APH-1 variants. J Biol Chem. 2004 Oct 1;279(40):41340-5.

Sperling RA, Aisen PS, Beckett LA, Bennett DA, Craft S, Fagan AM, Iwatsubo T, Jack CR Jr, Kaye J, Montine TJ, Park DC, Reiman EM, Rowe CC, Siemers E, Stern Y, Yaffe K, Carrillo MC, Thies B, Morrison-Bogorad M, Wagster MV, Phelps CH. Toward defining the preclinical stages of Alzheimer's disease: recommendations from the National Institute on Aging-Alzheimer's

Association workgroups on diagnostic guidelines for Alzheimer's disease. Alzheimers Dement. 2011 May;7(3):280-92.

Steiner H, Capell A, Pesold B, Citron M, Kloetzel PM, Selkoe DJ, Romig H, Mendla K, Haass C. Expression of Alzheimer's disease-associated presenilin-1 is controlled by proteolytic degradation and complex formation. J Biol Chem. 1998 Nov 27;273(48):32322-31.

Takasugi N, Tomita T, Hayashi I, Tsuruoka M, Niimura M, Takahashi Y, Thinakaran G, Iwatsubo T. The role of presenilin cofactors in the gamma-secretase complex. Nature. 2003 Mar 27;422(6930):438-41.

Thies B, Morrison-Bogorad M, Wagster MV, Phelps CH. Toward defining the preclinical stages of Alzheimer's disease: recommendations from the National Institute on Aging-Alzheimer's Association workgroups on diagnostic guidelines for Alzheimer's disease. Alzheimers Dement. 2011 May;7(3):280-92.

Thinakaran G, Harris CL, Ratovitski T, Davenport F, Slunt HH, Price DL, Borchelt DR, Sisodia SS. Evidence that levels of presenilins (PS1 and PS2) are coordinately regulated by competition for limiting cellular factors. J Biol Chem. 1997 Nov 7;272(45):28415-22.

Takami M, Nagashima Y, Sano Y, Ishihara S, Morishima-Kawashima M, Funamoto S, Ihara Y. gamma-Secretase: successive tripeptide and tetrapeptide release from the transmembrane domain of beta-carboxyl terminal fragment. J Neurosci. 2009 Oct 14;29(41):13042-52.

Tanzi RE, Bertram L. Twenty years of the Alzheimer's disease amyloid hypothesis: a genetic perspective.Cell. 2005 Feb 25;120(4):545-55.

Terry RD, Masliah E, Salmon DP, Butters N, DeTeresa R, Hill R, Hansen LA, Katzman R. Physical basis of cognitive alterations in Alzheimer's disease: synapse loss is the major correlate of cognitive impairment. Ann Neurol. 1991 Oct;30(4):572-80.

Urban S, Lee JR, Freeman M. A family of Rhomboid intramembrane proteases activates all Drosophila membrane-tethered EGF ligands. EMBO J. 2002 Aug 15;21(16):4277-86.

Urban S, Freeman M.Substrate specificity of rhomboid intramembrane proteases is governed by helix-breaking residues in the substrate transmembrane domain.Mol Cell. 2003 Jun;11(6): 1425-34.

Vassar R, Bennett BD, Babu-Khan S, Kahn S, Mendiaz EA, Denis P, Teplow DB, Ross S, Amarante P, Loeloff R, Luo Y, Fisher S, Fuller J, Edenson S, Lile J, Jarosinski MA, Biere AL, Curran E, Burgess T, Louis JC, Collins F, Treanor J, Rogers G, Citron M. Beta-secretase cleavage of Alzheimer's amyloid precursor protein by the transmembrane aspartic protease BACE. Science. 1999 Oct 22;286(5440):735-41.

Walsh DM, Klyubin I, Fadeeva JV, Cullen WK, Anwyl R, Wolfe MS, Rowan MJ, Selkoe DJ. Naturally secreted oligomers of amyloid beta protein potently inhibit hippocampal long-term potentiation in vivo. Nature. 2002 Apr 4;416(6880):535-9.

Walsh DM, Selkoe DJ. A beta oligomers - a decade of discovery. J Neurochem. 2007 Jun; 101(5):1172-84.

Wang HY, Lee DH, Davis CB, Shank RP. Amyloid peptide Abeta(1-42) binds selectively and with picomolar affinity to alpha7 nicotinic acetylcholine receptors. J Neurochem. 2000 Sep; 75(3):1155-61.

Weidemann A, Eggert S, Reinhard FB, Vogel M, Paliga K, Baier G, Masters CL, Beyreuther K, Evin G. A novel epsilon-cleavage within the transmembrane domain of the Alzheimer amyloid precursor protein demonstrates homology with Notch processing. Biochemistry. 2002 Feb 26;41(8):2825-35.

Wang B, Yang W, Wen W, Sun J, Su B, Liu B, Ma D, Lv D, Wen Y, Qu T, Chen M, Sun M, Shen Y, Zhang X. Gamma-secretase gene mutations in familial acne inversa. Science. 2010 Nov 19;330(6007):1065.

Weihofen A, Binns K, Lemberg MK, Ashman K, Martoglio B. Identification of signal peptide peptidase, a presenilin-type aspartic protease.Science. 2002 Jun 21;296(5576):2215-8.

Weingarten MD, Lockwood AH, Hwo SY, Kirschner MW. A protein factor essential for microtubule assembly. Proc Natl Acad Sci U S A. 1975 May;72(5):1858-62.

Wippold FJ 2nd, Cairns N, Vo K, Holtzman DM, Morris JC. Neuropathology for the neuroradiologist: plaques and tangles. AJNR Am J Neuroradiol. 2008 Jan;29(1):18-22.

Wolfe MS, Xia W, Ostaszewski BL, Diehl TS, Kimberly WT, Selkoe DJ. Two transmembrane aspartates in presenilin-1 required for presenilin endoproteolysis and gamma-secretase activity. Nature. 1999 Apr 8;398(6727):513-7.

Wolfe MS. Gamma-secretase: structure, function, and modulation for Alzheimer's disease. Curr Top Med Chem. 2008;8(1):2-8.

Wolfe MS. Intramembrane proteolysis. Chem Rev. 2009 Apr;109(4):1599-612.

Wolfe MS. The role of tau in neurodegenerative diseases and its potential as a therapeutic target. Scientifica. 2012a 2012:796024.

Wolfe MS. Processive proteolysis by γ-secretase and the mechanism of Alzheimer's disease. Biol Chem. 2012b Sep;393(9):899-905.

Wong PC, Zheng H, Chen H, Becher MW, Sirinathsinghji DJ, Trumbauer ME, Chen HY, Price DL, Van der Ploeg LH, Sisodia SS. Presenilin 1 is required for Notch1 and DII1 expression in the paraxial mesoderm. Nature. 1997 May 15;387(6630):288-92.

Xia D, Watanabe H, Wu B, Lee SH, Li Y, Tsvetkov E, Bolshakov VY, Shen J, Kelleher RJ 3rd. Presenilin-1 Knockin Mice Reveal Loss-of-Function Mechanism for Familial Alzheimer's Disease. Neuron. 2015 Mar 4;85(5):967-81.

Xie T, Yan C, Zhou R, Zhao Y, Sun L, Yang G, Lu P, Ma D, Shi Y. Crystal structure of the γ-secretase component nicastrin. Proc Natl Acad Sci U S A. 2014 Sep 16;111(37):13349-54.

Yankner BA, Lu T. Amyloid beta-protein toxicity and the pathogenesis of Alzheimer disease. J Biol Chem. 2009 Feb 20;284(8):4755-9.

Ye J, Davé UP, Grishin NV, Goldstein JL, Brown MS.Asparagine-proline sequence within membrane-spanning segment of SREBP triggers intramembrane cleavage by site-2 protease.Proc Natl Acad Sci U S A. 2000 May 9;97(10):5123-8.

Zempel H, Thies E, Mandelkow E, Mandelkow EM. Abeta oligomers cause localized Ca(2+) elevation, missorting of endogenous Tau into dendrites, Tau phosphorylation, and destruction of microtubules and spines. J Neurosci. 2010 Sep 8;30(36):11938-50.

Zhao B, Yu M, Neitzel M, Marugg J, Jagodzinski J, Lee M, Hu K, Schenk D, Yednock T, Basi G. Identification of gamma-secretase inhibitor potency determinants on presenilin. J Biol Chem. 2008 Feb 1;283(5):2927-38.

Zhao G, Mao G, Tan J, Dong Y, Cui MZ, Kim SH, Xu X. Identification of a new presenilin-dependent zeta-cleavage site within the transmembrane domain of amyloid precursor protein. J Biol Chem. 2004 Dec 3;279(49):50647-50. Epub 2004 Oct 13.

Chapter 2:

Alzheimer presenilin-1 mutations dramatically reduce trimming of long amyloid β-peptides (Aβ) by γ-secretase to increase 42-to-40-residue Aβ

Authors: Marty A. Fernandez, Julia A. Klutkowski, Taylor Freret, and Michael S. Wolfe

Contributors: This project was designed by M.A.F. and M.S.W. J.A.K. cloned APP constructs, and T.F. assisted with *in vitro* assays for the kinetic analysis of Aβ trimming. All other experiments were carried out by M.A.F. The manuscript was written by M.A.F. and M.S.W.

Publication: This chapter has been published in the Journal of Biological Chemistry.

Abstract

The presenilin-containing γ-secretase complex produces the amyloid β-peptide (Aβ) through intramembrane proteolysis, and over 100 presenilin mutations are associated with familial early-onset Alzheimer's disease (AD). The question of whether these mutations result in AD through a gain or a loss of function remains highly controversial. Mutations in presenilins increase ratios of 42- to 40-residue Aβ critical to pathogenesis, but other Aβs of 38 to 49 residues are also formed by γ-secretase. Evidence in cells suggests the protease first cleaves substrate within the transmembrane domain at the ε site to form 48- or 49-residue Aβ. Subsequent cleavage almost every three residues from the C-terminus is thought to occur along two pathways toward shorter secreted forms of Aβ: Aβ49→Aβ46→Aβ43→Aβ40 and Aβ48→Aβ45→Aβ42→Aβ38. Here we show that addition of synthetic long Aβ peptides (Aβ45-49) directly into purified preparations of γ-secretase leads to the formation of Aβ40 and Aβ42, whether the protease complex is detergent-solubilized or reconstituted into lipid vesicles, and the ratios of products Aβ42 to Aβ40 follow a pattern consistent with the dual-pathway hypothesis. Kinetic analysis of five different AD-causing mutations in presenilin-1 revealed that all result in drastic reduction of normal carboxypeptidase function. Altered trimming of long Aβ peptides to Aβ40 and Aβ42 by mutant proteases occurs at multiple levels, independent of effects on initial endoproteolysis at the ε site, all conspiring to increase the critical Aβ42/Aβ40 ratio implicated in AD pathogenesis. Taken together, these results suggest that specific reduction of carboxypeptidase function of γ-secretase leads to the gain of toxic Aβ42/Aβ40.

Introduction

Deposition of the amyloid β-peptide (Aβ) in the form of neuritic plaques in the brain is a defining pathological characteristic of Alzheimer's disease (AD) (1). A large body of evidence points to Aβ as the pathogenic initiator, most notably the identification of dominant missense mutations in the amyloid β-protein precursor (APP) and the presenilins that cause early-onset familial AD (FAD) (2) and the discovery of presenilin as the catalytic component of γ-secretase responsible for generation of the Aβ C-terminus (3). More than 100 FAD presenilin mutations have been identified, and these mutations can cause a decrease in γ-secretase cleavage of substrates as well as an increase in the ratio of the more aggregation-prone 42-residue Aβ (Aβ42) over the major secreted 40-residue Aβ (Aβ40). These findings have led to a still unresolved controversy over whether presenilin mutations cause FAD through a loss or a gain of function (4-8).

In deciphering the effects of presenilin FAD mutations, it is critical to consider the various proteolytic functions of γ-secretase. First, upon assembly with the other three components of the protease complex, presenilin undergoes autoproteolysis (3, 9) within a large loop located between transmembrane domains 6 and 7 to form an N-terminal fragment (NTF) and C-terminal fragment (CTF) (10), resulting in activation of the enzyme for cleavage of substrates. FAD-mutant presenilins likewise undergo NTF/CTF formation, with one notable exception (Δexon9, which is active as a holoprotein (10)). Second, γ-secretase has endoproteolytic activity toward membrane stubs of APP and other substrates generated upon ectodomain release by sheddases (11). This cleavage occurs within the substrate transmembrane domain to release the intracellular domain. For APP, the endoproteolytic site (called the ε site) is located close to the

transmembrane/cytosolic boundary (Figure 2.1A) (12), with cleavage here releasing the APP intracellular domain (AICD). Reduction of ε cleavage is seen with many, although not all, FAD presenilin mutations (7, 13, 14).

In recent years, evidence has mounted in support of a third type of proteolytic function of the γ-secretase complex, a carboxypeptidase activity that trims membrane-associated long Aβ peptides of 48 or 49 residues to shorter secreted forms of 38-43 amino acids (15-19). Biochemical and cellular studies suggest that the endoproteolytic ε cleavage of APP substrate occurs first and that the resultant long Aβ peptides are primarily trimmed in intervals of three amino acids along two product lines (Figure 2.1A), with Aβ49 leading to Aβ46, Aβ43 and Aβ40 and Aβ48 leading to Aβ45, Aβ42 and Aβ38 (this last event removing a tetrapeptide). The expected tri- and tetrapeptide products have been detected by mass spectrometry (18). Despite the evidence, however, other studies suggest that Aβ and AICD production can be dissociated (20, 21) or that there is no precursor-product relationship between Aβ42 and Aβ38 (22, 23). The former contention has been disproven by the determination of equimolar Aβ and AICD production (24), and the latter has been unambiguously settled recently with the demonstration that synthetic Aβ42 is converted to Aβ38 by isolated γ-secretase (25).

In this study, we developed a method for examining the carboxypeptidase cleavage of synthetic Aβ48 and Aβ49 by isolated or purified enzyme complexes, independent of their initial formation through ε proteolysis of APP substrate. In so doing, we confirm that these long Aβ peptides are indeed intermediates towards Aβ40 and Aβ42, provide support for the dual-pathway model, and determine the degree to which long Aβ peptides contribute to the critical Aβ42-to-Aβ40 ratio. This biochemical system also allowed evaluation of the role of the membrane in the

Figure 2.1. γ-Secretase trims synthetic Aβ49 and Aβ48 to Aβ40 and Aβ42 *in vitro*. (A) APP substrate is thought to be cleaved sequentially by γ-secretase at the ε, ζ, and γ sites, indicated by arrowheads. These cleavage events result in Aβ peptides with the indicated C-termini. Ihara and co-workers (16, 18) have proposed Aβ40- and Aβ42-generating pathways (top and bottom, respectively), in which ε cleavage that produces AICD50-99 primarily leads to Aβ40, while ε cleavage that produces AICD49-99 mainly produces Aβ42. (B, C) Aβ40 and Aβ42 production from synthetic Aβ49 and Aβ48 and CHAPSO-solubilized membranes from CHO cells overexpressing the four γ-secretase components (B) or purified γ-secretase complexes reconstituted into lipid vesicles (C). Aβ40 and Aβ42 were detected using specific ELISAs. Assays were performed in triplicate, with control reactions as follows: + I reactions contain 1.5 μM γ-secretase inhibitor L-685,458; D1 reactions contain γ-secretase with an inactive D257A mutant PS1; boiled reactions contain heat-inactivated γ-secretase; γ reactions have no substrate added to the assay mixtures; and Aβ reactions have no enzyme added to the reaction mixtures. For all of the non-control reactions, the level of Aβ40 produced was significantly different than that of Aβ42 ($p<0.01$, Student's *t* test). n=3; error bars: S.D.

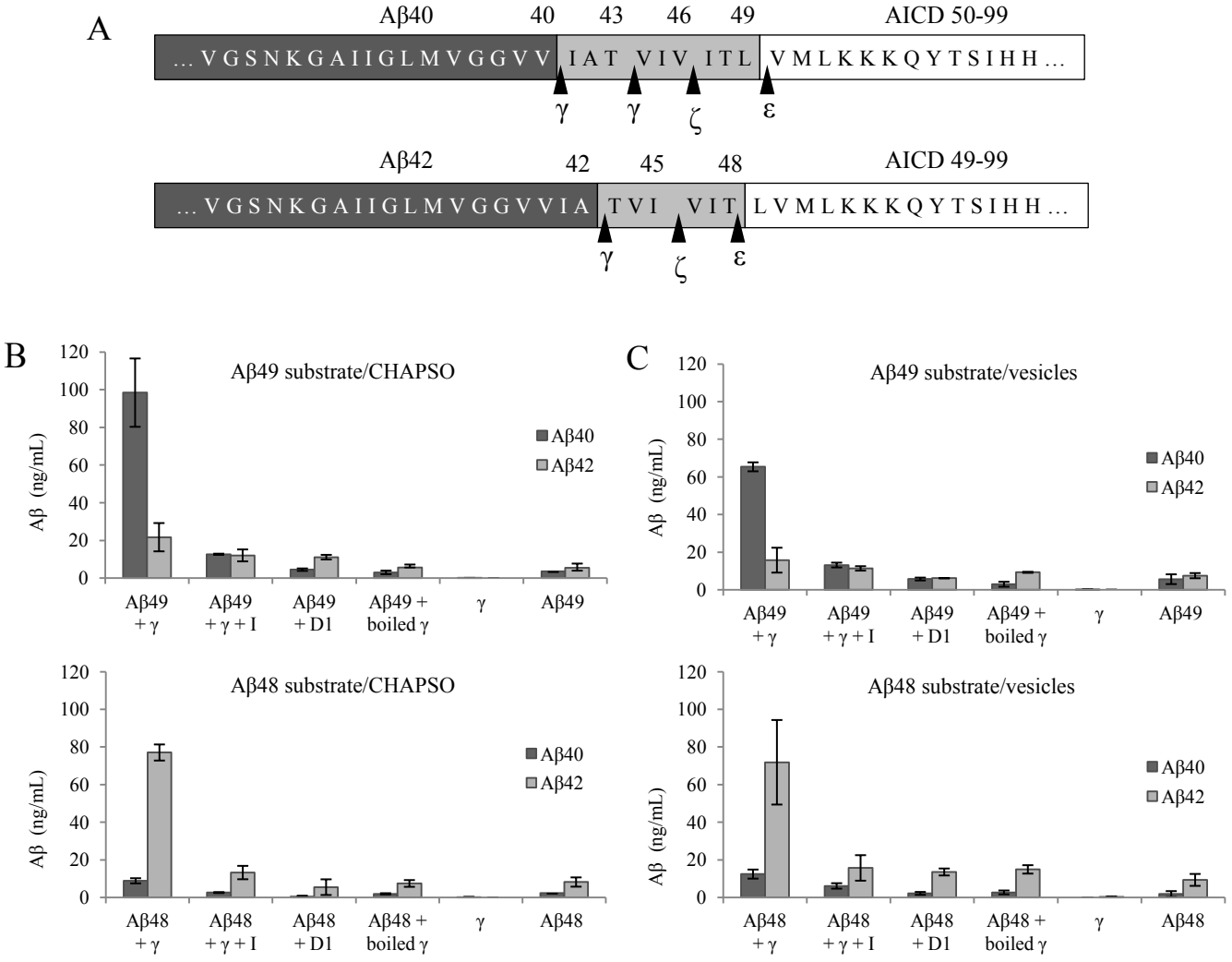

Figure 2.1 continued. γ-Secretase trims synthetic Aβ49 and Aβ48 to Aβ40 and Aβ42 *in vitro*.

carboxypeptidase activity. Most notably, kinetic analysis of Aβ40 and Aβ42 production from long Aβ peptides by FAD mutant presenilin-1/γ-secretase complexes revealed striking reductions in carboxypeptidase activity that have important implications for resolving the loss-of-function versus gain-of-function controversy and providing a unifying model for the pathogenic mechanism of presenilin mutations.

Experimental procedures

γ-Secretase preparations. CHAPSO-solubilized membranes from S20 cells, which are CHO cells overexpressing all four γ-secretase components, were prepared as previously described (26). Briefly, 20 confluent 15-cm plates were scraped and lysed using a French pressure cell at 1000 p.s.i. The lysate was spun at low speed to remove nuclei and unbroken cells, and then at 100,000 X *g*. The resulting membrane pellet was washed in sodium bicarbonate buffer and solubilized in 2 mL of 1% CHAPSO. For purified γ-secretase preparations, membranes from 160 confluent 15-cm plates of S20 cells were isolated, washed and solubilized as described above, and γ-secretase complexes were purified by sequential affinity purifications via Ni-NTA agarose beads (Sigma-Aldrich) and M2 immobilized anti-Flag agarose beads (Sigma-Aldrich). For the inactive mutant enzyme controls, both solubilized membranes and purified complexes were prepared from CHO D1 cells (overexpressing all four γ-secretase components, but with D257A mutant PS1 containing an N-terminal Myc tag) in the same way as above, except the first affinity purification step involved anti-Myc antibody agarose beads (Sigma-Aldrich). For the analysis of FAD PS1 mutant complexes, membranes were prepared from CHO cells overexpressing Pen2, Aph1, nicastrin, and either WT or mutant PS1 as previously reported (14).

For these preparations, membranes were isolated from 20 confluent 15-cm plates and resuspended in 160 μL of 1% CHAPSO.

γ-Secretase assays. For assays performed in CHAPSO (27), solubilized membranes were incubated with substrate in HEPES buffer at pH 7.0 with 0.1% phosphatidylcholine, 0.025% phosphatidylethanolamine, 0.00625% cholesterol, and a final CHAPSO concentration of 0.25%. For assays performed in vesicles (28), purified γ-secretase, 0.1% phosphatidylcholine, 0.025% phosphatidylethanolamine, 0.00625% cholesterol were solubilized in 0.25% CHAPSO and incubated with styrene-based Biobeads (Biorad) for 2 h at 4 °C to remove detergent. Substrate was added to the resulting detergent-solubilized preparations or proteoliposomes, followed by incubation at 37 °C. To validate trimming of long Aβ substrates, reactions were carried out for 4 h, which was within the time frame needed for maximal product formation; to analyze the rate of trimming by WT or FAD mutant PS1/γ-secretase and to examine the effects of modulators (GSM-1 (22) and compound 2 (29), obtained courtesy of T. Golde (U. Florida)) on the trimming process, reactions were carried out for 1.5 h, which was within the linear range of product formation. Synthetic, purified long Aβ substrates were purchased from Anaspec, and APP C100-FLAG substrate was prepared as previously described (27, 30). Aβ40 and Aβ42 generated from Aβ49-45 were detected using Aβ40- and Aβ42-specific ELISAs (Invitrogen).

Kinetic analysis. Samples of WT and FAD mutant membrane preparations were run on 4-12% Bis-Tris gels, followed by western blotting with mAb1563 (Millipore), which detects PS1 NTF. The signal was captured using ECL (GE Healthcare), densitometry was performed on the films using ImageQuant (GE Healthcare), and the amount of enzyme added to each reaction was normalized based on the measured level of PS1 NTF (or holoprotein in the case of the

uncleavable Δexon9). Time course experiments were first performed with the FAD mutants to establish the linear range of product formation. Reactions were then carried out with varying concentrations of substrate within this linear time frame. Aβ40 and Aβ42 products were quantified by specific ELISAs (Invitrogen), and non-linear regression analysis, with K_m and V_{max} determination, was performed using GraphPad Prism 4.

Cloning, cell culture, transfections and analysis. All CHO cell lines were grown in DMEM with 10% fetal bovine serum. For the analysis of long Aβ trimming in cells, APP truncated at residues 49 and 48 (Aβ numbering) and harboring the Swedish double mutation were cloned and expressed using the Tet-On system (Clontech). 100,000 CHO cells/well were seeded into 24-well plates. Upon reaching ~50% confluence, cells were transiently co-transfected with a 1:5 ratio of the pTet-On Advanced plasmid (Clontech) and a pTRE-Tight plasmid (Clontech) carrying the truncated APP sequence. Six h post-transfection, the medium was changed to DMEM complete containing 1μg/mL doxycycline to induce the expression of the truncated APP. Inhibitor control transfections were also treated with 10 μM DAPT at this time. After 24 h, cells and conditioned media were harvested. Aβ40 and Aβ42 in the media were measured by specific ELISAs (Meso Scale Discovery). Cells from each well were lysed in RIPA buffer, and the intracellular protein concentration was measured by BCA assay (Pierce). Western blot analysis for APPε49 and APPε48 in cell lysates was carried out using anti-APP antibody 22C11 (Millipore).

Statistical analysis. Comparisons of more than two groups were carried out using one-way analysis of variance (ANOVA) and Dunnett's post hoc test, using WT values as the control group. Statistical significance between two groups was determined by unpaired two-tailed Student's *t* test.

Results

γ-Secretase trims ε-site Aβ peptides to Aβ40 and Aβ42--We first examined the production of Aβ40 and Aβ42 from synthetic Aβ48 and Aβ49 *in vitro*, which allowed us to demonstrate the C-terminal trimming of ε-site Aβ peptides by γ-secretase using isolated enzyme and substrate. We could also directly examine the model that Aβ48 processing leads primarily to Aβ42 and Aβ49 primarily to Aβ40 (18). We performed these assays in CHAPSO detergent (27, 30) as well as with purified enzyme complexes reconstituted into lipid vesicles (28) to ensure that the results are not artifacts arising from detergent solubilization and to determine if the membrane is critical to the trimming process. We and others have previously described the use of urea polyacrylamide gel electrophoresis followed by western blotting with an N-terminally directed anti-Aβ antibody to detect the range of C-terminal variants of Aβ produced in *in vitro* γ-secretase reactions (7, 14, 17, 31). However, trimmed Aβ generated from the synthetic long Aβ substrates could not be detected by this method, because the signal from the excess substrate streaked throughout the lane, completely obscuring any signals from the Aβ products (data not shown). The levels of Aβ40 and Aβ42 produced from each synthetic long Aβ were instead quantified using specific ELISAs. The data reveal that Aβ48 and Aβ49 are indeed trimmed by γ-secretase to Aβ40 and Aβ42 in both the CHAPSO-solubilized (Figure 2.1B) and proteoliposome systems (Figure 2.1C). Control reactions with Aβ substrate alone (in which no enzyme was added to the reaction mixture) give the baseline levels of cross-reactivity of the large amounts of long Aβ substrates in the assays with each ELISA detection antibody. Although there is some cross-reactivity, the results indicate that the signal obtained in the reactions with enzyme present is not simply background. Furthermore, the addition of the γ-secretase transition-state analog inhibitor

L-685,458 to the assays results in inhibition of Aβ40 and Aβ42 production. Heat-inactivated or inactive PS1 D257A (D1) γ-secretase showed no Aβ production above background. In addition, no Aβ40 or Aβ42 was detected from solubilized membranes or proteoliposomes incubated without substrate, ensuring that the Aβ40 and Aβ42 produced is not due to cleavage of endogenous substrate present in the enzyme preparations. γ-Secretase modulators (GSMs) also had the effect on trimming that they typically have on Aβ production (32): levels of Aβ42 generated from Aβ48 and Aβ49 were decreased by two different GSMs (22, 29), whereas Aβ40 levels were not altered, providing further validation of C-terminal trimming by γ-secretase *in vitro* (Figure 2.2A and B). However, only the more potent GSM-1 compound showed a robust dose-response effect. Kinetic analysis of the levels of Aβ42 generated from APP C100FLAG and Aβ48 in the presence and absence of GSM-1 indicates that this modulator reduces the V_{max} in both cases and does not alter the K_m of these conversions (Figure 2.2C). This result is consistent with a recent report demonstrating that modulators increase the k_{cat} of Aβ42 conversion to Aβ38 (25).

The ratios of Aβ42 to Aβ40 produced from each Aβ substrate in each system (taking into account the background signal that each substrate alone has in each ELISA) are shown in Table 2.1 and indicate that γ-secretase cleavage of Aβ49 primarily leads to Aβ40, with an Aβ42/40 ratio of ~1:7, and cleavage of Aβ48 primarily leads Aβ42, with an Aβ42/40 ratio of ~9:1 in detergent and ~6:1 in vesicles (with no statistically significant differences in trimming between the CHAPSO and vesicle assays). These results are consistent with the model proposed by Ihara and co-workers of two pathways in which Aβ49 is primarily converted to Aβ40 and Aβ48 primarily to Aβ42 (18). We show that C-terminal trimming along these pathways is an inherent

Figure 2.2. γ-Secretase modulators lower Aβ42 produced from Aβ49 and Aβ48. Both GSM-1 and Rivkin-2 (compound 2 in ref. 29) have previously been shown to selectively lower Aβ42 levels and concomitantly increase Aβ38 levels (22, 29). (A) As expected, both compounds lower Aβ42 and increase Aβ38 in a concentration-dependent manner using APP C100-FLAG as substrate in CHAPSO-solubilized γ-secretase assays, as detected using a bicine/urea-polyacrylamide gel electrophoresis system. (B) Both compounds decreased the amount of Aβ42 generated from Aβ48 and Aβ49 without altering Aβ40 levels. n = 3; error bars: S.D. * indicate values that were significantly different from the Aβ42 value with no compound added ($p<0.05$). Aβ40 values were not significantly different at any concentration tested. (C) Cleavage reactions were performed in CHAPSO with the indicated concentrations of substrate. The levels of Aβ42 generated from C100-FLAG (left) or Aβ48 (right) were measured by ELISA. +GSM: reactions contained 25 μM GSM-1, -GSM: reactions with vehicle alone. V_{max} values for C100 and Aβ48 substrates were significantly reduced in the presence of GSM-1 ($p<0.05$, Student's *t* test). n=2; error: S.D.

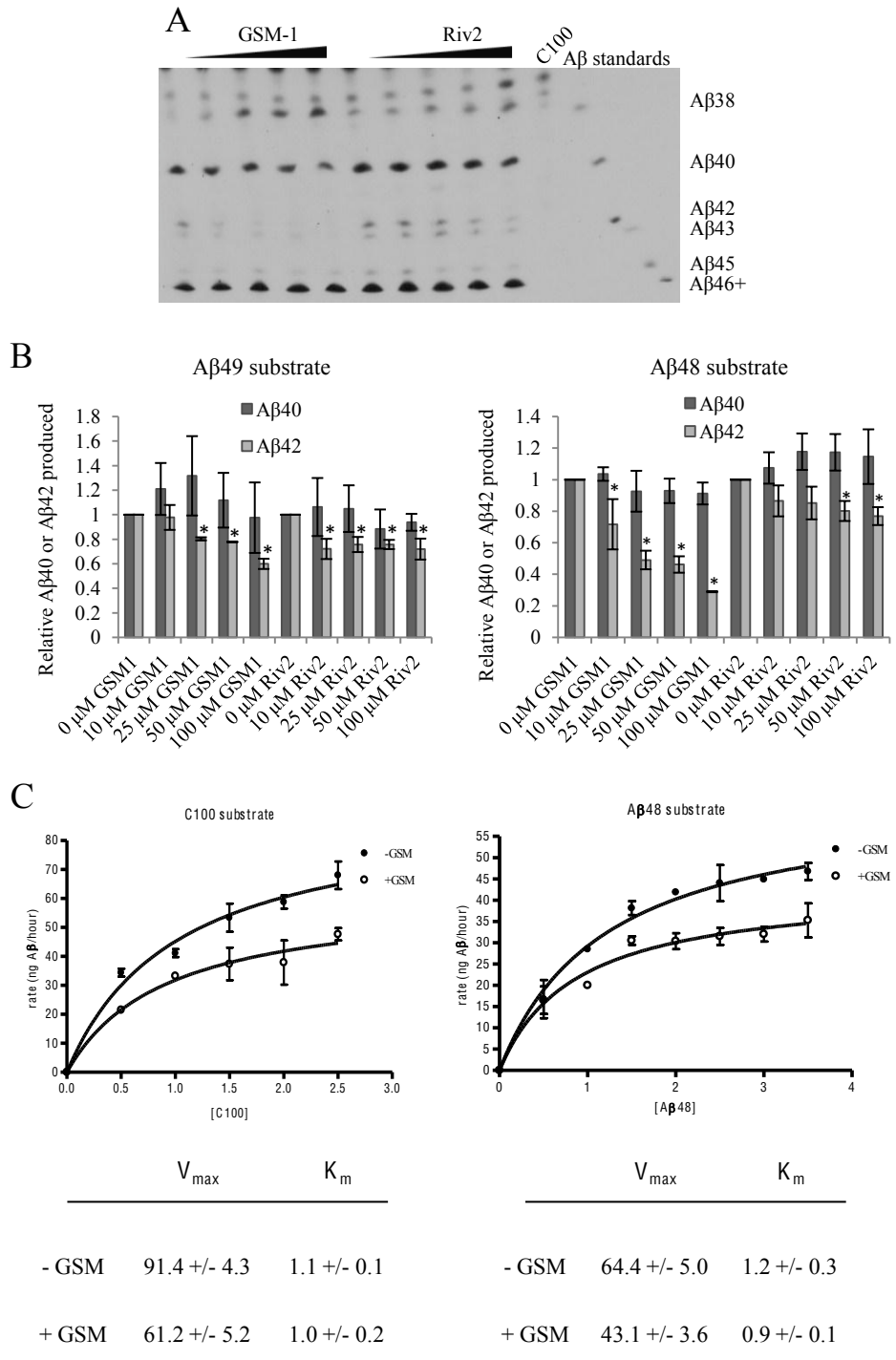

	V_{max}	K_m
- GSM	91.4 +/- 4.3	1.1 +/- 0.1
+ GSM	61.2 +/- 5.2	1.0 +/- 0.2

	V_{max}	K_m
- GSM	64.4 +/- 5.0	1.2 +/- 0.3
+ GSM	43.1 +/- 3.6	0.9 +/- 0.1

Figure 2.2 continued. γ-Secretase modulators lower Aβ42 produced from Aβ49 and Aβ48.

Table 2.1. Aβ42/Aβ40 ratios from trimming of ε- and ζ-cleaved Aβs. Ratios are calculated from the ELISA data in Figures 2.1 and 2.4. The background of each substrate in each ELISA (i.e. Aβ alone controls) was first subtracted. Error: S.D.

Conversion	Aβ45	Aβ46	Aβ48	Aβ49
CHAPSO	41 ± 2.4	0.14 ± 0.03	8.8 ± 1.1	0.14 ± 0.06
Vesicles	40 ± 10	0.18 ± 0.06	6.1 ± 1.4	0.14 ± 0.08

property of γ-secretase, whether it is solubilized in detergent or incorporated in a membrane, and also demonstrate that Aβ40 and Aβ42 can be produced by a small degree of crossover between the two pathways.

Although these results demonstrate the trimming of ε-site Aβ peptides *in vitro*, we nonetheless sought to validate our findings in a cellular assay. Previous studies have attempted to examine the trimming of Aβ49 and Aβ48 by γ-secretase in cells by direct expression of these long Aβs with a signal sequence (15). Although this system was used to demonstrate that Aβ49 expression primarily leads to Aβ40 secretion, the 1:1 ratio for Aβ42/40 observed from Aβ48 was inconclusive, as the levels of secreted Aβ were highly variable and apparently below the detection limits, likely due to the observed poor expression of Aβ48. Alternatively, APP truncated at position 49 (APPε49) can be expressed at high levels, inserted into the membrane and sorted to the cell surface (33). Moreover, APPε49 was processed by β- or α-secretase and then γ-secretase to generate quantifiable amounts of secreted Aβ or p3, an N-terminally truncated Aβ generated through α/γ-secretase cleavage. Therefore, we generated constructs for the expression of APPε49 and the previously unreported APPε48 and introduced them into CHO cells overexpressing all four γ-secretase components (14). Expression of these truncated APPs was confirmed by western blot of the cell lysates (Figure 2.3A), and the levels of p3/Aβ40 and p3/Aβ42 secreted into the media were measured by specific ELISAs (Figure 2.3B). We used 4G8, targeting the middle region of Aβ, as the detection antibody in the ELISA because it detects both p3 and Aβ, as secretion of Aβ alone from these cells was too low for quantification. The results confirm our *in vitro* findings, as APP49 expression primarily led to p3/Aβ40 secretion, and APP48 expression led mainly to p3/Aβ42 secretion. p3/Aβ production from each construct

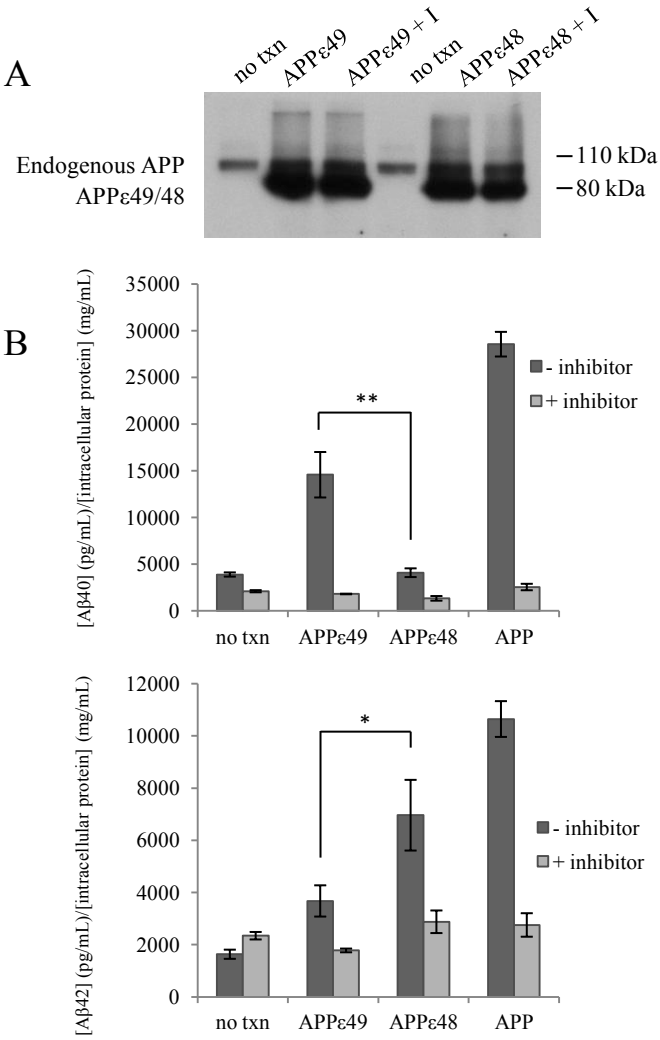

Figure 2.3. γ-Secretase trims p3/Aβ49 and p3/Aβ48 to p3/Aβ40 and p3/Aβ42 in cells. (A) The expression of APPε49 and APPε48 in CHO cells was confirmed by western blot of cell lysates using anti-APP antibody 22C11. The truncated APPs run slightly faster than full-length, endogenous APP. (B) p3/Aβ40 and p3/Aβ42 secretion by cells expressing APPε49, APPε48, or full-length APP. Untransfected controls (no txn) show the endogenous background signal from the cells; for + inhibitor transfections, cells were treated with 10 μM DAPT. *P<0.05, **p<0.01 (Student's *t* test). n = 3; error bars: S.E.M.

could be inhibited by the γ-secretase inhibitor DAPT. In principle, we could obtain Aβ42/40 ratios by subtracting the background observed from endogenous APP in untransfected cells; however, this may not be appropriate, as the overexpressed truncated APPs may compete with endogenous substrate for binding to secretases. The inability to accurately quantify ε-independent Aβ40 and Aβ42 production in this cellular system emphasizes the value of direct biochemical analysis with isolated or purified enzyme. In any event, whether production of p3/Aβ from endogenous substrate is completely inhibited or uninhibited by the overexpression, the conclusions about product preference (Aβ40 from APPε49 and Aβ42 from APPε48) still stand.

γ-Secretase trims ζ-cleaved Aβs to Aβ40 and Aβ42--We next explored the cleavage of synthetic ζ-site Aβs 45 and 46, as well as Aβ47, a long Aβ that is not naturally observed (Figure 2.4). Aβ45 and Aβ46 were also trimmed to Aβ40 and Aβ42 in a γ-secretase-dependent manner. In addition, the proportions of Aβ40 and Aβ42 generated from each long Aβ were again consistent with a dual pathway model: using Aβ46 as a substrate primarily resulted in Aβ40 production with an Aβ42/40 ratio of ~1:7, whereas Aβ45 led to Aβ42 almost exclusively, with a large Aβ42/40 ratio of ~40:1. A higher ratio of Aβ42/40 generated from Aβ45 than from Aβ48 is also consistent with the Ihara model, which posits only one cleavage event between Aβ45 and Aβ42. Importantly, we again found that the Aβ42/40 ratios from each substrate were the same in both the solubilized and proteoliposome systems (Table 2.1). These results consistently indicate that dual-pathway C-terminal trimming is an intrinsic property of γ-secretase and that the membrane is not essential for the enzyme to trim with apparent precision along these two pathways. We also attempted to confirm these results in cells by expressing APPε46 and APPε45 in the same CHO cell line that was used for APPε49 and APPε48 expression; however, we could

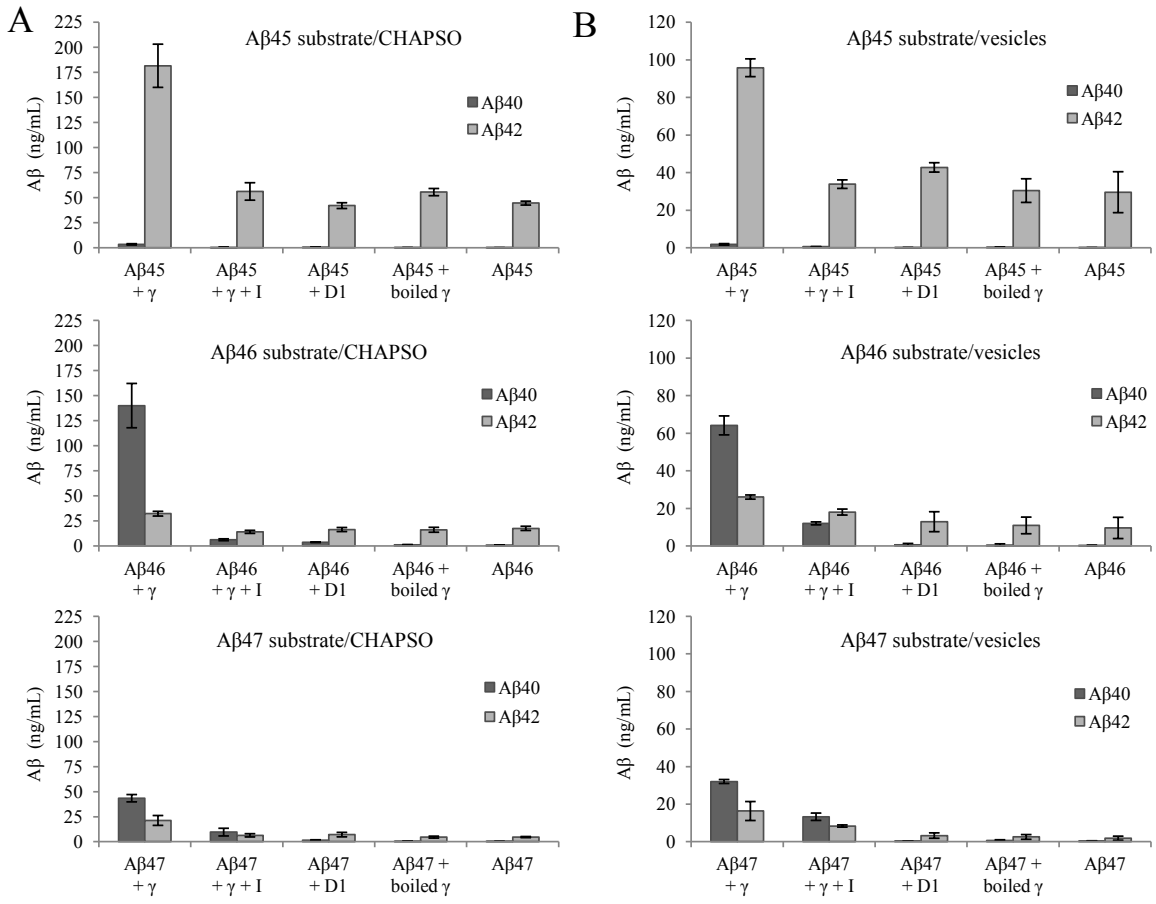

Figure 2.4. γ-Secretase trims synthetic Aβ45, Aβ 46, and Aβ47 to Aβ40 and Aβ42 *in vitro*. (A) Enzyme assays using CHAPSO-solubilized membranes from CHO cells overexpressing the four γ-secretase components. (B) Enzyme assays using purified γ-secretase complexes reconstituted into lipid vesicles. Control reactions are the same as in Figure 2.1. The level of Aβ40 generated in all non-control reactions was significantly different than that of Aβ42 ($p<0.01$ for Aβ45 and Aβ46 substrates, $p<0.05$ for Aβ47 substrate, Students *t* test). n=3; error bars: S.D

not detect an increase in the level of secreted p3/Aβ above endogenous background when these constructs were expressed, likely due to the inability of these truncated APPs to remain inserted in the membrane. With synthetic Aβ47 as a substrate for isolated γ-secretase, we found that the levels of Aβ40 and Aβ42 produced were substantially reduced compared with that seen with the natural long Aβ substrates. This is consistent with the fact that the expected major cleavage products of Aβ47 based on the Ihara model are Aβ44 and Aβ41, which, like Aβ47, are not naturally observed γ-secretase products.

C-terminal trimming by FAD-mutant γ-secretase--Having established a system to examine γ-secretase trimming of synthetic long Aβ from the ε to γ sites, we next examined the effects of FAD mutations in PS1 on this trimming process. To accomplish this, we determined the levels of Aβ40 and Aβ42 that five FAD-mutant PS1/γ-secretase complexes produced from Aβ49 and Aβ48 and their rates of formation compared with wild-type (WT) complexes. In this system, the levels of Aβ40 and Aβ42 generated are solely based on the efficiency of trimming, independent of effects on cleavage at the ε site (which could either alter the rate of ε site cleavage or the specificity of cleavage at positions 48 and 49). The PS1 mutations are G384A, Δexon9, L166P, A246E and L286V, and all except L286V have been previously shown to reduce the endoproteolytic cleavage at the ε site that leads to AICD production (14). However, all five mutations have been shown to generate an increased proportion of long Aβ peptides (Aβ42+) compared with WT enzyme (14). Membranes from CHO cells stably overexpressing the four γ-secretase components with either WT or mutant PS1 were solubilized in CHAPSO, and equal amounts of each enzyme were used in the reactions based on PS1 NTF levels (or PS1 holoprotein in the case of the uncleavable but proteolytically active Δexon9) in each enzyme

preparation. We first performed time course experiments to determine the linear range for Aβ40 and Aβ42 production from Aβ48 and Aβ49, followed by kinetic analysis of C-terminal trimming by each mutant. The rates of Aβ40 and Aβ42 production for each mutant were measured across different concentrations of substrate, and curves were generated for each possible conversion (Aβ49→Aβ40, Aβ49→Aβ42, Aβ48→Aβ40, and Aβ48→Aβ42) using non-linear regression analysis (Figure 2.5). The K_m and V_{max} values were then calculated from these curves (Table 2.2). Because each reaction contained equal amounts of enzyme, k_{cat} is proportional to V_{max}, and V_{max}/K_m is therefore a measure of catalytic efficiency (Table 2.2). When the efficiencies of these conversions by WT PS1 are set to 100% and compared to the efficiencies of the mutants (Table 2.3), all of the FAD mutant complexes displayed clear and substantial reduction of the normal carboxypeptidase trimming function of γ-secretase, with efficiencies ranging from 2-9% of WT for Aβ49 trimming, and from 17-40% of WT for Aβ48 trimming. The K_m and V_{max} values in Table 2.2 indicate that these reductions in trimming efficiencies are primarily the result of dramatic decreases in V_{max}, suggesting that the mutations affect the turnover of the long Aβs more than their affinity for the enzyme. Moreover, the trimming of these synthetic ε-cleaved Aβs was altered in ways that contribute to an increase in the Aβ42/Aβ40 ratio. First, as shown in Table 2.3, the trimming of Aβ49 to Aβ40 was significantly more reduced than the trimming of Aβ48 to Aβ42 by all of the mutant complexes when compared with WT. The catalytic efficiency values in Table 2.2 show that, while the WT enzyme trimmed Aβ49 to Aβ40 about 2.5 times more efficiently than Aβ48 to Aβ42, the Δexon9 and L286V complexes trimmed Aβ48 to Aβ42 more efficiently than Aβ49 to Aβ40, and the L166P, G384A and A246E complexes trimmed Aβ48 to Aβ42 with nearly equal efficiency as Aβ49 to Aβ40.

Figure 2.5. Aβ49 and Aβ48 conversions to Aβ40 and Aβ42 by γ-secretase are dramatically reduced by PS1 FAD mutations. (A) Equal amounts of each enzyme were used in the reactions, normalizing for PS1 NTF levels in each enzyme preparation based on densitometry of PS1 NTF western blots (or of full-length PS1 for the uncleaved but proteolytically active Δexon9 mutation). (B) Cleavage reactions with WT (top panels) or the indicated FAD-mutant PS1 (bottom panels) were carried out in CHAPSO with the indicated concentration of substrate. Left panels: Aβ49 substrate; right panels: Aβ48 substrate. Levels of Aβ40 (solid lines) and Aβ42 (dashed lines) were determined by ELISA, and data were fit using GraphPad prism 4 non-linear regression analysis. n= 3; error bars: S.E.M. Note the difference in scale for Aβ levels from WT (top panels) and FAD-mutant PS1 (bottom panels).

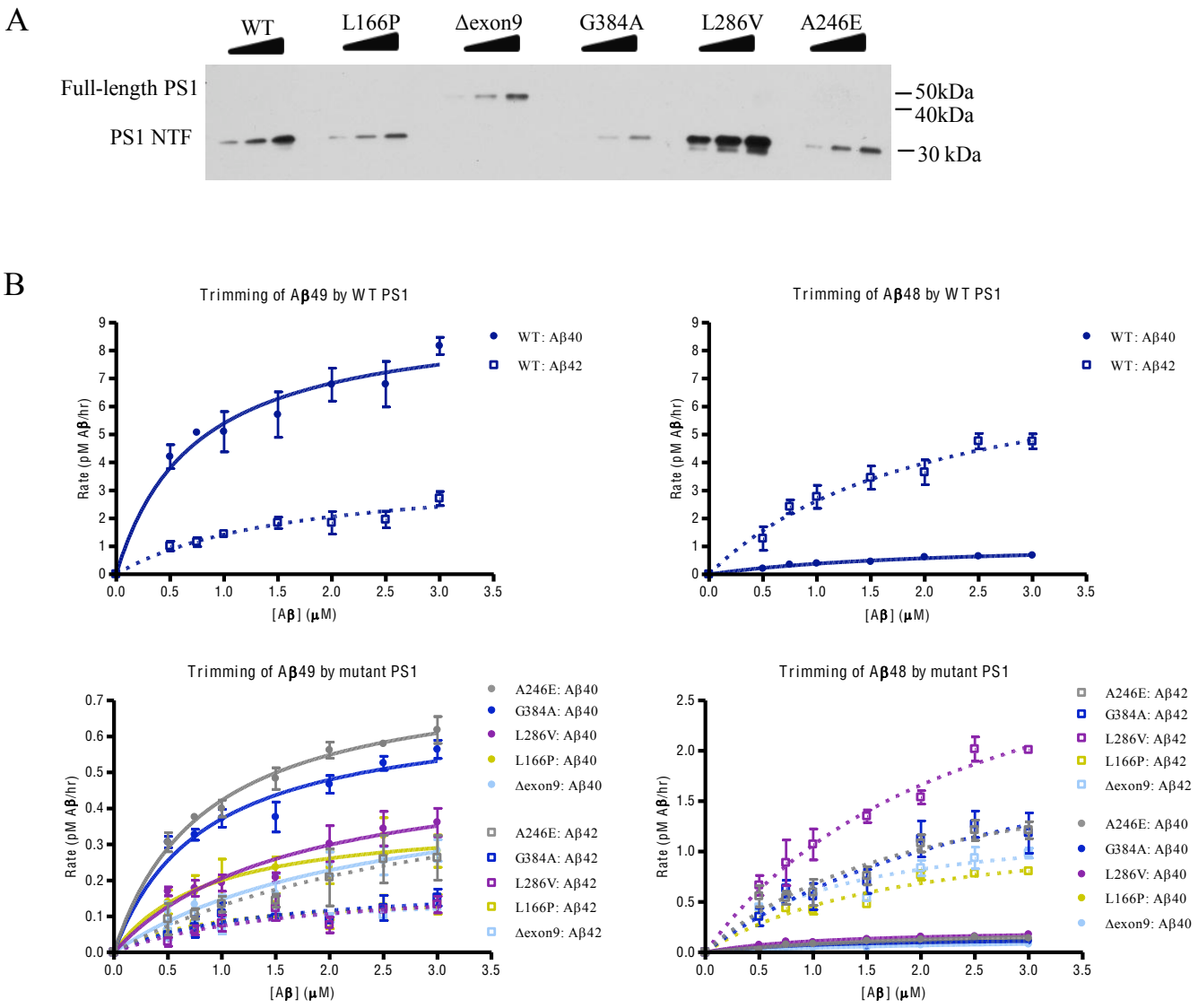

Figure 2.5 continued. Aβ49 and Aβ48 conversions to Aβ40 and Aβ42 by γ-secretase are dramatically reduced by PS1 FAD mutations.

Table 2.2. V_{max} and K_m of Aβ trimming events from WT and PS1 FAD-mutant γ-secretase. V_{max} and K_m values were calculated from the non-linear regression analyses in Figure 2.5. Equal amounts of enzyme were used in each reaction; therefore, K_{cat} is proportional to V_{max}, and V_{max}/K_m is a measure of catalytic efficiency. For all of the mutants, the V_{max} and catalytic efficiency values for each conversion were significantly lower than the values obtained with WT enzyme ($p<0.01$, one-way ANOVA and Dunnett's post test). No significant changes in K_m values were measured. n=3; error: S.D.

Table 2.2 continued. V_{max} and K_m of Aβ trimming events from WT and PS1 FAD-mutant γ-secretase.

Conversion	V_{max}	K_m	Catalytic efficiency
	pM/h	*μM*	V_{max}/K_m
Aβ49 →Aβ40			
WT	9.18 ± 0.70	0.84 ± 0.17	11.13 ± 2.03
L166P	0.35 ± 0.11	0.73 ± 0.33	0.50 ± 0.12
Δexon9	0.53 ± 0.13	2.56 ± 1.46	0.25 ± 0.12
G384A	0.74 ± 0.07	1.07 ± 0.49	0.75 ± 0.22
L286V	0.60 ± 0.30	2.10 ± 1.92	0.37 ± 0.20
A246E	0.79 ± 0.04	0.89 ± 0.34	0.94 ± 0.24
Aβ49 →Aβ42			
WT	3.83 ± 0.93	1.76 ± 0.53	2.21 ± 0.16
L166P	0.18 ± 0.05	1.02 ± 0.44	0.18 ± 0.03
Δexon9	0.17 ± 0.06	1.48 ± 0.42	0.17 ± 0.07
G384A	0.20 ± 0.01	1.45 ± 0.64	0.15 ± 0.08
L286V	0.22 ± 0.02	2.01 ± 1.15	0.13 ± 0.06
A246E	0.56 ± 0.25	3.06 ± 0.76	0.18 ± 0.04
Aβ48 →Aβ42			
WT	7.40 ± 0.08	1.85 ± 0.50	4.17 ± 0.95
L166P	1.49 ± 0.47	2.41 ± 1.58	0.70 ± 0.19
Δexon9	1.43 ± 0.29	1.50 ± 0.65	0.98 ± 0.27
G384A	2.59 ± 0.24	3.18 ± 0.80	0.83 ± 0.13
L286V	3.18 ± 0.02	2.05 ± 0.57	1.62 ± 0.44
A246E	2.13 ± 0.32	2.13 ± 0.15	1.00 ± 0.08
Aβ48 →Aβ40			
WT	1.07 ± 0.34	1.53 ± 0.49	0.70 ± 0.05
L166P	0.13 ± 0.02	1.18 ± 0.23	0.12 ± 0.04
Δexon9	0.17 ± 0.08	1.48 ± 0.42	0.11 ± 0.02
G384A	0.19 ± 0.06	1.20 ± 0.43	0.16 ± 0.01
L286V	0.22 ± 0.05	1.46 ± 0.01	0.15 ± 0.04
A246E	0.27 ± 0.04	2.24 ± 0.20	0.12 ± 0.01

Table 2.3. Catalytic efficiencies of trimming of Aβ49 and Aβ48 to Aβ40 and Aβ42 as a percent of WT PS1. Percentages are calculated from the catalytic efficiency values in Table 2.2. For all of the mutants, the values for each conversion were significantly lower than WT ($p<0.01$, one-way ANOVA and Dunnett's post test). In addition, all mutations resulted in a greater reduction of the trimming of Aβ49 to Aβ40 than Aβ48 to Aβ42 ($p<0.05$, Student's *t* test). For L166P and Δexon9, the conversion of Aβ49 to Aβ40 was more reduced than Aβ49 to Aβ42, and for L286V and Δexon9, the conversion of Aβ48 to 42 was less reduced than Aβ48 to Aβ40 ($p<0.05$, Students *t* test). Error: S.D.

Conversion	WT	L166P	Δexon9	G384A	L286V	A246E
Aβ49 →Aβ40	100	5 ± 1	2 ± 1	7 ± 1	4 ± 2	9 ± 1
Aβ49 →Aβ42	100	8 ± 1	7 ± 3	7 ± 3	6 ± 2	8 ± 2
Aβ48 →Aβ42	100	17 ± 1	23 ± 2	21 ± 9	40 ± 2	27 ± 5
Aβ48 →Aβ40	100	17 ± 4	16 ± 3	23 ± 2	21 ± 4	18 ± 2

In addition to these differences seen between the processing of Aβ49 and Aβ48, the L166P and Δexon9 mutations resulted in a significantly greater reduction of the major Aβ49 to Aβ40 conversion compared with the crossover Aβ49 to Aβ42 conversion, and the Δexon9 and L286V mutations led to a greater reduction of the crossover Aβ48 to Aβ40 conversion compared to the major Aβ48 to Aβ42 conversion (Table 2.3).

We also attempted to examine the effects of FAD mutations on the trimming of ζ-site Aβs (Aβ46 and Aβ45) in an effort to determine if a specific step in the trimming process is reduced more than others. However, due to the high background that the Aβ45 and Aβ46 substrates have in the Aβ42 ELISA (Figure 2.4), we were not able to detect any Aβ42 signal above background when we attempted to monitor the rates of trimming of these substrates by the FAD mutants (data not shown). In addition, due to the low efficiency of the conversion of Aβ45 to Aβ40 (Figure 2.4), we were unable to detect any Aβ40 production from Aβ45 by the mutants (data not shown). We were, however, able to quantitate the trimming of Aβ46 to Aβ40. When compared with wild type, each mutant showed a substantial reduction of the rate of Aβ46 conversion to Aβ40 (Table 2.4). Moreover, these low rates of Aβ46 trimming by the mutants were comparable to those observed for Aβ49 (Table 2.4), suggesting that the individual cleavage step from Aβ49 to Aβ46 is not one that is significantly impaired by the FAD mutations.

FAD mutant complexes increase Aβ42/40 from a fixed Aβ49/48 mixture-- Some FAD mutations in PS1 have been shown to lead to an increased proportion of ε site cleavage at Aβ48 compared with cleavage at Aβ49 than is seen for WT PS1 (34). Because, as we have demonstrated above, Aβ48 is the ε product that primarily leads to Aβ42, this alteration in the ε

Table 2.4. Rate of trimming of Aβ46 and Aβ49 to Aβ40 as a percent of WT PS1. The rates of trimming (ng Aβ/hr) of 1 μM Aβ46 and Aβ49 were measured by ELISA. For both conversions, the values for the mutants were significantly lower than wildtype ($p<0.01$, one-way ANOVA and Dunnett's post test). n=3; error: S.D.

Conversion	WT	L166P	Δexon9	G384A	L286V	A246E
Aβ46 →Aβ40	100	1.2 ± 0.2	1.4 ± 0.2	0.7 ± 0.2	2.3 ± 0.2	5.1 ± 1.6
Aβ49 →Aβ40	100	3.8 ± 0.7	2.9 ± 0.3	0.8 ± 0.6	3.7 ± 0.5	11.5 ± 3.8

cleavage site is one mechanism by which these mutations may increase Aβ42/40. However, not all FAD PS1 mutations have this effect (35), and our data suggest that the more substantial reduction in the efficiency of trimming of Aβ49 to Aβ40 compared to that of Aβ48 to Aβ42 by the FAD mutant complexes should be sufficient to increase the Aβ42/40 ratio, regardless of effects on the specificity of ε site cleavage. We measured the levels of Aβ42 and Aβ40 generated from a fixed mixture of Aβ49 and Aβ48, with 70% Aβ49 and 30% Aβ48, as this has been shown to be the normal proportions generated from WT PS1 γ-secretase complexes (34). The Aβ42/40 ratios generated by isolated WT and mutant γ-secretase complexes are shown in Figure 2.6. The ratios for the mutant complexes are 2- to 4-fold higher than the ratio generated by the WT complex, suggesting that the differential reduction in the rates of trimming of each substrate associated with each FAD mutant alone, independent of ε proteolysis, can indeed increase the Aβ42/40 ratio.

Discussion

Our findings have important implications for the normal biochemical function of the γ-secretase complex as well as for the mechanism of pathogenesis of FAD presenilin mutations. First, we demonstrate that the carboxypeptidase activity is an intrinsic function of the enzyme, independent of the membrane. Synthetic Aβ peptides of 45-49 amino acids in length were converted to Aβ40 and Aβ42 in a γ-secretase-dependent manner, whether the enzyme was isolated from membranes and detergent-solubilized or purified and reconstituted into lipid vesicles. Little or no difference in the ratio of Aβ42/Aβ40 was seen between detergent-solubilized and membrane-incorporated protease complexes. Our results are consistent with the

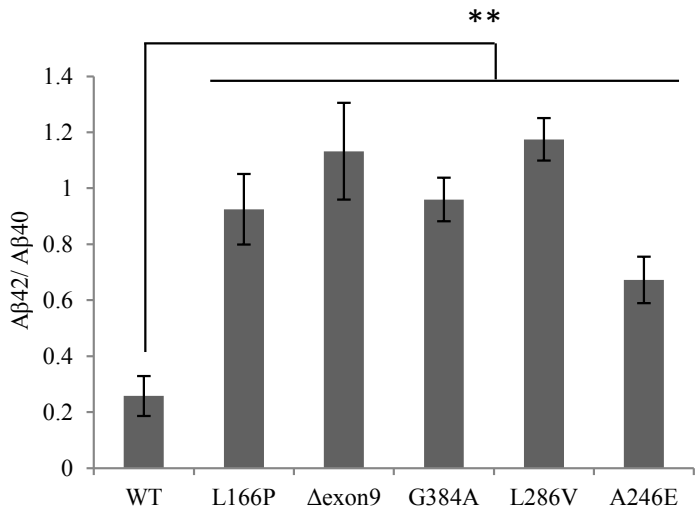

Figure 2.6. FAD-mutant PS1/γ-secretase complexes increase Aβ42/40 independent of effects on ε site endoproteolysis. Aβ42/40 ratios generated in *in vitro* γ-secretase assays with either WT or the indicated FAD-mutant PS1 from a 70:30 mixture of Aβ49/48 (similar to what is observed normally from APP). **p<0.01 (one-way ANOVA and Dunnett's post test). n= 3; error bars: S.D.

model that Aβ48 and Aβ49, formed upon initial ε endoproteolysis by γ-secretase, are intermediates toward Aβ40 and Aβ42.

Second, our results are completely consistent with the dual-pathway model originally hypothesized by Ihara and co-workers, in which Aβ49→Aβ46→Aβ43→Aβ40 and Aβ48→Aβ45→Aβ42→Aβ38 (16, 18). Aβ49 substrate resulted in Aβ40 along with a small level of Aβ42, and Aβ48 gave Aβ42 as well as some Aβ40. Nevertheless, the production of Aβ42 from Aβ49 and Aβ40 from Aβ48 reveals that crossover between the two pathways does occur to some degree, and therefore these crossover pathways contribute to the overall Aβ42-to-Aβ40 ratio. In addition, Aβ46 trimming results in Aβ40 in high preference to Aβ42, and Aβ45 is cleaved to Aβ42 to the virtual exclusion of Aβ40, again consistent with the dual-pathway model. Interestingly, use of Aβ47 as substrate resulted in only small degrees of conversion to either Aβ40 or Aβ42. This peptide, along with its expected trimmed products Aβ44 and Aβ41, is virtually absent in analyses of Aβ from *in vitro* γ-secretase assays, cell culture or brain tissue. The corresponding tripeptide intermediates have also not been detected (18). Further study of Aβ47 is needed to determine if Aβ44 and Aβ41 are indeed produced as expected.

Most importantly, we uncovered a surprising and striking effect of PS1 FAD mutations on the carboxypeptidase function of the γ-secretase complex. Our biochemical system provided a means to study trimming by these mutant complexes independently of ε proteolysis. All mutant complexes that we examined, located in different regions of PS1 and associated with average ages of onset from 24 to 53 years displayed dramatic reductions in rates of conversion of Aβ49 and Aβ48 to Aβ40 and Aβ42. Most unexpectedly, the rates of Aβ49 conversion to Aβ40 with the PS1 mutants were extremely low, with catalytic efficiencies 2-9% that of wild-type

enzyme. These relative conversion rates of Aβ49 to Aβ40 by the PS1 mutants were much lower than those seen from Aβ48 to Aβ42, which gave catalytic efficiencies ranging from 17 to 40% that of wild-type enzyme. As Aβ49 is the major ε cleavage product leading to Aβ40 (34), this difference in FAD-mutant PS1/γ-secretase in handling Aβ49 and Aβ48 leads to increased Aβ42/Aβ40, primarily through reduction in Aβ40.

Differences were also revealed in the rates of Aβ49 conversion to Aβ40 and Aβ42, as the crossover conversion of Aβ49 to Aβ42 was not decreased as much as its primary conversion to Aβ40 for two of the PS1 mutations (L166P and Δexon9). Moreover, the crossover conversion of Aβ48 to Aβ40 was decreased more than the major conversion to Aβ42 for two PS1 mutations (L286V and Δexon9). These effects, while minor in comparison to the overall difference in handling between Aβ49 and Aβ48, likewise contribute to net increases in Aβ42/Aβ40. Interestingly, some (34), but not all (35), PS1 mutations have been reported to shift ε cleavage to increase AICD51-99 versus AICD50-99, the other products generated along with Aβ48 and Aβ49, respectively (Figure 2.1). Shifting ε cleavage toward Aβ48 in this way would also increase Aβ42/Aβ40. Finally, a new report showed that PS1 FAD mutations can also slow the conversion of Aβ42 to Aβ38 (25). Thus, multiple effects of PS1 FAD mutations all conspire to raise Aβ42/Aβ40.

Despite these multiple effects, the most striking and consistent change is the decreased carboxypeptidase trimming of ε cleavage products Aβ48 and Aβ49 to Aβ40 and Aβ42, most particularly the dramatic reduction in the Aβ49 (or Aβ46) to Aβ40 conversion. This loss, while not complete, is severe and clearly leads to increases in Aβ42/Aβ40 by virtue of reducing Aβ40 formation, providing a simple reconciliation of the loss-of-function versus gain-of-function

controversy. These mutations do cause a loss of function: a specific loss of carboxypeptidase function, particularly the ability to trim Aβ49 or Aβ46 to Aβ40. Our findings are consistent with recent reports suggesting that FAD-mutant presenilins can cause a reduction in the conversion of Aβ43 and Aβ42 to Aβ40 and Aβ38 (7, 25). This loss of carboxypeptidase function results in a gain of function: the elevation of the critical Aβ42/Aβ40, thereby increasing the propensity of Aβ to aggregation and neurotoxicity (36). It should be noted that this specific loss of function also elevates longer Aβ peptides (7, 14), and that the gain of neurotoxic function may be through these forms of Aβ. Investigation of this possibility is, therefore, warranted and currently underway.

Abbreviations-- Aβ, amyloid β-peptide; AD, Alzheimer's disease; AICD, amyloid β-protein precursor intracellular domain; APP, amyloid β-protein precursor; CTF, C-terminal fragment; NTF, N-terminal fragment; FAD, familial Alzheimer's disease; GSM, γ-secretase modulator; CHAPSO, 3-[(3-cholamidopropyl)dimethylammonio]-2-hydroxymethyl)propane- 1,3-diol; ANOVA, analysis of variance; D1, PS1 D257A; Bicine, N,N-bis(2-hydroxyethyl)glycine; DAPT, N-[N-(3,5-difluorophenacetyl)-L-alanyl]-S-phenylglycine t-butyl ester; WT, wildtype

Acknowledgements-- We thank colleague O. Holmes for CHO D1 cells expressing γ-secretase with the inactive PS1 D257A mutation and T. Golde (University of Florida) for γ-secretase modulators GSM-1 and Riv2.

References

1. Goedert, M., and Spillantini, M. G. (2006) A century of Alzheimer's disease. *Science* **314**, 777-781

2. Tanzi, R. E., and Bertram, L. (2005) Twenty years of the Alzheimer's disease amyloid hypothesis: a genetic perspective. *Cell* **120**, 545-555

3. Wolfe, M. S., Xia, W., Ostaszewski, B. L., Diehl, T. S., Kimberly, W. T., and Selkoe, D. J. (1999) Two transmembrane aspartates in presenilin-1 required for presenilin endoproteolysis and γ-secretase activity. *Nature* **398**, 513-517

4. Shen, J., and Kelleher, R. J., 3rd. (2007) The presenilin hypothesis of Alzheimer's disease: evidence for a loss-of-function pathogenic mechanism. *Proc Natl Acad Sci U S A* **104**, 403-409

5. De Strooper, B. (2007) Loss-of-function presenilin mutations in Alzheimer disease. Talking Point on the role of presenilin mutations in Alzheimer disease. *EMBO Rep* **8**, 141-146

6. Wolfe, M. S. (2007) When loss is gain: reduced presenilin proteolytic function leads to increased Abeta42/Abeta40. Talking Point on the role of presenilin mutations in Alzheimer disease. *EMBO Rep* **8**, 136-140

7. Chavez-Gutierrez, L., Bammens, L., Benilova, I., Vandersteen, A., Benurwar, M., Borgers, M., Lismont, S., Zhou, L., Van Cleynenbreugel, S., Esselmann, H., Wiltfang, J., Serneels, L., Karran, E., Gijsen, H., Schymkowitz, J., Rousseau, F., Broersen, K., and De Strooper, B. (2012) The mechanism of gamma-secretase dysfunction in familial Alzheimer disease. *EMBO J* **31**, 2261-2274

8. Heilig, E. A., Gutti, U., Tai, T., Shen, J., and Kelleher, R. J., 3rd. (2013) Trans-dominant negative effects of pathogenic PSEN1 mutations on gamma-secretase activity and Abeta production. *J Neurosci* **33**, 11606-11617

9. Fukumori, A., Fluhrer, R., Steiner, H., and Haass, C. (2010) Three-amino acid spacing of presenilin endoproteolysis suggests a general stepwise cleavage of gamma-secretase-mediated intramembrane proteolysis. *J Neurosci* **30**, 7853-7862

10. Thinakaran, G., Borchelt, D. R., Lee, M. K., Slunt, H. H., Spitzer, L., Kim, G., Ratovitsky, T., Davenport, F., Nordstedt, C., Seeger, M., Hardy, J., Levey, A. I., Gandy, S. E., Jenkins, N. A., Copeland, N. G., Price, D. L., and Sisodia, S. S. (1996) Endoproteolysis of presenilin 1 and accumulation of processed derivatives in vivo. *Neuron* **17**, 181-190

11. Haapasalo, A., and Kovacs, D. M. (2011) The many substrates of presenilin/gamma-secretase. *J Alzheimers Dis* **25**, 3-28

12. Weidemann, A., Eggert, S., Reinhard, F. B., Vogel, M., Paliga, K., Baier, G., Masters, C. L., Beyreuther, K., and Evin, G. (2002) A Novel var epsilon-Cleavage within the Transmembrane Domain of the Alzheimer Amyloid Precursor Protein Demonstrates Homology with Notch Processing. *Biochemistry* **41**, 2825-2835.

13. Song, W., Nadeau, P., Yuan, M., Yang, X., Shen, J., and Yankner, B. A. (1999) Proteolytic release and nuclear translocation of Notch-1 are induced by presenilin-1 and impaired by pathogenic presenilin-1 mutations. *Proc Natl Acad Sci U S A* **96**, 6959-6963

14. Quintero-Monzon, O., Martin, M. M., Fernandez, M. A., Cappello, C. A., Krzysiak, A. J., Osenkowski, P., and Wolfe, M. S. (2011) Dissociation between the processivity and total activity of gamma-secretase: implications for the mechanism of Alzheimer's disease-causing presenilin mutations. *Biochemistry* **50**, 9023-9035

15. Funamoto, S., Morishima-Kawashima, M., Tanimura, Y., Hirotani, N., Saido, T. C., and Ihara, Y. (2004) Truncated carboxyl-terminal fragments of beta-amyloid precursor protein are processed to amyloid beta-proteins 40 and 42. *Biochemistry* **43**, 13532-13540

16. Qi-Takahara, Y., Morishima-Kawashima, M., Tanimura, Y., Dolios, G., Hirotani, N., Horikoshi, Y., Kametani, F., Maeda, M., Saido, T. C., Wang, R., and Ihara, Y. (2005) Longer forms of amyloid beta protein: implications for the mechanism of intramembrane cleavage by gamma-secretase. *J Neurosci* **25**, 436-445

17. Yagishita, S., Morishima-Kawashima, M., Ishiura, S., and Ihara, Y. (2008) Abeta46 is processed to Abeta40 and Abeta43, but not to Abeta42, in the low density membrane domains. *J Biol Chem* **283**, 733-738

18. Takami, M., Nagashima, Y., Sano, Y., Ishihara, S., Morishima-Kawashima, M., Funamoto, S., and Ihara, Y. (2009) gamma-Secretase: successive tripeptide and tetrapeptide release from the transmembrane domain of beta-carboxyl terminal fragment. *J Neurosci* **29**, 13042-13052

19. Zhao, G., Cui, M. Z., Mao, G., Dong, Y., Tan, J., Sun, L., and Xu, X. (2005) gamma-Cleavage is dependent on zeta-cleavage during the proteolytic processing of amyloid precursor protein within its transmembrane domain. *J Biol Chem* **280**, 37689-37697

20. Chen, F., Hasegawa, H., Schmitt-Ulms, G., Kawarai, T., Bohm, C., Katayama, T., Gu, Y., Sanjo, N., Glista, M., Rogaeva, E., Wakutani, Y., Pardossi-Piquard, R., Ruan, X., Tandon, A., Checler, F., Marambaud, P., Hansen, K., Westaway, D., St George-Hyslop, P., and

Fraser, P. (2006) TMP21 is a presenilin complex component that modulates gamma-secretase but not epsilon-secretase activity. *Nature* **440**, 1208-1212

21. He, G., Luo, W., Li, P., Remmers, C., Netzer, W. J., Hendrick, J., Bettayeb, K., Flajolet, M., Gorelick, F., Wennogle, L. P., and Greengard, P. (2010) Gamma-secretase activating protein is a therapeutic target for Alzheimer's disease. *Nature* **467**, 95-98

22. Page, R. M., Baumann, K., Tomioka, M., Perez-Revuelta, B. I., Fukumori, A., Jacobsen, H., Flohr, A., Luebbers, T., Ozmen, L., Steiner, H., and Haass, C. (2008) Generation of Abeta38 and Abeta42 is independently and differentially affected by familial Alzheimer disease-associated presenilin mutations and gamma-secretase modulation. *J Biol Chem* **283**, 677-683

23. Czirr, E., Cottrell, B. A., Leuchtenberger, S., Kukar, T., Ladd, T. B., Esselmann, H., Paul, S., Schubenel, R., Torpey, J. W., Pietrzik, C. U., Golde, T. E., Wiltfang, J., Baumann, K., Koo, E. H., and Weggen, S. (2008) Independent generation of Abeta42 and Abeta38 peptide species by gamma-secretase. *J Biol Chem* **283**, 17049-17054

24. Kakuda, N., Funamoto, S., Yagishita, S., Takami, M., Osawa, S., Dohmae, N., and Ihara, Y. (2006) Equimolar production of amyloid beta-protein and amyloid precursor protein intracellular domain from beta-carboxyl-terminal fragment by gamma-secretase. *J Biol Chem* **281**, 14776-14786

25. Okochi, M., Tagami, S., Yanagida, K., Takami, M., Kodama, T. S., Mori, K., Nakayama, T., Ihara, Y., and Takeda, M. (2013) gamma-secretase modulators and presenilin 1 mutants act differently on presenilin/gamma-secretase function to cleave Abeta42 and Abeta43. *Cell Rep* **3**, 42-51

26. Cacquevel, M., Aeschbach, L., Osenkowski, P., Li, D., Ye, W., Wolfe, M. S., Li, H., Selkoe, D. J., and Fraering, P. C. (2008) Rapid purification of active gamma-secretase, an intramembrane protease implicated in Alzheimer's disease. *J Neurochem* **104**, 210-220

27. Kimberly, W. T., Esler, W. P., Ye, W., Ostaszewski, B. L., Gao, J., Diehl, T., Selkoe, D. J., and Wolfe, M. S. (2003) Notch and the amyloid precursor protein are cleaved by similar gamma-secretase(s). *Biochemistry* **42**, 137-144.

28. Osenkowski, P., Ye, W., Wang, R., Wolfe, M. S., and Selkoe, D. J. (2008) Direct and potent regulation of gamma-secretase by its lipid microenvironment. *J Biol Chem* **283**, 22529-22540

29. Rivkin, A., Ahearn, S. P., Chichetti, S. M., Hamblett, C. L., Garcia, Y., Martinez, M., Hubbs, J. L., Reutershan, M. H., Daniels, M. H., Siliphaivanh, P., Otte, K. M., Li, C., Rosenau, A., Surdi, L. M., Jung, J., Hughes, B. L., Crispino, J. L., Nikov, G. N.,

Middleton, R. E., Moxham, C. M., Szewczak, A. A., Shah, S., Moy, L. Y., Kenific, C. M., Tanga, F., Cruz, J. C., Andrade, P., Angagaw, M. H., Shomer, N. H., Miller, T., Munoz, B., and Shearman, M. S. (2010) Purine derivatives as potent gamma-secretase modulators. *Bioorg Med Chem Lett* **20**, 2279-2282

30. Li, Y. M., Lai, M. T., Xu, M., Huang, Q., DiMuzio-Mower, J., Sardana, M. K., Shi, X. P., Yin, K. C., Shafer, J. A., and Gardell, S. J. (2000) Presenilin 1 is linked with gamma -secretase activity in the detergent solubilized state. *Proc Natl Acad Sci U S A* **97**, 6138-6143

31. Shimojo, M., Sahara, N., Mizoroki, T., Funamoto, S., Morishima-Kawashima, M., Kudo, T., Takeda, M., Ihara, Y., Ichinose, H., and Takashima, A. (2008) Enzymatic characteristics of I213T mutant presenilin-1/gamma-secretase in cell models and knock-in mouse brains: familial Alzheimer disease-linked mutation impairs gamma-site cleavage of amyloid precursor protein C-terminal fragment beta. *J Biol Chem* **283**, 16488-16496

32. Golde, T. E., Koo, E. H., Felsenstein, K. M., Osborne, B. A., and Miele, L. (2013) gamma-Secretase inhibitors and modulators. *Biochim Biophys Acta* **1828**, 2898-2907

33. Lefranc-Jullien, S., Sunyach, C., and Checler, F. (2006) APPepsilon, the epsilon-secretase-derived N-terminal product of the beta-amyloid precursor protein, behaves as a type I protein and undergoes alpha-, beta-, and gamma-secretase cleavages. *J Neurochem* **97**, 807-817

34. Sato, T., Dohmae, N., Qi, Y., Kakuda, N., Misonou, H., Mitsumori, R., Maruyama, H., Koo, E. H., Haass, C., Takio, K., Morishima-Kawashima, M., Ishiura, S., and Ihara, Y. (2003) Potential link between amyloid beta-protein 42 and C-terminal fragment gamma 49-99 of beta-amyloid precursor protein. *J Biol Chem* **278**, 24294-24301.

35. Mori, K., Okochi, M., Tagami, S., Nakayama, T., Yanagida, K., Kodama, T. S., Tatsumi, S., Fujii, K., Tanimukai, H., Hashimoto, R., Morihara, T., Tanaka, T., Kudo, T., Funamoto, S., Ihara, Y., and Takeda, M. (2010) The production ratios of AICDepsilon51 and Abeta42 by intramembrane proteolysis of betaAPP do not always change in parallel. *Psychogeriatrics* **10**, 117-123

36. Kuperstein, I., Broersen, K., Benilova, I., Rozenski, J., Jonckheere, W., Debulpaep, M., Vandersteen, A., Segers-Nolten, I., Van Der Werf, K., Subramaniam, V., Braeken, D., Callewaert, G., Bartic, C., D'Hooge, R., Martins, I. C., Rousseau, F., Schymkowitz, J., and De Strooper, B. (2010) Neurotoxicity of Alzheimer's disease Abeta peptides is induced by small changes in the Abeta42 to Abeta40 ratio. *Embo J* **29**, 3408-3420

Chapter 3:

Transmembrane substrate determinants for γ-secretase processing of APP CTFβ

Authors: Marty A. Fernandez, Kelly Biette, Georgia Dolios, Rong Wang, and Michael S. Wolfe

Contributors: This project was designed by M.A.F. and M.S.W. G.D. and R.W. performed mass spectrometry analysis, and K.B. assisted with analyses of helical mutant substrates. All other experiments were carried out by M.A.F.

Abstract

The amyloid beta-peptide (Aβ), thought to play a central role in the pathogenesis of Alzheimer's disease (AD), is generated by proteolysis of the C-terminal fragment of the amyloid β protein-precursor, known as APP CTFβ, by the γ-secretase complex. γ-secretase cleavage of CTFβ generates a range of Aβ products of 38-49 residues. Evidence suggests that this spectrum of Aβs is the result of successive γ-secretase cleavages, with endoproteolysis first occurring at the ε sites to generate Aβ48 or Aβ49, followed by C-terminal trimming mostly every three residues along two product lines to generate shorter, secreted forms of Aβ: the primary Aβ49-46-43-40 line and a minor Aβ48-45-42-38 line. The major secreted Aβ species are Aβ40 and Aβ42, and an increased level of the longer, aggregation-prone Aβ42 compared to Aβ40 is widely thought to be important in AD pathogenesis. We examined substrate determinants of the specificity and efficiency of ε site endoproteolysis and carboxypeptidase trimming of CTFβ by γ-secretase. We found that the C-terminal charge of the long intermediate Aβ49 does not play a role in its trimming by γ-secretase every three residues. Peptidomimetic probes suggest that γ-secretase has S1', S2', and S3' pockets, through which trimming by tripeptides may be determined. However, deletion of residues around the ε sites demonstrates that a depth of three residues within the transmembrane domain is not a determinant of the location of endoproteolytic cleavage of CTFβ. We also show that instability of the CTFβ transmembrane helix near the ε site significantly increases endoproteolysis, and that instability near the carboxypeptidase cleavage sites facilitates C-terminal trimming by γ-secretase. Taken together, these results enhance our understanding of how γ-secretase cleaves and trims CTFβ to generate the Aβ peptides implicated in AD.

Introduction

The production and aggregation of the amyloid β-peptide (Aβ) is thought to initiate the pathogenesis of Alzheimer's disease (AD) (Hardy and Selkoe, 2002). Aβ is generated by successive proteolysis of the amyloid β-protein precursor (APP), a type I transmembrane protein. Initial β-secretase cleavage within the luminal portion of APP releases the soluble ectodomain and leaves the remaining C-terminal stub, known as CTFβ, in the membrane (Vassar et al., 1999). CTFβ then undergoes scission within its transmembrane domain (TMD) by the presenilin (PS)-containing γ-secretase complex, releasing the APP intracellular domain (AICD) and generating the Aβ peptide (Wolfe, 2009). Cleavage of CTFβ by γ-secretase is heterogeneous, yielding a range of secreted Aβs of 38-43 residues in length varying at their C-termini. While Aβ40 is the major secreted species, Aβ42, with its two additional hydrophobic transmembrane residues, is more prone to aggregation (Jarrett et al, 1993) and is the predominant Aβ species deposited in neuritic plaques, a defining pathological feature of AD (Iwatsubo et al., 1994). Many dominant mutations in PS1 and APP that cause early-onset familial AD (FAD) increase the ratio of Aβ42 produced relative to Aβ40, suggesting the importance of the production of aggregation-prone long Aβ in precipitating AD pathogenesis (Bentahir et al., 2006; Citron et al., 1997; Duff et al., 1996; Scheuner et al., 1996; Selkoe, 2001; Tanzi and Bertram, 2005). In addition to Aβ42, the amyloidogenicity and potential pathogenic role of Aβ43 has recently been suggested (Saito et al., 2011).

Evidence in cells and *in vitro* demonstrates that these various Aβ species are the result of successive γ-secretase cleavages of CTFβ, starting with an initial endoproteolytic cut at the ε sites (Gu et al., 2001; Sastre et al., 2001; Weidemann et al., 2002); this cut releases AICD and

generates Aβ48 or Aβ49, which remain in the membrane and undergo C-terminal trimming by γ-secretase mostly every three residues at the ζ and then γ sites to produce the shorter, secreted forms of Aβ. Specifically, two product lines are thought to exist depending on the initial ε site: a primary line with ε cleavage producing Aβ49 and subsequent trimming generating Aβ46→43→40, and a minor line with ε cleavage first generating Aβ48 and leading to Aβ45→42→38 (this last step trimming off a tetrapeptide) (Funamoto et al, 2004; Okochi et al., 2013; Sato et al., 2003; Qi-Takahara et al., 2005; Takami et al. 2009; Zhao et al., 2004). This model of γ-secretase cleavage is outlined in Figure 3.1A.

γ-secretase is a membrane-embedded aspartyl protease complex consisting of PS, presenilin enhancer 2 (Pen-2), anterior pharynx-defective 1 (Aph1), and nicastrin (Edbauer et al., 2003; Kimberly et al., 2003; Takasugi et al., 2003). The active site of γ-secretase, contained within PS (Wolfe et al., 1999), is sequestered from the hydrophobic membrane environment; substrates first bind to a docking site on the external surface of the enzyme, followed by lateral entry to gain to access to the active site (Esler et al., 2002; Kornilova et al., 2005; Wolfe 2009). γ-secretase exhibits broad substrate specificity and cleaves the stubs of many type I membrane proteins with shed ectodomains (Haapasalo and Kovacs, 2011), including that of the Notch receptor (De Strooper et al, 1999). While not as well characterized as APP processing, γ-secretase has been shown to cleave Notch and CD44 substrates in an analogous manner, with cleavage occurring both at ε-like sites near the membrane-cytoplasm border and at γ-like sites in the middle of the TMD (Lammich et al., 2002; Okochi et al., 2002). Thus, the γ-secretase complex can cut a broad range of TMDs, some at multiple sites.

Figure 3.1 γ-secretase trims Aβ49 and Aβ49 with a C-terminal amide to generate primarily Aβ40. A. The transmembrane domain of APP CTFβ is processed by γ-secretase by sequential cleavage at the ε, ζ, and γ sites to generate the Aβ peptides with the indicated C-termini. ε site cleavage at position Aβ49 leads to subsequent trimming at Aβ46, 43, and 40 to generate primarily secreted AB40 (left), while ε cleavage at position Aβ48 leads to cleavage at position Aβ45, Aβ42, and Aβ38 to generate primarily secreted Aβ42 (right). B. A model for γ-secretase trimming of long Aβ intermediates every three residues. The negatively charged C-terminus, generated upon scission at the ε site, would move three residues due to attraction to positive charges on the cytosolic side of the enzyme, setting set up the next cut at the subsequent cleavage site. This process would then repeat until the Aβ is secreted from the membrane. C. Aβ40 and Aβ42 production from Aβ49 or Aβ49 with a C-terminal amide and CHAPSO-solubilized membranes containing overexpressed γ-secretase. Aβ40 and Aβ42 products were measured by ELISA. n=1, with three technical replicates.

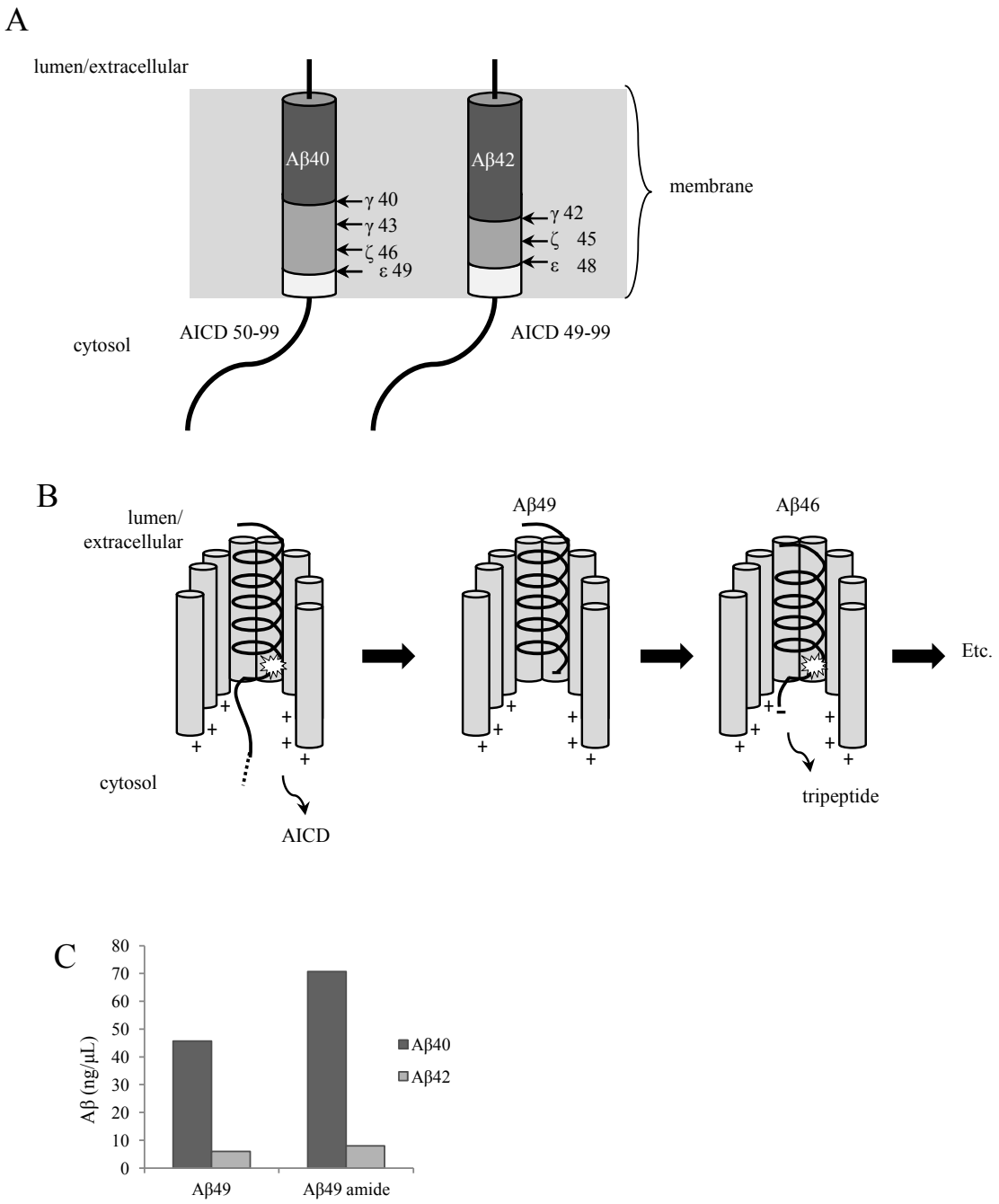

Figure 3.1 continued. γ-secretase trims Aβ49 and Aβ49 with a C-terminal amide to generate primarily Aβ40.

Because γ-secretase is capable of cleaving such a wide range of hydrophobic amino acid sequences, and because the production of aggregation-prone Aβ42 relative to Aβ40 closely correlates with AD, determinants of the precise location of γ-secretase cleavage along the CTFβ TMD to generate Aβ40 and Aβ42 are of great interest. Mutagenesis of the APP TMD has shown that the production of Aβ42 versus Aβ40 is sensitive to point mutations and is therefore influenced by the TMD amino acid sequence (Lichtenthaler et al., 1997; Lichtenthaler et al., 1999). In addition, naturally-occurring FAD-causing point mutations within the APP TMD have been shown to increase the ratio of Aβ42 to Aβ40 (Selkoe, 2001; Tanzi and Bertram, 2005). It is now clear based on the sequential cleavage model, however, that the production of Aβ42 versus Aβ40 is primarily dictated by the specific upstream ε site that is used to generate either Aβ48 or Aβ49 and subsequent proteolysis every three residues at the trimming sites. While some studies have shown that FAD mutations within the APP TMD can shift the site of ε cleavage (Chávez-Gutiérrez et al., 2012; Sato et al., 2003), many previous studies of TMD mutations that alter Aβ42 and Aβ40 production were performed before the clear demonstration of the model for sequential proteolysis, and thus the effects of many of these mutations on the precise location of ε site cleavage and the entire trimming pathway were not examined. Therefore, little is known about determinants of the specific sites of initial ε cleavage and subsequent C-terminal trimming by γ-secretase. It is also clear from the sequential cleavage model that, in addition to the efficiency of ε site endoprotoeolysis, which determines the level of total Aβ generated (Kakuda et al., 2006), the extent of trimming is another critical determinant of the production of toxic Aβs, as reduced trimming can result in the production of increased Aβ42 and Aβ43 compared to shorter Aβ38 and Aβ40. While specific residues within the juxtamembrane region of APP have

been shown to affect the lengths of Aβ peptides generated (Kukar et al., 2011; Ren et al., 2007), little is known about transmembrane determinants of the degree of cleavage at the trimming sites.

In this study we examined determinants of the specificity and efficiency of ε site endoproteolysis and C-terminal trimming of CTFβ by γ-secretase. We show that the C-terminal charge of long Aβ intermediates is not necessary for γ-secretase trimming every three residues. We also analyzed whether depth within the TMD determines the location of ε site cleavage. Additionally, we show that instability of the CTFβ transmembrane helix plays an important role in endoproteolysis and C-terminal trimming by γ-secretase.

Experimental procedures

γ-Secretase preparations. Purified γ-secretase complexes from S20 cells, CHO cells overexpressing all four γ-secretase components, were prepared as previously described (Cacquevel et al., 2008). S20 cells were scraped from plates and lysed in buffer containing 50 mM MES, pH 6.0, 150 mM NaCl, 5mM $MgCl_2$, and 5 mM $CaCl_2$ using a French pressure cell at 1000 p.s.i. The lysate was spun at low speed to remove nuclei and unbroken cells, and then at 100,000 X *g*. The resulting membrane pellet was washed in sodium bicarbonate buffer and solubilized in 1% CHAPSO. γ-secretase complexes were then purified from this CHAPSO-solubilized fraction by sequential affinity purifications via Ni-NTA agarose beads (Sigma-Aldrich) and M2 anti-Flag agarose beads (Sigma-Aldrich).

Plasmids and C100-FLAG mutagenesis. The pET2-21b plasmid containing the coding sequence for C100-FLAG has been previously described (Li et al., 2000). Helix-stabilizing,

helix-destabilizing, and deletion mutations were introduced into C100-FLAG using the Quick-Change Lightning Site Directed Mutagenesis kit (Agilent).

C100-FLAG preparation. C100-FLAG substrates (APP CTFβ with an N-terminal methionine and a C-terminal FLAG tag) were expressed in *E. coli* BL21(DE3) cells (Stratagene) (with the exception of the mutant with LL inserted between the ε and ζ sites, which would not express in BL21(DE3) cells, but did express in C43(DE3) cells (Lucigen)). Cells were grown to an OD of 0.8, and C100-FLAG expression was induced with 1 mM IPTG for 2 h at 37 °C. Cells were pelleted and lysed in buffer containing 10 mM Tris pH 7.0, 150 mM NaCl, 1% TritonX-100, and a protease inhibitor cocktail by 3 passages through a French pressure cell at 1000 p.s.i. The lysate was spun at 3000 X *g* to remove unbroken cells and larger debris, and the lysate was bound to M2 anti-FLAG affinity gel (Sigma) by rocking overnight at 4 °C. The resin was then washed twice for 20 min at room temperature in lysis buffer, and C100-FLAG was eluted from the resin by rocking in buffer containing 100 mM glycine, pH 2.7, and 1% NP-40 for 2 h at room temperature. The protein concentration in each purified C100-FLAG preparation was determined by BCA assay (Pierce).

γ-secretase assays. γ-secretase was incubated with substrate in assay buffer (50 mM HEPES pH 7.0 and 150 mM NaCl) with 0.1% phosphatidylcholine, 0.025% phosphatidylethanolamine, 0.00625% cholesterol, and a final CHAPSO concentration of 0.25%. To compare the trimming of Aβ49 to the trimming of Aβ49 with a C-terminal amide (both from AnaSpec), reactions were carried out for 4 h, which was within the time frame needed for maximal product formation; to analyze the cleavage of C100-FLAG deletion and helical mutants, 2 μM substrate was used, and reactions were carried out for 1.5 h, which was within the linear range of product formation.

Gel electrophoresis and western blotting. For analysis of AICD-FLAG generated from C100-FLAG, reaction samples were prepared in SDS sample buffer and incubated at room temperature for 10 min. The samples were run on 12% Bis Tris gels (Biorad), followed by transfer to PVDF membrane and western blotting with M2 anti-FLAG antibody (Sigma). The signal was captured using ECL (GE Healthcare), and densitometry was performed using ImageQuant software (GE Healthcare).

The Aβ products generated from C100-FLAG substrates were analyzed by bicine urea gel electrophoresis as previously described (Quintero-Monzon et al., 2011). Briefly, bicine urea gels were hand-cast with a 13.5 cm separating layer containing 8 M urea and an acrylamide concentration of 11% T/2.6% C, a 10.5 cm spacer layer with 4 M urea and the same acrylamide concentration as the separating layer, and comb layer with 4% T/3.3% C acrylamide. Reaction samples were incubated with SDS sample buffer at room temperature for 10 min and loaded into the wells of the gel, and the gel was run at 12 mA for 1 h and at 34 W for approximately 4 h, until the dye front reached the bottom of the gel. The gel was cut based on the mobility of the standards in Novex Sharp prestained protein ladder (Invitrogen), and proteins running below the 15 kDa marker were transferred to a PVDF membrane for 2 hours at 400 mA in Tris-glycine transfer buffer containing 20% methanol. The membranes were blotted for Aβ using 6E10 (Covance); the epitope for 6E10 is at the N-terminus of Aβ, and thus it detects all C-terminal Aβ species.

Mass spectrometry analysis. Aβ products were immunoprecipitated from reaction mixtures using 4G8 (Covance), which targets Aβ residues 17-24, followed by mass spectrometric analysis as previously described (Wang et al., 1996).

Statistical analysis. Statistical significance was determined by one-way analysis of variance (ANOVA) and Dunnett's post hoc test, using WT values as the control group.

Results

The C-terminal charge of Aβ intermediates plays no role in trimming-- We first sought to examine how γ-secretase measures by three amino acids in carrying out C-terminal trimming of long Aβ intermediates. Upon endoproteolysis of CTFβ by γ-secretase at the ε sites, a new C-terminus is generated. We considered whether this newly-formed, negatively-charged C-terminus would then move a distance of roughly three residues due to attraction to positively charged residues on the cytosolic side of the enzyme, extending the substrate and setting up the subsequent cut 3 residues from the initial cleavage site. This cut would then generate a new C-terminus, and the process could be repeated until the trimmed Aβ peptide is released from the enzyme (Figure 3.1B).

We have previously reported that ε-cleaved Aβs are trimmed by γ-secretease *in vitro* to generate Aβ40 and Aβ42 (Fernandez et al., 2014). Specifically, we found that synthetic Aβ49 substrate is primarily trimmed to Aβ40, and synthetic Aβ48 to Aβ42. These results were consistent with tripeptide trimming of each ε-cleaved Aβ, but also demonstrated that a small degree of crossover of the primary Aβ40 and Aβ42 generating pathways is possible, as the trimming of Aβ49 led to a minor amount of Aβ42, and Aβ48 to a minor amount of Aβ40. Having established this system for monitoring C-terminal trimming by γ-secretase, we could examine the role of the C-terminal charge of Aβ intermediates in this process by comparing the

trimming of Aβ49 to that of Aβ49 with a C-terminal amide, which has a neutral C-terminus. As shown in Figure 3.1C, the amide was not only able to be trimmed, but it was trimmed in the same way as Aβ49, with γ-secretase able to generate the same ratio of Aβ42 to Aβ40 from each. In addition, we found that a transition-state analogue inhibitor with three C-terminal residues extending from the hydroxyl moiety was equally potent whether the C-terminus of the inhibitor contained a methyl ester or a carboxylic acid; if the charge hypothesis had been correct, the carboxylic acid should have been the more potent inhibitor (data not shown). Thus, we conclude that the C-terminal charge of long Aβ intermediates are not involved in setting up a trimming event every three residues.

Determinants of ε site specificity-- The residues of protease substrates on either side of the scissile amide bond are referred to as P1, P2, P3, etc moving toward the N-terminus, and as P1', P2', P3', etc moving toward the C-terminus. These substrate residues around the cleavage site bind to the enzyme active site in an extended conformation, each interacting with a corresponding pocket on the enzyme; the pockets interacting with the P residues are referred to as S1, S2, S3, etc, and the pockets interacting with the P' residues as S1', S2', S3', etc (Wolfe 2009). The S2-S4' pockets of the γ-secretase active site have been previously examined using transition state analogue inhibitors with systematically varied amino acid substituents to probe the corresponding pocket on the enzyme (Esler et al., 2004). The data obtained using these peptidomimetics suggests that γ-secretase has an S1', an S2', and an S3' pocket (but no S4' pocket): the addition of a substituent to the P3' position of the peptidomimetic increased the potency of the compounds, while the addition of a substituent at the P4' position had no effect on potency (Figure 3.2). Once the substrate binds to the γ-secretase active site for proteolysis,

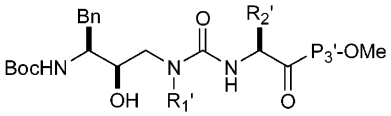

Compd	R1′	R2′	P3′	IC_{50} (μM)[a]
6	Me	*i*-Bu	Phe	3.1
7	*i*-Pr	*i*-Bu	Phe	22
8	*i*-Bu	*i*-Bu	Phe	0.40
9	Bn	*i*-Bu	Phe	0.40
10	Bn	Me	Phe	0.14
11	Bn	*i*-Pr	Phe	0.40
12	Bn	*i*-Bu	Phe	0.39
13	Bn	Bn	Phe	18
14	Bn	*i*-Bu	Ala	2.0
15	Bn	*i*-Bu	Val	0.22
16	Bn	*i*-Bu	Leu	0.65
2	Bn	*i*-Bu	Phe	0.39
17	Bn	*i*-Bu	—	8.0

[a] Values are means of three experiments.

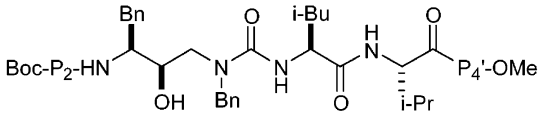

Compd	P2	P4′	IC_{50} (μM)[a]
15	—	—	0.22
18	—	Ala	0.67
19	—	Val	0.53
20	—	Leu	0.54
21	—	Ile	0.27
22	—	Phe	0.25
23	Ala	—	0.15
24	Val	—	0.07
25	Leu	—	0.23
26	Phe	—	0.50

[a] Values are means of three experiments.

Figure 3.2. γ-secretase has S1', S2', and S3' pockets. Taken from Esler et al, 2004. Hydroxyethylurea-type transition-state analogue γ-secretase inhibitors were used to probe the pockets of the γ-secretase active site that accommodate substrate residues around the scissile amide bond. The potency of the compounds was examined by measuring Aβ production in cells. These data indicate that the enzyme has an S3' pocket and no S4' pocket.

these three hydrophobic pockets can accommodate three residues downstream of the scissile amide bond; therefore we asked if a depth of three hydrophobic residues within the TMD, dictated by these three pockets, is a determinant of which peptide bond will be cleaved. This model could potentially account for not only trimming by three residues, but also for the site of ε cleavage: ε cleavage primarily occurs exactly three residues within the CTFβ TMD to generate Aβ49 and subsequently Aβ40 after AICD dissociates from the enzyme and tripeptide trimming occurs.

If the site of the initial ε cut is primarily determined by a distance of three residues from the cytosolic triple lysine sequence of CTFβ, then deletion of one residue from the C-terminus of the TMD (L52, Aβ numbering) should shift the primary site of ε cleavage by one residue, maintaining the location of ε cleavage as three residues within the TMD and therefore generating Aβ48 as the predominant ε cleavage product. Subsequent trimming would result in Aβ42 as the predominant final product (Figure 3.3A). Deletion of an additional residue (both M51 and L52) should shift ε cleavage to generate Aβ47, and Aβ41 as the primary trimmed product; deletion of one more residue, for a total of three (V50, M51, and L52), should result in Aβ46 production, thus restoring cleavage back to the original register and leading to Aβ40 as the major product (Figure 3.3A). Systematic deletion of residues L49, T48, and I47 would yield similar shifts in cleavage products if endoproteolysis primarily occurs three residues within the TMD: deletion of residue L49 should result in endoproteolysis generating Aβ48 and therefore Aβ42 as the primary trimmed product. Deletion of both L49 and T48 should result in Aβ47 production and subsequently Aβ41, and deletion of I47-L49 should lead to Aβ46 generation and restore Aβ40 as the primary final product (Figure 3.3A). However, as shown in Figure 3.3B, deletion of residue

Figure 3.3. Deletion of residues around the ε sites does not alter the primary Aβ cleavage products. (A) C100-FLAG deletion mutants. One, two, or three residues on either side of the primary ε site (between Aβ residues 49 and 50) were deleted. The transmembrane domain is in bold. The predicted site of ε cleavage is indicated by an arrow, and the expected ε-cleaved Aβ products are in parentheses. Residue V40 (Aβ numbering) is in red for reference. (B) C100-FLAG deletion mutants were used as substrates in *in vitro* enzyme assays, and the Aβ products were separated by bicine urea gel electrophoresis. Aβ signal was visualized by western blotting with 6E10. A representative result of five independent experiments is shown. (C) A summary of the mass spectrometric analysis of the Aβ products of each deletion mutant. The C-termini of the Aβ species detected by mass spectrometry are indicated by vertical bars, and the larger bars indicate products with larger peaks in the mass spectra. Residue V40 (Aβ numbering) is in red for reference (D) AICD production from the deletion mutants was monitored by anti-FLAG western blotting, and was quantified and normalized to WT. For each mutant, AICD production was significantly lower than for WT. *$p<0.05$, **$p<0.01$, ***$p<0.001$ versus WT. n=2. Error: S.E.M

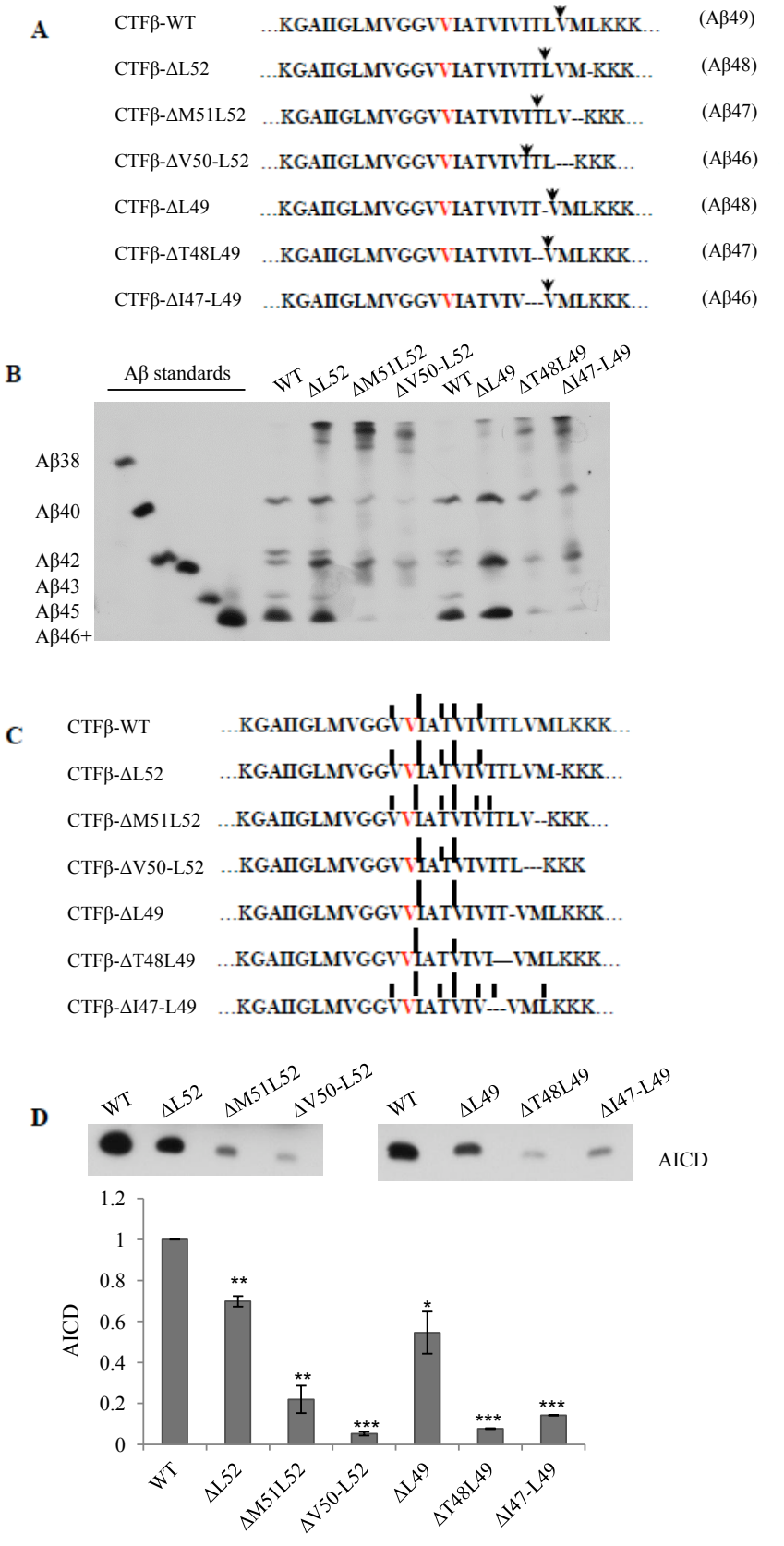

Figure 3.3. continued. Deletion of residues around the ε sites does not alter the primary Aβ cleavage products.

L52 from APP C100-FLAG substrate resulted in little change in the spectrum of Aβs generated by γ-secretase compared to wildtype (WT), with a slight shift toward increased Aβ40 and Aβ43 production. Deletion of an additional C-terminal residue resulted in the production of primarily Aβ40, Aβ43, and Aβ46+ and reduced Aβ42 production compared to WT. Deletion of all three residues C-terminal to the primary ε cleavage site at position 49 (residues V50, M51, and L52) resulted in the production of primarily Aβ43 and Aβ40. Systematic deletion of residues 47-49 also gave results that were inconsistent with our hypothesis, with each deletion resulting in cleavage mainly along the Aβ49-46-43-40 pathway: the single deletion of residue L49 and the double deletion of residues T48 and L49 resulted in solely Aβ40, Aβ43, and Aβ46+ production, and the triple deletion of I47-L49 resulted in primarily Aβ40 and Aβ43 production and reduced Aβ42 compared to WT. These results indicate that upstream sequences, and not a depth of three hydrophobic residues within the TMD, are the determinants of ε site cleavage specificity. This suggests that the sequence of amino acids arranged along the CTFβ transmembrane helix dictates the initial interaction between γ-secretase and the substrate; this interaction between enzyme and substrate sets up the site of endoproteolysis and does not change when deletions are made near the C-terminal end of the TMD (Figure 3.4).

We then performed mass spectrometry analysis of the Aβ products to confirm the results obtained by urea gel electrophoresis. It is important to note that this analysis is not quantitative, and that longer Aβ peptides are difficult to detect by mass spectrometry due to their hydrophobicity. Therefore, Aβ43-Aβ49, although readily detected by gel, were not reliably detected by mass spectrometry. Even so, the mass spectrometry results largely confirm what we observed by gel, with the deletions generating primarily Aβ40 and Aβ43, and not leading to

Figure 3.4. Depth within the TMD is not a determinant of ε-site specificity. The top row of helices demonstrates how the cleavage sites would be predicted to shift if initial ε site cleavage always occurred three residues within the transmembrane domain. The bottom row of helices summarizes the results obtained in Figure 3.3. The primary γ-cleaved product from each mutant was Aβ40, with cleavage always occurring on the same face of the transmembrane helix regardless of deletions at the C-terminal end.

Depth-in-membrane model

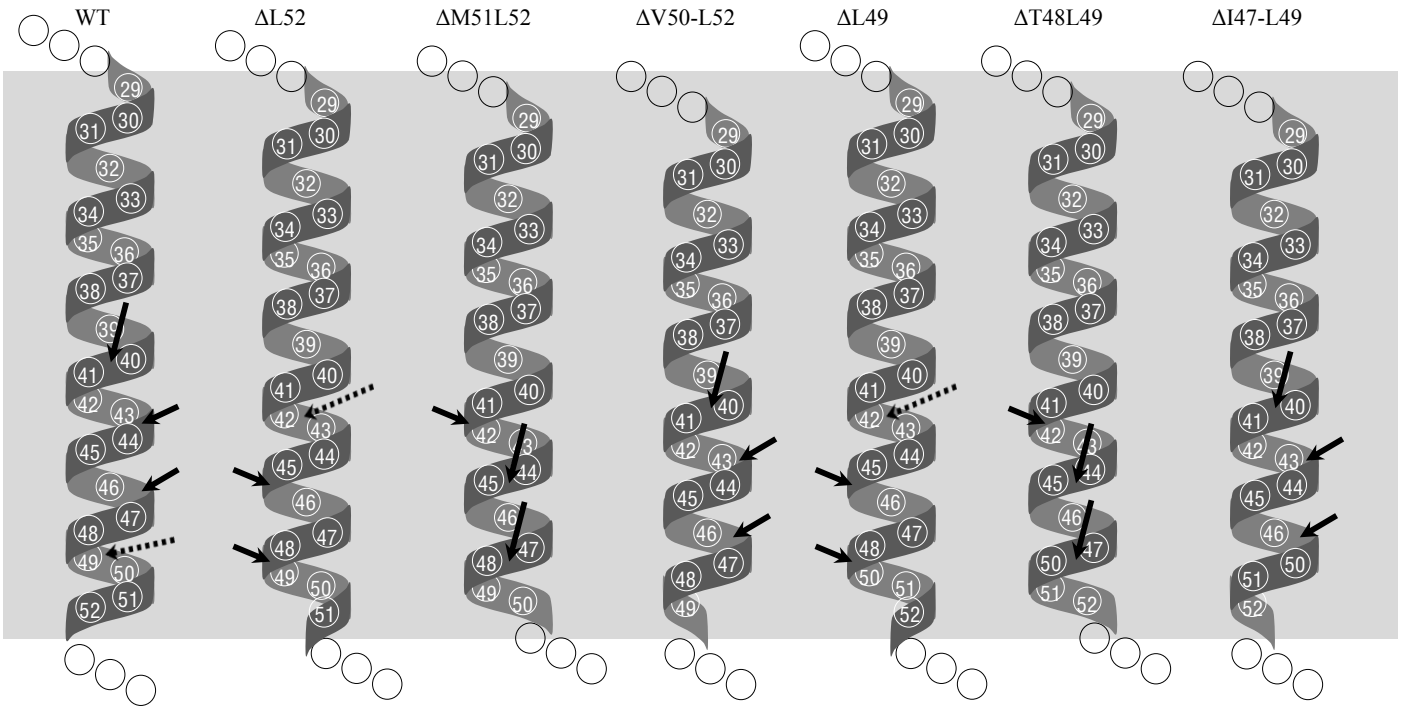

TMD sequence model

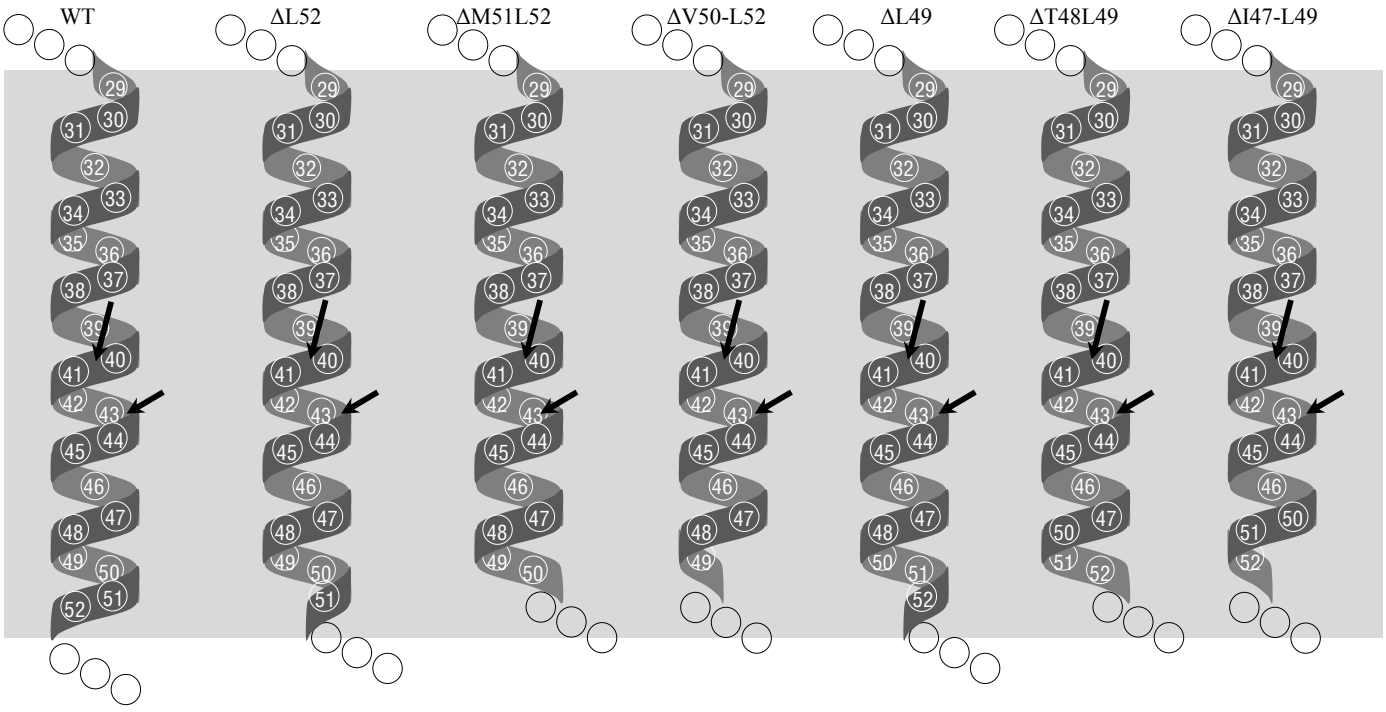

Figure 3.4 continued. Depth within the TMD is not a determinant of ε-site specificity

shifts toward Aβ42 and Aβ41 products (Figure 3.3C and Figure S1). Although the analysis of the Aβ spectrum makes clear that fundamental shifts in product lines did not occur with C-terminal TMD deletions, we are currently optimizing the analysis of AICD species by mass spectrometry to determine the precise locations of ε site cleavage for each of these mutants. Analysis of the level of AICD product by western blot shows that each deletion resulted in a decrease in γ-secretase proteolysis at the ε site (Figure 3.3D).

Helical stability of CTFβ and γ-secretase processing-- The transmembrane substrates of intramembrane cleaving proteases are typically folded into α helices (Urban et al., 2003; Wolfe, 2009); this conformation is energetically favored for single pass TMDs, as the polar groups of the peptide backbone form hydrogen bonds with each other within the hydrophobic membrane environment. Experimental evidence demonstrates that CTFβ is indeed α helical upon initial binding to γ-secretase (Barrett et al., 2012; Lichtenthaler et al., 1999). In addition, helical peptides based on the APP TMD are potent inhibitors of γ-secretase, and disruption of their helical conformation abolishes their inhibitory activity; this is consistent with the APP TMD being in a helical conformation upon initial interaction with γ-secretase (Bihel et al., 2004; Das et al., 2003). Moreover, the data we obtained from the deletion mutants highlights the importance of the initial binding of the α helical substrate to the enzyme, as this interaction apparently dictates the position of ε site endoproteolysis. However, upon access to the internal active site, this α helical structure would render amide bonds inaccessible for hydrolysis (Wolfe, 2009). Therefore, at least partial instability of the helical substrate should be important for exposing peptide bonds for proteolysis. A requirement for helix-destabilizing residues in substrates has been demonstrated for other intramembrane-cleaving proteases (Lemberg and

Martoglio, 2002; Urban and Freeman, 2003; Ye et al., 2000), but has never been shown for γ-secretase, and the role of CFTβ helical stability in trimming has not been investigated.

We examined the role of helical instability in endoproteolysis and trimming by γ-secretase by introducing helix-destabilizing (GG and GA) and helix-promoting (LL) motifs between the ε, ζ, and γ cleavage sites of C100-FLAG as shown in Figure 3.5A. Glycine and alanine have more conformational flexibility than larger amino acids and thus destabilize constrained α helical structures, while leucine has a high propensity to form α helices (O'Neil and Degrado, 1990; Urban and Freeman, 2003). The effects of these mutations on endoproteolysis at the ε site were measured by quantitating the levels of AICD generated from each mutant substrate in *in vitro* γ-secretase reactions, and the effects on trimming were analyzed by monitoring the spectrum of Aβs products.

We first analyzed the effects of the mutations most proximal to the ε site (Figure 3.5B). We found that the helix-destabilizing residues inserted between the ε and ζ sites significantly increase ε site cleavage when compared to WT by roughly 3.5-fold, while this cleavage was significantly decreased for the helix-promoting residues by about 4-fold (Figure 3.5B). This result is consistent with the hypothesis that at least partial instability of the CTFβ transmembrane helix is important for exposing the peptide bond at the ε site for endoproteolysis by γ-secretase. Once endoproteolysis occurs, the mutation is still present in the resulting long Aβ, so the effects of these ε to ζ site mutations on subsequent trimming could also be examined. The helix-destabilizing mutations decreased the proportion of Aβ46-49 to the trimmed Aβ40-43 products compared to WT substrate, and the helix-promoting mutation increased the proportion of

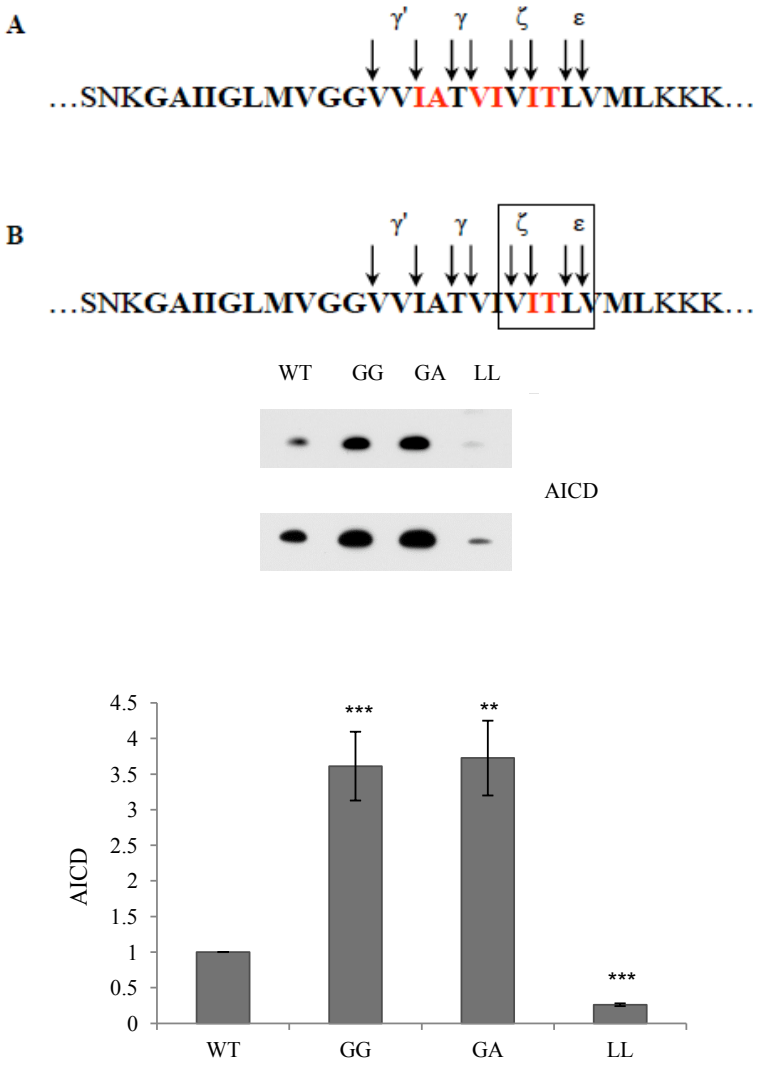

Figure 3.5. Helical instability between the ε and ζ sites is important for endoproteolysis at the ε site. (A) Helix-promoting (LL) and helix-destabilizing motifs (GG and GA) were inserted between cleavage sites. The mutated residues are indicated in red. (B) C100-FLAG substrates with GG, GA, and LL mutations between the ε and ζ sites (outlined with a box) were used as substrates in *in vitro* γ-secretase assays. AICD production was monitored by anti-FLAG western blotting. AICD signal was quantified by densitometry and normalized to WT. A representative blot of 4 independent experiments is shown, and the lower blot is a longer exposure of the upper blot. ** $p<0.01$, ***$p<0.001$ versus WT. n=4. error: S.E.M.

Aβ46-49 to Aβ40-45 compared to WT (Figure 3.6A). This data is consistent with the hypothesis that, after endoproteolysis, helical instability facilitates subsequent trimming at the ζ site.
In addition, the GG and GA mutants resulted in cleavage only along the Aβ49-46-40-43 pathway, with no Aβ42 or Aβ45 detected. We suggest that this pattern of products is a result of the nature of the amino acids that have been substituted into the WT amino acid sequence. Previous studies have demonstrated that small residues at the P1 and P2 positions of substrates or transition state analog inhibitors are disfavored for binding to the apparently large S1 and S2 pockets of the enzyme (Chau et al., 2012; Moore et al., 2000). Substrate binding to the active site to generate Aβ48 would place a disfavored small residue in both the S1 and S2 positions, while binding to generate Aβ49 would only result in one disfavored interaction. We also note that, because small residues have shown to be disfavored for binding to the S1 and S2 pockets of the active site, the increase in endoproteolysis observed with the GG and GA mutations present in the corresponding substrate positions are likely a result of decreased helical stability of the substrate. Alternatively, it is possible that ε cleavage occurs at Aβ46 for these mutants. Again, we are currently optimizing the analysis of AICD species by mass spectrometry to investigate this possibility.

We next verified our analysis of Aβ production by mass spectrometry (Figure 3.6B and Figure S2). Again, the analysis was not quantitative, and the longest Aβ peptides were not consistently detected. However, the production of solely Aβ40 and Aβ43, and the lack of Aβ42, from the GG and GA mutant substrates were confirmed by this analysis.

We next examined the effects of these helix-promoting and helix-destabilizing mutations on endoproteolysis when they are inserted between the ζ and γ sites and between the γ and γ'

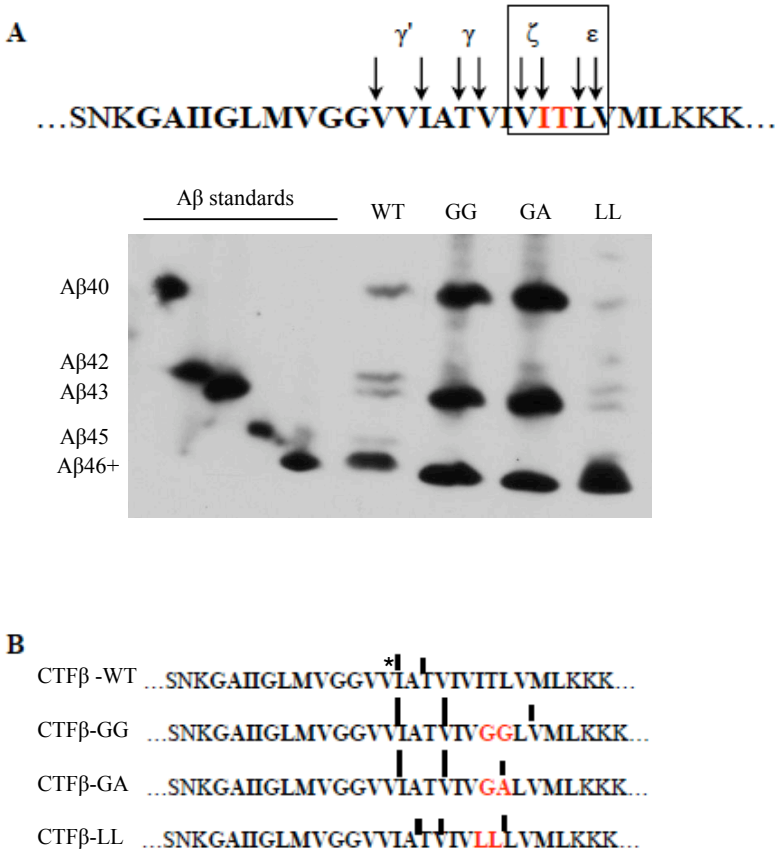

Figure 3.6. Helical instability between the ε and ζ sites and trimming. (A) Aβ generated in enzyme assays using the same substrates in Figure 5 were analyzed by bicine urea gel electrophoresis. Aβ signal was captured by 6E10 western blot. A representative blot of four independent experiments is shown. (B) A summary of the mass spectrometric analysis of the Aβ species generated in these reactions. The data are labeled as in Figure 3.3C. The C-terminus of Aβ40 (residue V40) is indicated with an asterisk above the WT sequence for reference.

sites. As shown in Figure 3.7A, the placement of these mutations between these trimming sites did not have a significant effect on endoproteolysis at the ε site, with the notable exceptions of the GG and GA γ to γ' mutants, which were not cleaved by γ-secretase. During purification, we found that the GG γ to γ' site mutant runs as an SDS stable dimer on a gel (Figure 3.7B), and inspection of the CTFβ sequence reveals that the insertion of the GG and GA mutations between the γ and γ' sites generates an additional contiguous GxxxG motif along the CTFβ TMD (Figure 3.6A). The dimerization of CTFβ through three existing contiguous TMD GxxxG motifs, which promote helix-helix interactions (Brosig and Langosch, 1998), and the cleavage of CTFβ dimers by γ-secretase has been previously suggested (Munter et al., 2007). Moreover, this dimerization has been linked to increased pathogenic Aβ42 production. However, our results suggest that the dimerization of substrate completely prevents γ-secretase cleavage.

To examine the effects of these mutations on trimming, we again performed urea gel electrophoresis of the reactions to analyze the Aβ spectrum. Our results were at first unclear because several bands, indicated with asterisks in Figure 3.8A, were running aberrantly in the gel compared to the Aβ standards, most likely because the presence of the mutations in the Aβ products altered the mobility of those Aβs in the gel. Therefore, mass spectrometric analysis was essential to determine the identity of these Aβ products. Based on the mass spectrometry data (Figure 3.8B and Figure S3), we were able to identify the product bands as follows: the bands running aberrantly in the GG, GA, and LL ζ to γ lanes are mutant Aβ45, and the bands in the LL γ to γ' lane are mutant Aβ42 and Aβ43. Comparison of the relative levels of Aβ products detected by western blot shows that, for the LL ζ to γ substrate, the major product band is Aβ45; there is hardly any Aβ40, Aβ42, or Aβ43, suggesting that trimming is impaired after Aβ45 is

Figure 3.7. Helical instability between ζ and γ sites and γ and γ' sites does not affect endoproteolysis at the ε site. (A) Enzyme assays were performed using C100-FLAG substrates with helix-promoting and helix-destabilizing residues between the ζ and γ and γ and γ' sites (outlined with boxes). AICD production was detected by anti-FLAG western blot. A representative blot of 5 independent experiments is shown. AICD signal was quantified by densitometry and normalized to WT. No significant differences in AICD levels were found between the mutants and WT, with the exception of the γ to γ' site GG and GA mutants, for which AICD product levels were too low to be consistently quantified. error: S.E.M. (B) All C100-FLAG substrates were purified by anti-FLAG affinity chromatography and the purifications were examined by SDS-PAGE. The GG γ to γ' mutant runs as an SDS-stable dimer, and is shown alongside a purification of WT C100-FLAG, which largely runs as a monomer, for comparison.

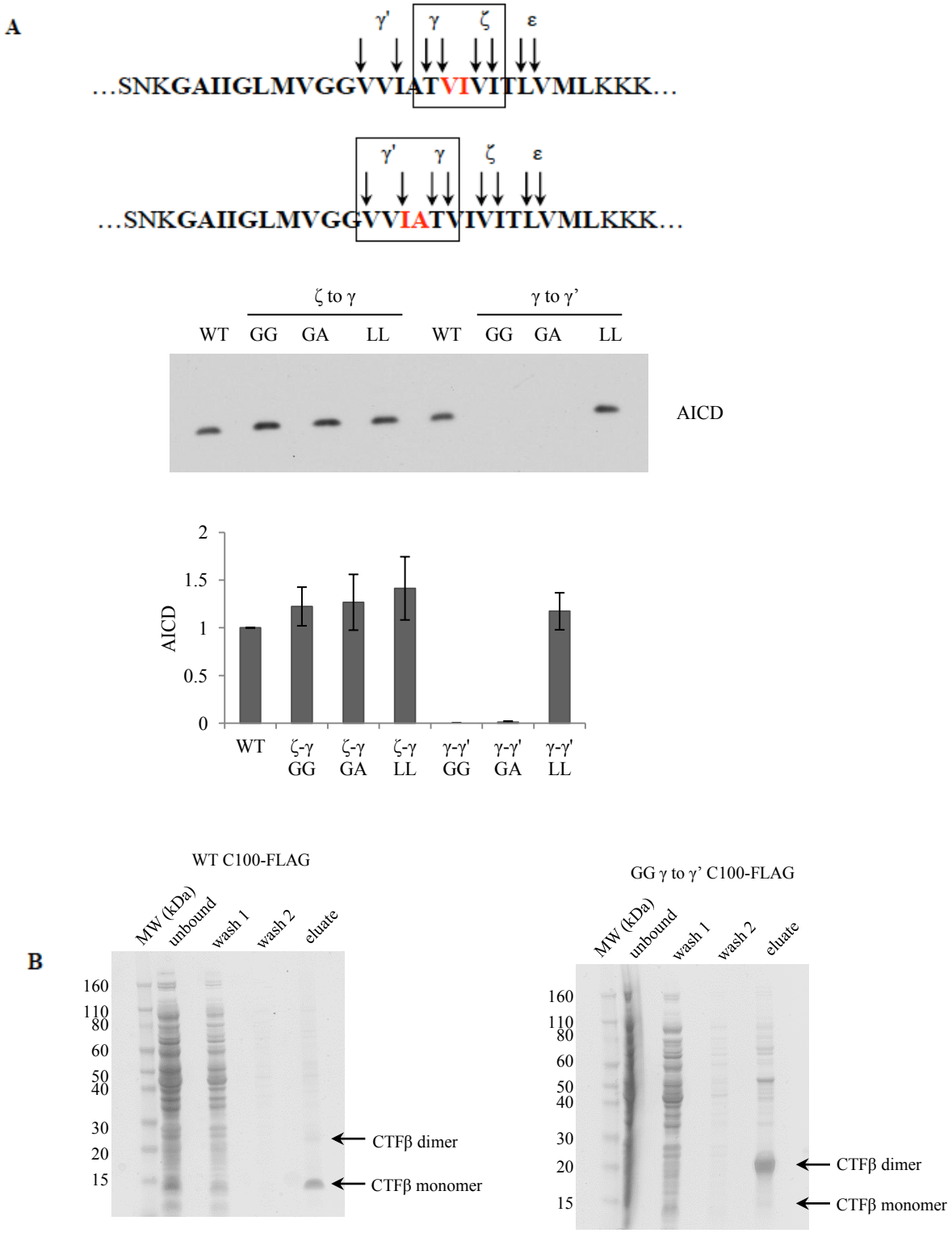

Figure 3.7 continued. Helical instability between ζ and γ sites and γ and γ' sites does not affect endoproteolysis at the ε site.

Figure 3.8. Helical propensity between ζ and γ sites and γ and γ' sites and trimming. (A) Aβ products generated from the same substrates used in Figure 3.7 were analyzed by bicine urea gel electrophoresis. Asterisks indicate Aβ products running differently than the Aβ standards. These bands were identified by mass spectrometry as follows: the products in the GG ζ to γ lane, GA ζ to γ lane, and LL ζ to γ lane are Aβ45 containing each respective mutation, and the products in the LL γ to γ' lane are Aβ42 and Aβ43 containing the LL mutation. A representative blot of three independent experiments is shown. (B) A summary of the mass spectrometric analysis of the Aβ products generated from these substrates. The data are labeled as in Figure 3.3C. The C-terminus of Aβ40 (residue V40) is indicated with an asterisk above WT sequence for reference.

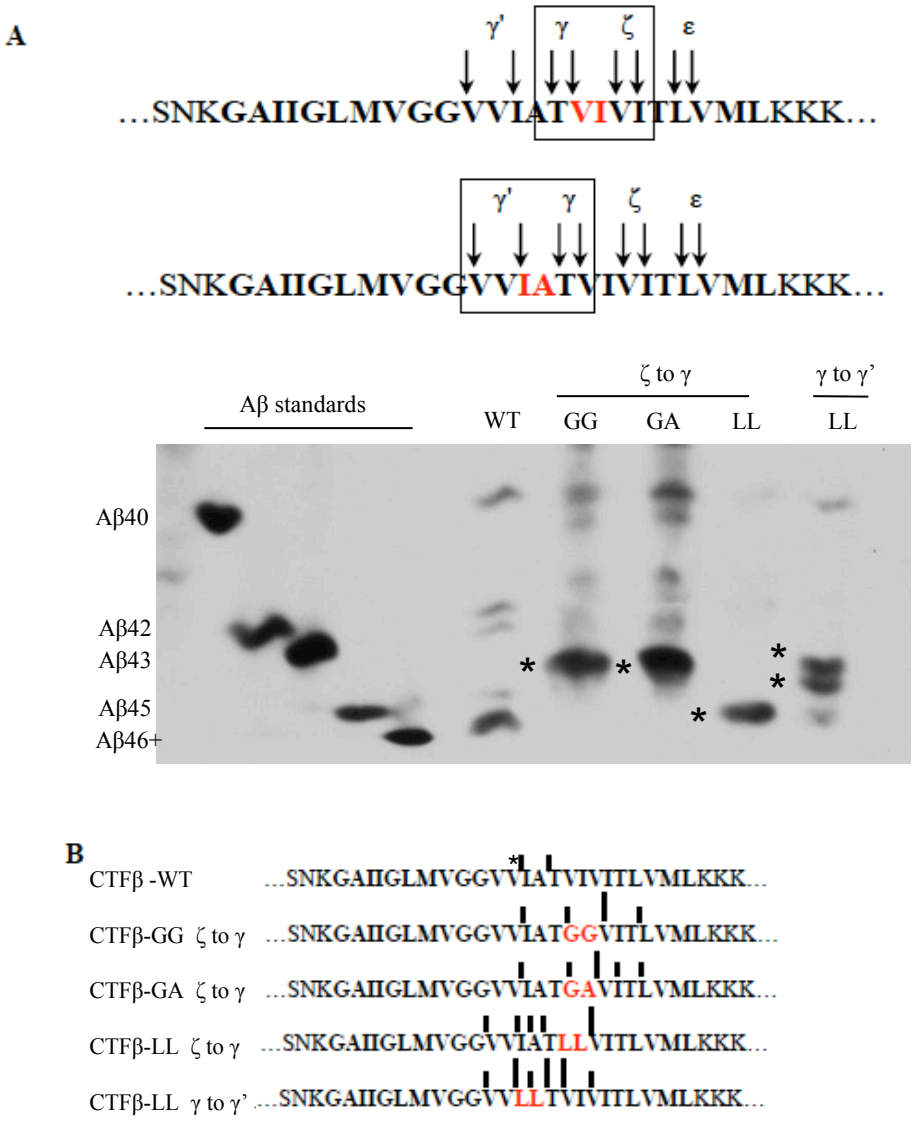

Figure 3.8 continued. Helical propensity between ζ and γ sites and γ and γ' sites and trimming.

formed. Similarly, for LL γ to γ', Aβ42 and Aβ43 are accumulating at the expense of Aβ40. For each of these LL mutants, the presence of the helix-stabilizing residues seems to impair further trimming at the subsequent site compared to WT substrate (Figure 3.8A). However, the destabilizing mutations inserted between the ζ and γ sites did not have the opposite effect of the LL mutation inserted at the same site, as the level of shorter products that would be generated by trimming past the mutation site does not seem to be increased compared to the longer Aβ45 product (Figure 3.8A). It may be that, once the TMD is cut at the ζ site, it is so destabilized that further helix disruption is not facilitating further trimming. The effects of the GG and GA γ to γ' mutations on trimming could not be examined, as these mutants are not cleaved at all, giving no AICD-FLAG product. Again, we are currently in the process of optimizing mass spectrometric analysis of the AICD species generated in these reactions.

Discussion

The intramembrane cleavage of transmembrane substrates by γ-secretase is an important event in biology and in disease. Our results provide novel information about how γ-secretase interacts with, cleaves, and trims the TMD of CTFβ to generate the Aβ peptides implicated in AD pathogenesis. We first examined determinants of ε site and trimming site specificity. We found that the C-terminal charge of long Aβ intermediates is not involved in proteolysis every three residues at the trimming sites, as Aβ49 and Aβ49 with a C-terminal amide were trimmed the same way, with the same ratio of Aβ42 to Aβ40 generated from each substrate. We next examined the hypothesis that initial endoproteolysis and subsequent proteolysis at the trimming sites all occur three residues within the transmembrane domain, dictated by the hydrophobic S1',

S2', and S3' pockets on the enzyme. We instead found that the deletion of residues from the C-terminus of the TMD, predicted to shift the position of the ε cleavage site, did not result in shifts in the primary Aβ product line, suggesting that depth within the TMD is not a determinant of ε site specificity. These results are consistent with the model that the arrangement of amino acid side chains along the transmembrane helix of CTFβ determines the initial binding mode to the enzyme, and that this binding determines the position of endoproteolytic cleavage and the subsequent trimming pathway; this interaction does not change due to deletions at the C-terminal end of the helix. Our results are consistent with similar studies in which C-terminal residues of the APP TMD were deleted. These previous studies found that such deletions did not have a dramatic effect on the Aβ40 to Aβ42 ratio (Lichtenthaler et al., 2002; Murphy et al., 1999). Moreover, a previous study of systematic insertions at the APP C-terminus demonstrated that Aβ42/40 was increased no matter how many residues were added to the C-terminal end, and thus shifts in product lines did not correlate with the number of C-terminal residues added (Ousson et al., 2013). However, all of these studies were performed in cells, where the expression and trafficking of mutants can be issues that affect Aβ production; thus our examination of CTFβ C-terminal deletions provides important direct, *in vitro* validation of these previous studies. Our results suggesting that the sequence of amino acids along the TMD, and not simply depth within the membrane, is important in dictating the location of the ε site are also supported by the demonstration that some missense FAD mutations within the APP TMD can increase the degree of ε site cleavage at position 48 compared to WT APP (Chávez-Gutiérrez et al., 2012; Sato et al., 2003). Detailed mutagenesis studies should now be carried out to determine what specific upstream sequence elements dictate the location of ε site cleavage.

We also examined requirements for γ-secretase endoproteolysis and carboxypeptidase trimming. Specifically, we analyzed the role of flexibility of the APP transmembrane helix in CTFβ processing. A requirement for helix-destabilizing residues within the TMD of substrates has been previously demonstrated for signal peptide peptidase, site-2 protease, and rhomboid protease, with specific helix-destabilizing motifs distinguishing substrates from non-substrates (Lemberg and Martoglio, 2002; Moin and Urban 2012; Urban and Freeman, 2003; Ye et al., 2000). Not only has such a requirement not been demonstrated for γ-secretase, but it is often thought that helical instability is actually not a requirement for γ-secretase cleavage (Urban and Freeman, 2003). This is partly because γ-secretase exhibits such broad sequence specificity and, in contrast to the other intramembrane proteases, there is no apparent motif or sequence that distinguishes a protein as a γ-secretase substrate. In addition, it is likely that a requirement for helix-destabilization for γ-secretase cleavage of CTFβ was not previously uncovered experimentally because endoproteolytic cleavage by γ-secretase had historically been assumed to occur in the middle of the TMD to generate Aβ40 and Aβ42, as those were the major species detected, and has only recently been appreciated to occur further C-terminal at the ε sites. As we show, altering helical stability near the γ sites does not affect overall endoproteolytic cleavage by γ-secretase, so previous mutagenesis in this area could have led to erroneous conclusions about γ-secretase cleavage and substrate helicity. Our results show that helix destabilization near the site of endoproteolysis does in fact increase endoproteolysis by γ-secretase; to our knowledge, no other mutations within CTFβ that increase γ-secretase cleavage have been reported. Significantly, we found that CTFβ substrate with a helix-promoting mutation inserted near the ε site substantially decreased γ-secretase endoproteolysis below the WT level. Interestingly, the

CTFβ sequence has β-branched amino acids proximal to the ε site (threonine at Aβ position 47 and isoleucine at Aβ position 48) that were mutated in this study. β-branched residues are also known to destabilize α helices, most likely due to their increased bulkiness near the peptide backbone caused by the branching of the side chains (O'Neil and Degrado, 1990; Urban and Freeman, 2003). Therefore, this motif could provide the necessary flexible conformation for WT CTFβ endoproteolysis.

We also examined the effects of conformational flexibility on substrate trimming by γ-secretase. A helix-promoting mutation inserted between each cleavage site led to a reduction in trimming past that site compared to WT, resulting in the accumulation of longer Aβ species, and the helix-destabilizing mutations proximal to the ε site resulted in reduced accumulation of longer Aβ products. Interestingly, these same destabilizing mutations inserted between the ζ and γ sites did not seem to affect trimming. These results suggest that unwinding and extension of the helix is necessary for cleavage at the trimming sites, but that ζ-cleaved products are perhaps flexible enough that further destabilization does not facilitate trimming. As with the residues near the ε site, β-branched isoleucines and valines predominate along the CTFβ TMD at the trimming sites and were mutated in this study, and again they potentially provide the instability needed for γ-secretase trimming.

Although we demonstrate these effects for APP, the role of helical stability and requirements for helix destabilization within other γ-secretase substrates should be investigated experimentally. Such an analysis could reveal if some degree of helical instability is a defining feature of all γ-secretase substrates or if the degree of instability within different substrate TMDs influences how efficiently they are cleaved by γ-secretase. In addition, although γ-secretase has

seemingly loose substrate requirements, it does exhibit some degree of selectivity, as certain TMDs have been identified that are not cleaved by γ-secretase (Hemming et al, 2008). It would be interesting to examine these non-substrate TMDs in the same way to determine if conformational flexibility provides a basis for this observed selectivity.

This mutagenesis study, while designed to test the effects of helicity on γ-secretase cleavage, also allowed us to examine the effects of substrate dimerization. The dimerization of APP and the effects of this dimerization on Aβ production have been widely studied. Full length APP has dimerization motifs within the ectodomain, as well as three consecutive GxxxG motifs within the TMD (Scheuermann et al., 2001; Munter et al., 2007). The dimerization of full-length APP has been clearly demonstrated, and has also been shown to affect β-secretase cleavage and therefore Aβ production (Kaden et al., 2008). Moreover, small molecule inhibitors of APP dimerization have been identified that lower Aβ production by reducing β-secretase cleavage (So et al., 2012). However, the dimerization of CTFβ via the transmembrane GxxxG motifs and the effects of this dimerization on γ-secretase cleavage have remained unclear and controversial. It has been suggested that CTFβ dimers are cleaved by γ-secretase, and that CTFβ dimerization is specifically linked to an increase in Aβ42 production (Munter et al., 2007). Moreover, binding to the dimerization site and interfering with CTFβ dimer formation has been proposed as the mechanism of action of certain γ-secretase modulators, compounds that increase Aβ38 production and reduce Aβ42 levels (Richter et al., 2010). A subsequent study in which the CTFβ GxxxG motifs were mutated reported that increased dimerization of CTFβ did not affect AICD levels, but led to decreased Aβ40 and Aβ42 levels (Kienlen-Campard et al., 2008). In contrast, multiple studies have reported that γ-secretase does not cleave dimerized substrates. For

example, a study in drosophila demonstrated that the glycophorin A TMD was not cleaved by γ-secretase as a dimer, but was cleaved as monomer (Struhl and Adachi, 2000). In addition, inducing APP or CTFβ dimerization via an FKBP/rapamycin system has been reported to result in reduced Aβ production by reducing γ-secretase cleavage (Eggert et al., 2009). We realized that the insertion of GG and GA motifs between the γ and γ' sites of C100-FLAG added a GxxxG motif into the TMDs of these substrates; the GG mutant indeed runs as an SDS-stable dimer when examined by SDS-PAGE. Our *in vitro* system, using purified C100-FLAG substrates, the direct substrate for γ-secretase, and isolated enzyme directly demonstrates that dimerization of CTFβ does not allow γ-secretase cleavage. Our results are consistent with a similar report in which CTFβ dimerization, induced via a triple lysine mutation at the ectodomain-TMD border, also eliminated γ-secretase cleavage *in vitro* (Jung et al., 2014). Thus, our results suggest that reducing the dimerization of CTFβ is not an effective therapeutic strategy.

.

Abbreviations-- Aβ, amyloid β-peptide; AD, Alzheimer's disease; AICD, amyloid β-protein precursor intracellular domain; APP, amyloid β-protein precursor; CTF, C-terminal fragment; FAD, familial Alzheimer's disease; CHAPSO, 3-[(3-cholamidopropyl)dimethylammonio]-2-hydroxymethyl)propane- 1,3-diol; ANOVA, analysis of variance; Bicine, N,N-bis(2-hydroxyethyl)glycine; SDS, sodium dodecyl sulfate; TMD, transmembrane domain; WT, wildtype

References

Bentahir M, Nyabi O, Verhamme J, Tolia A, Horré K, Wiltfang J, Esselmann H, De Strooper B. Presenilin clinical mutations can affect gamma-secretase activity by different mechanisms.J Neurochem. 2006 Feb;96(3):732-42. Epub 2006 Jan 9.

Barrett PJ, Song Y, Van Horn WD, Hustedt EJ, Schafer JM, Hadziselimovic A, Beel AJ, Sanders CR. The amyloid precursor protein has a flexible transmembrane domain and binds cholesterol. Science. 2012 Jun 1;336(6085):1168-71.

Bihel F, Das C, Bowman MJ, Wolfe MS. Discovery of a Subnanomolar helical D-tridecapeptide inhibitor of gamma-secretase. J Med Chem. 2004 Jul 29;47(16):3931-3.

Brosig B, Langosch D. The dimerization motif of the glycophorin A transmembrane segment in membranes: importance of glycine residues. Protein Sci. 1998 Apr;7(4):1052-6.

Cacquevel M, Aeschbach L, Osenkowski P, Li D, Ye W, Wolfe MS, Li H, Selkoe DJ, Fraering PC. Rapid purification of active gamma-secretase, an intramembrane protease implicated in Alzheimer's disease. J Neurochem. 2008 Jan;104(1):210-20.

Chau DM, Crump CJ, Villa JC, Scheinberg DA, Li YM.Familial Alzheimer disease presenilin-1 mutations alter the active site conformation of γ-secretase. J Biol Chem. 2012 May 18;287(21): 17288-96.

Chávez-Gutiérrez L, Bammens L, Benilova I, Vandersteen A, Benurwar M, Borgers M, Lismont S, Zhou L, Van Cleynenbreugel S, Esselmann H, Wiltfang J, Serneels L, Karran E, Gijsen H, Schymkowitz J, Rousseau F, Broersen K, De Strooper B. The mechanism of γ-Secretase dysfunction in familial Alzheimer disease. EMBO J. 2012 May 16;31(10):2261-74.

Citron M, Westaway D, Xia W, Carlson G, Diehl T, Levesque G, Johnson-Wood K, Lee M, Seubert P, Davis A, Kholodenko D, Motter R, Sherrington R, Perry B, Yao H, Strome R, Lieberburg I, Rommens J, Kim S, Schenk D, Fraser P, St George Hyslop P, Selkoe DJ. Mutant presenilins of Alzheimer's disease increase production of 42-residue amyloid beta-protein in both transfected cells and transgenic mice. Nat Med. 1997 Jan;3(1):67-72.

Das C, Berezovska O, Diehl TS, Genet C, Buldyrev I, Tsai JY, Hyman BT, Wolfe MS.Designed helical peptides inhibit an intramembrane protease. J Am Chem Soc. 2003 Oct 1;125(39): 11794-5.

De Strooper B, Annaert W, Cupers P, Saftig P, Craessaerts K, Mumm JS, Schroeter EH, Schrijvers V, Wolfe MS, Ray WJ, Goate A, Kopan R. A presenilin-1-dependent gamma-secretase-like protease mediates release of Notch intracellular domain. Nature. 1999 Apr 8;398(6727):518-22.

Duff K, Eckman C, Zehr C, Yu X, Prada CM, Perez-tur J, Hutton M, Buee L, Harigaya Y, Yager D, Morgan D, Gordon MN, Holcomb L, Refolo L, Zenk B, Hardy J, Younkin S.Increased

amyloid-beta42(43) in brains of mice expressing mutant presenilin 1.Nature. 1996 Oct 24;383(6602):710-3.

Edbauer D, Winkler E, Regula JT, Pesold B, Steiner H, Haass C. Reconstitution of gamma-secretase activity. Nat Cell Biol. 2003 May;5(5):486-8.

Eggert S, Midthune B, Cottrell B, Koo EH. Induced dimerization of the amyloid precursor protein leads to decreased amyloid-beta protein production. J Biol Chem. 2009 Oct 16;284(42): 28943-52.

Esler WP, Kimberly WT, Ostaszewski BL, Ye W, Diehl TS, Selkoe DJ, Wolfe MS. Activity-dependent isolation of the presenilin- gamma -secretase complex reveals nicastrin and a gamma substrate. Proc Natl Acad Sci U S A. 2002 Mar 5;99(5):2720-5.

Esler WP, Das C, Wolfe MS. Probing pockets S2-S4' of the gamma-secretase active site with (hydroxyethyl)urea peptidomimetics.Bioorg Med Chem Lett. 2004 Apr 19;14(8):1935-8.

Fernandez MA, Klutkowski JA, Freret T, Wolfe MS.Alzheimer presenilin-1 mutations dramatically reduce trimming of long amyloid β-peptides (Aβ) by γ-secretase to increase 42-to-40-residue Aβ. J Biol Chem. 2014 Nov 7;289(45):31043-52.

Funamoto S, Morishima-Kawashima M, Tanimura Y, Hirotani N, Saido TC, Ihara Y. Biochemistry. 2004 Oct 26;43(42):13532-40.Truncated carboxyl-terminal fragments of beta-amyloid precursor protein are processed to amyloid beta-proteins 40 and 42.Biochemistry. 2004 Oct 26;43(42):13532-40.

Gu Y, Misonou H, Sato T, Dohmae N, Takio K, Ihara Y. Distinct intramembrane cleavage of the beta-amyloid precursor protein family resembling gamma-secretase-like cleavage of Notch. J Biol Chem. 2001 Sep 21;276(38):35235-8. Epub 2001 Aug 1.

Haapasalo A, Kovacs DM. The many substrates of presenilin/γ-secretase.J Alzheimers Dis. 2011;25(1):3-28.

Hardy J, Selkoe DJ.The amyloid hypothesis of Alzheimer's disease: progress and problems on the road to therapeutics. Science. 2002 Jul 19;297(5580):353-6.

Hemming ML, Elias JE, Gygi SP, Selkoe DJ. Proteomic profiling of gamma-secretase substrates and mapping of substrate requirements. PLoS Biol. 2008 Oct 21;6(10):e257

Iwatsubo T, Odaka A, Suzuki N, Mizusawa H, Nukina N, Ihara Y. Visualization of A beta 42(43) and A beta 40 in senile plaques with end-specific A beta monoclonals: evidence that an initially deposited species is A beta 42(43).Neuron. 1994 Jul;13(1):45-53.

Jarrett JT, Berger EP, Lansbury PT Jr. The carboxy terminus of the beta amyloid protein is critical for the seeding of amyloid formation: implications for the pathogenesis of Alzheimer's disease. Biochemistry. 1993 May 11;32(18):4693-7.

Jung JI, Premraj S, Cruz PE, Ladd TB, Kwak Y, Koo EH, Felsenstein KM, Golde TE, Ran Y. Independent relationship between amyloid precursor protein (APP) dimerization and γ-secretase processivity. PLoS One. 2014 Oct 28;9(10):e111553.

Kaden D, Munter LM, Joshi M, Treiber C, Weise C, Bethge T, Voigt P, Schaefer M, Beyermann M, Reif B, Multhaup G. Homophilic interactions of the amyloid precursor protein (APP) ectodomain are regulated by the loop region and affect beta-secretase cleavage of APP. J Biol Chem. 2008 Mar 14;283(11):7271-9.

Kakuda N, Funamoto S, Yagishita S, Takami M, Osawa S, Dohmae N, Ihara Y. Equimolar production of amyloid beta-protein and amyloid precursor protein intracellular domain from beta-carboxyl-terminal fragment by gamma-secretase.J Biol Chem. 2006 May 26;281(21):14776-86. Epub 2006 Apr 4.

Kienlen-Campard P, Tasiaux B, Van Hees J, Li M, Huysseune S, Sato T, Fei JZ, Aimoto S, Courtoy PJ, Smith SO, Constantinescu SN, Octave JN.Amyloidogenic processing but not amyloid precursor protein (APP) intracellular C-terminal domain production requires a precisely oriented APP dimer assembled by transmembrane GXXXG motifs. J Biol Chem. 2008 Mar 21;283(12):7733-44.

Kimberly WT, LaVoie MJ, Ostaszewski BL, Ye W, Wolfe MS, Selkoe DJ. Gamma-secretase is a membrane protein complex comprised of presenilin, nicastrin, Aph-1, and Pen-2.Proc Natl Acad Sci U S A. 2003 May 27;100(11):6382-7.

Kornilova AY, Bihel F, Das C, Wolfe MS. The initial substrate-binding site of gamma-secretase is located on presenilin near the active site. Proc Natl Acad Sci U S A. 2005 Mar 1;102(9): 3230-5.

Kukar TL, Ladd TB, Robertson P, Pintchovski SA, Moore B, Bann MA, Ren Z, Jansen-West K, Malphrus K, Eggert S, Maruyama H, Cottrell BA, Das P, Basi GS, Koo EH, Golde TE. Lysine 624 of the amyloid precursor protein (APP) is a critical determinant of amyloid β peptide length: support for a sequential model of γ-secretase intramembrane proteolysis and regulation by the amyloid β precursor protein (APP) juxtamembrane region. Biol Chem. 2011 Nov 18;286(46): 39804-12.

Lammich S, Okochi M, Takeda M, Kaether C, Capell A, Zimmer AK, Edbauer D, Walter J, Steiner H, Haass C. Presenilin-dependent intramembrane proteolysis of CD44 leads to the liberation of its intracellular domain and the secretion of an Abeta-like peptide. J Biol Chem. 2002 Nov 22;277(47):44754-9.

Lemberg MK, Martoglio B. Requirements for signal peptide peptidase-catalyzed intramembrane proteolysis.Mol Cell. 2002 Oct;10(4):735-44.

Li YM, Lai MT, Xu M, Huang Q, DiMuzio-Mower J, Sardana MK, Shi XP, Yin KC, Shafer JA, Gardell SJ. Presenilin 1 is linked with gamma-secretase activity in the detergent solubilized state. Proc Natl Acad Sci U S A. 2000 May 23;97(11):6138-43.

Lichtenthaler SF, Ida N, Multhaup G, Masters CL, Beyreuther K.Mutations in the transmembrane domain of APP altering gamma-secretase specificity. Biochemistry. 1997 Dec 9;36(49):15396-403.

Lichtenthaler SF, Wang R, Grimm H, Uljon SN, Masters CL, Beyreuther K. Mechanism of the cleavage specificity of Alzheimer's disease gamma-secretase identified by phenylalanine-scanning mutagenesis of the transmembrane domain of the amyloid precursor protein. Proc Natl Acad Sci U S A. 1999 Mar 16;96(6):3053-8.

Lichtenthaler SF, Beher D, Grimm HS, Wang R, Shearman MS, Masters CL, Beyreuther K. The intramembrane cleavage site of the amyloid precursor protein depends on the length of its transmembrane domain. Proc Natl Acad Sci U S A. 2002 Feb 5;99(3):1365-70. Epub 2002 Jan 22.

Moin SM, Urban S.Membrane immersion allows rhomboid proteases to achieve specificity by reading transmembrane segment dynamics.Elife. 2012 Nov 13;1:e00173.

Moore CL, Leatherwood DD, Diehl TS, Selkoe DJ, Wolfe MS. Difluoro ketone peptidomimetics suggest a large S1 pocket for Alzheimer's gamma-secretase: implications for inhibitor design. J Med Chem. 2000 Sep 7;43(18):3434-42.

Munter LM, Voigt P, Harmeier A, Kaden D, Gottschalk KE, Weise C, Pipkorn R, Schaefer M, Langosch D, Multhaup G. GxxxG motifs within the amyloid precursor protein transmembrane sequence are critical for the etiology of Abeta42.EMBO J. 2007 Mar 21;26(6):1702-12.

Murphy MP, Hickman LJ, Eckman CB, Uljon SN, Wang R, Golde TE. gamma-Secretase, evidence for multiple proteolytic activities and influence of membrane positioning of substrate on generation of amyloid beta peptides of varying length. J Biol Chem. 1999 Apr 23;274(17): 11914-23.

Okochi M, Steiner H, Fukumori A, Tanii H, Tomita T, Tanaka T, Iwatsubo T, Kudo T, Takeda M, Haass C. Presenilins mediate a dual intramembranous gamma-secretase cleavage of Notch-1. EMBO J. 2002 Oct 15;21(20):5408-16.

Okochi M, Tagami S, Yanagida K, Takami M, Kodama TS, Mori K, Nakayama T, Ihara Y, Takeda M.γ-secretase modulators and presenilin 1 mutants act differently on presenilin/γ-secretase function to cleave Aβ42 and Aβ43. Cell Rep. 2013 Jan 31;3(1):42-51.

O'Neil KT, DeGrado WF. A thermodynamic scale for the helix-forming tendencies of the commonly occurring amino acids.Science. 1990 Nov 2;250(4981):646-51.

Ousson S, Saric A, Baguet A, Losberger C, Genoud S, Vilbois F, Permanne B, Hussain I, Beher D. Substrate determinants in the C99 juxtamembrane domains differentially affect γ-secretase cleavage specificity and modulator pharmacology. J Neurochem. 2013 May;125(4):610-9. doi: 10.1111/jnc.12129. Epub 2013 Jan 18.

Qi-Takahara Y, Morishima-Kawashima M, Tanimura Y, Dolios G, Hirotani N, Horikoshi Y, Kametani F, Maeda M, Saido TC, Wang R, Ihara Y. Longer forms of amyloid beta protein: implications for the mechanism of intramembrane cleavage by gamma-secretase.J Neurosci. 2005 Jan 12;25(2):436-45.

Quintero-Monzon O, Martin MM, Fernandez MA, Cappello CA, Krzysiak AJ, Osenkowski P, Wolfe MS. Dissociation between the processivity and total activity of γ-secretase: implications for the mechanism of Alzheimer's disease-causing presenilin mutations. Biochemistry. 2011 Oct 25;50(42):9023-35.

Ren Z, Schenk D, Basi GS, Shapiro IP. Amyloid beta-protein precursor juxtamembrane domain regulates specificity of gamma-secretase-dependent cleavages. J Biol Chem. 2007 Nov 30;282(48):35350-60.

Richter L, Munter LM, Ness J, Hildebrand PW, Dasari M, Unterreitmeier S, Bulic B, Beyermann M, Gust R, Reif B, Weggen S, Langosch D, Multhaup G. Amyloid beta 42 peptide (Abeta42)-lowering compounds directly bind to Abeta and interfere with amyloid precursor protein (APP) transmembrane dimerization. Proc Natl Acad Sci U S A. 2010 Aug 17;107(33):14597-602. doi: 10.1073/pnas.1003026107.

Saito T, Suemoto T, Brouwers N, Sleegers K, Funamoto S, Mihira N, Matsuba Y, Yamada K, Nilsson P, Takano J, Nishimura M, Iwata N, Van Broeckhoven C, Ihara Y, Saido TC.Potent amyloidogenicity and pathogenicity of Aβ43.Nat Neurosci. 2011 Jul 3;14(8):1023-32. doi: 10.1038/nn.2858.

Sastre M, Steiner H, Fuchs K, Capell A, Multhaup G, Condron MM, Teplow DB, Haass C.Presenilin-dependent gamma-secretase processing of beta-amyloid precursor protein at a site corresponding to the S3 cleavage of Notch.EMBO Rep. 2001 Sep;2(9):835-41. Epub 2001 Aug 23.

Sato T, Dohmae N, Qi Y, Kakuda N, Misonou H, Mitsumori R, Maruyama H, Koo EH, Haass C, Takio K, Morishima-Kawashima M, Ishiura S, Ihara Y.Potential link between amyloid beta-

protein 42 and C-terminal fragment gamma 49-99 of beta-amyloid precursor protein.J Biol Chem. 2003 Jul 4;278(27):24294-301. Epub 2003 Apr 21.

Scheuermann S, Hambsch B, Hesse L, Stumm J, Schmidt C, Beher D, Bayer TA, Beyreuther K, Multhaup G. Homodimerization of amyloid precursor protein and its implication in the amyloidogenic pathway of Alzheimer's disease. J Biol Chem. 2001 Sep 7;276(36):33923-9.

Scheuner D, Eckman C, Jensen M, Song X, Citron M, Suzuki N, Bird TD, Hardy J, Hutton M, Kukull W, Larson E, Levy-Lahad E, Viitanen M, Peskind E, Poorkaj P, Schellenberg G, Tanzi R, Wasco W, Lannfelt L, Selkoe D, Younkin S. Secreted amyloid beta-protein similar to that in the senile plaques of Alzheimer's disease is increased in vivo by the presenilin 1 and 2 and APP mutations linked to familial Alzheimer's disease. Nat Med. 1996 Aug;2(8):864-70.

Selkoe DJ. Alzheimer's disease: genes, proteins, and therapy. Physiol Rev. 2001 Apr;81(2): 741-66.

So PP, Zeldich E, Seyb KI, Huang MM, Concannon JB, King GD, Chen CD, Cuny GD, Glicksman MA, Abraham CR. Lowering of amyloid beta peptide production with a small molecule inhibitor of amyloid-β precursor protein dimerization. Am J Neurodegener Dis. 2012;1(1):75-87.

Struhl G, Adachi A. Requirements for presenilin-dependent cleavage of notch and other transmembrane proteins. Mol Cell. 2000 Sep;6(3):625-36.

Takasugi N, Tomita T, Hayashi I, Tsuruoka M, Niimura M, Takahashi Y, Thinakaran G, Iwatsubo T. The role of presenilin cofactors in the gamma-secretase complex. Nature. 2003 Mar 27;422(6930):438-41.

Takami M, Nagashima Y, Sano Y, Ishihara S, Morishima-Kawashima M, Funamoto S, Ihara Y. gamma-Secretase: successive tripeptide and tetrapeptide release from the transmembrane domain of beta-carboxyl terminal fragment.J Neurosci. 2009 Oct 14;29(41):13042-52.

Tanzi RE, Bertram L. Twenty years of the Alzheimer's disease amyloid hypothesis: a genetic perspective.Cell. 2005 Feb 25;120(4):545-55.

Urban S, Freeman M.Substrate specificity of rhomboid intramembrane proteases is governed by helix-breaking residues in the substrate transmembrane domain.Mol Cell. 2003 Jun;11(6): 1425-34.

Vassar R, Bennett BD, Babu-Khan S, Kahn S, Mendiaz EA, Denis P, Teplow DB, Ross S, Amarante P, Loeloff R, Luo Y, Fisher S, Fuller J, Edenson S, Lile J, Jarosinski MA, Biere AL, Curran E, Burgess T, Louis JC, Collins F, Treanor J, Rogers G, Citron M. Beta-secretase cleavage of Alzheimer's amyloid precursor protein by the transmembrane aspartic protease BACE. Science. 1999 Oct 22;286(5440):735-41.

Wang R, Sweeney D, Gandy SE, Sisodia SS. The profile of soluble amyloid beta protein in cultured cell media. Detection and quantification of amyloid beta protein and variants by immunoprecipitation-mass spectrometry. J Biol Chem. 1996 Dec 13;271(50):31894-902.

Weidemann A, Eggert S, Reinhard FB, Vogel M, Paliga K, Baier G, Masters CL, Beyreuther K, Evin G. A novel epsilon-cleavage within the transmembrane domain of the Alzheimer amyloid precursor protein demonstrates homology with Notch processing. Biochemistry. 2002 Feb 26;41(8):2825-35.

Wolfe MS, Xia W, Ostaszewski BL, Diehl TS, Kimberly WT, Selkoe DJ. Two transmembrane aspartates in presenilin-1 required for presenilin endoproteolysis and gamma-secretase activity. Nature. 1999 Apr 8;398(6727):513-7.

Wolfe MS. Intramembrane proteolysis. Chem Rev. 2009 Apr;109(4):1599-612.

Ye J, Davé UP, Grishin NV, Goldstein JL, Brown MS.Asparagine-proline sequence within membrane-spanning segment of SREBP triggers intramembrane cleavage by site-2 protease.Proc Natl Acad Sci U S A. 2000 May 9;97(10):5123-8.

Zhao G, Mao G, Tan J, Dong Y, Cui MZ, Kim SH, Xu X. Identification of a new presenilin-dependent zeta-cleavage site within the transmembrane domain of amyloid precursor protein. J Biol Chem. 2004 Dec 3;279(49):50647-50. Epub 2004 Oct 13.

Chapter 4:

Investigation of the pathogenicity of ε- and ζ-cleaved Aβ peptides

Authors: Marty A. Fernandez, Margot Samson, and Michael S. Wolfe

Contributors: This project was designed by M.A.F. and M.S.W. M.S. assissted with generation of stable cell lines. All other experiments were carried out by M.A.F.

Abstract

The amyloid β-peptide (Aβ) is generated by proteolysis of the amyloid β-protein precursor C-terminal fragment, or CTFβ, by the presenilin (PS)-containing γ-secretase complex. A large body of evidence suggests that Aβ is the pathogenic initiator of AD. γ-secretase generates secreted Aβ peptides of 38-43 residues, and familial AD (FAD)-causing mutations within PS increase the proportion of Aβ42 generated relative to Aβ40. In recent years, longer, membrane-associated Aβs of 45-49 residues have been identified. Evidence suggests that these various Aβ species are generated by successive γ-secretase cleavages of CTFβ, which are thought to start at the initial ε sites to generate Aβ48 or Aβ49, followed by C-terminal trimming mostly every three residues to produce Aβ45 and Aβ46 and, finally, the shorter, secreted forms of Aβ. The C-terminal trimming function of γ-secretase is dramatically reduced by FAD mutations in PS, and, in addition to increasing the Aβ42/40 ratio, PS FAD mutations also increase the relative proportion of Aβ45-49. We investigated the potential pathogenic role of these long Aβs in AD. We could not detect these species in AD brains using available techniques. However, we did establish cell culture systems to examine their potential neurotoxicity and obtained preliminary data suggesting that these species could exhibit neurotoxic effects.

Introduction

Cerebral plaques composed of the amyloid β-peptide (Aβ) and neurofibrillary tangles composed of hyperphosphorylated tau protein are the two defining pathological features of Alzheimer's disease (AD) (Selkoe, 2001). A large body of evidence implicates Aβ as the initiator of AD pathogenesis and the trigger of downstream tau pathology and synaptic and neuronal loss (Hardy and Selkoe, 2002). Aβ is generated by sequential proteolysis of the transmembrane amyloid β-protein precursor (APP), first by β-secretase, which releases the soluble APP ectodomain (Vassar et al., 1999), and then by the presenilin (PS)-containing γ-secretase complex, which cleaves within the transmembrane domain of the remaining membrane-spanning stub, known as CTFβ; this cut by γ-secretase releases the APP intracellular domain (AICD) and generates the C-terminus of Aβ (Wolfe et al, 1999).

Cleavage of CTFβ by γ-secretase is heterogeneous and generates secreted Aβ species of 38-43 residues with varying C-termini. Aβ40 is the predominant secreted Aβ species. However, as the Aβ C-terminus is derived from the CTFβ transmembrane domain, Aβ42, and the less abundantly-secreted Aβ43, are more prone to aggregation and predominate in cerebral plaques (Iwatsubo et al., 1994; Jarrett et al., 1993). Mutations in APP that lead to early-onset familial forms of AD (FAD) either boost overall Aβ levels, increase Aβ's propensity to aggregate, or increase the ratio of Aβ42 generated relative to Aβ40 (Scheuner et al., 1996; Selkoe, 2001; Tanzi and Bertram, 2005). In addition, over 100 FAD mutations in PS have been identified, and they result in increased production of Aβ42 relative to Aβ40 (Bentahir et al., 2006; Citron et al., 1997; Duff et al., 1996; Scheuner et al., 1996; Selkoe, 2001). This genetic evidence suggests that Aβ

aggregation, and in particular the aggregation of longer species, is important in precipitating AD pathogenesis.

Data obtained in cells and *in vitro* demonstrates that the various secreted Aβ species are the result of successive γ-secretase cleavages of CTFβ. Initial endoproteolysis at the so-called ε sites near the membrane cytoplasm border produces Aβ48 or Aβ49 and releases the corresponding AICD fragments (AICD 49-99 or 50-99, respectively) (Gu et al., 2001; Sastre et al., 2001; Weidemann et al., 2001). Aβ48 and Aβ49, which are retained in the membrane, are then trimmed mostly every three residues, first at the so-called ζ sites to produce either Aβ45 or Aβ46, and then at the γ-sites to generate Aβ43 and Aβ42, which can be trimmed again to Aβ40 or Aβ38 (Funamoto et al, 2004; Okochi et al., 2013; Sato et al., 2003; Qi-Takahara et al., 2005; Takami et al. 2009; Zhao et al., 2004). These γ-site cleaved products apparently have enough of the transmembrane domain removed to be released from the membrane and secreted from cells.

Work on Aβ neurotoxicity has focused almost exclusively on aggregates formed by secreted Aβs. Early studies focused on the toxicity of fibrillar Aβ, which is the form present in plaques; however, the focus of the field has since shifted to soluble Aβ aggregates, as the level of soluble Aβ in the brain correlates better with AD than plaque burden (Walsh and Selkoe, 2007). The neurotoxic and synaptotoxic effects of soluble Aβ assemblies, including low-*n* oligomers, Aβ-derived diffusible ligands, and protofibrils have been examined (Hartley et al., 1999; Lambert et al., 1998; O'Nuallain et al., 2010; Walsh et al. 2002; Walsh and Selkoe, 2007). In particular, Aβ dimers, which have been isolated from human AD brains (Shankar et al., 2008) and are tightly associated with AD (Mc Donald et al., 2010), impair long term potentiation, reduce dendritic spine density in rodent hippocampal slices, and induce memory deficits in rats

(Shankar et al., 2008). Aβ dimers have also been shown to result in changes in tau phosphorylation and cytoskeletal alterations in rat primary neurons (Jin et al., 2011). More recently, injection of Aβ oligomers into the brains of macaques was shown to induce synapse loss and NFT formation (Forny-Germano et al., 2014). A potential role of intraneuronal Aβ has been considered, but any work on the pathogenicity of intraneuronal Aβ has primarily focused on Aβ42 (Abramowski et al., 2012, Tseng et al., 2004; Zhang et al. 2002). However, despite extensive evidence that Aβ leads to tau pathology (Choi et al., 2014; Götz et al, 2001; Hardy and Selkoe, 2002; Lewis et al. 2001) and that tau is a necessary downstream mediator of Aβ toxicity (Ittner et al., 2010; Rapoport et al., 2002; Roberson et al., 2007), the connections and pathways between Aβ and the NFTs observed in AD remain unclear (Ittner and Götz, 2011; Selkoe, 2011).

The long, membrane-associated Aβs produced by cleavage at the ε and ζ sites are not only precursors to the shorter, secreted forms of Aβ. They can also be released from γ-secretase before further trimming, and have been observed in *in vitro* assays, in cell culture, and in transgenic mouse brains (Chávez-Gutiérrez et al., 2011; Qi-Takahara et al., 2005; Quintero-Monzon et al., 2011; Zhao et al., 2004). The trimming function of γ-secretase is dramatically reduced by PS FAD mutations (Fernandez et al., 2014), and we and others have demonstrated that PS FAD mutations not only increase the Aβ42/40 ratio, but also increase the relative production of these longer Aβs (Chávez-Gutiérrez et al., 2012; Shimojo et al., 2008; Quintero-Monzon et al., 2011). Despite these findings, the potential role of intraneuronal ε- and ζ-cleaved species in initiating toxic tau pathology and AD pathogenesis has never been examined. Although they are membrane-associated and not secreted into the aqueous environment where they may self-associate into soluble aggregates, as is the traditional paradigm for Aβ toxicity, the

location of these Aβs within the neuronal membrane may place them in a prime position to elicit intracellular tau pathology. In fact, interaction with and disruption of the neuronal lipid bilayer, with downstream effects on the resident transmembrane proteins, is thought to be a way in which extracellular Aβ assemblies exert their cellular effects (Jin et al., 2011; Marchesi, 2005; Selkoe, 2011).

If these long Aβs are a pathogenic species in AD, they should be present in FAD and in sporadic AD (SAD) brains and not in control brains. To date, there is only one published report of these long Aβs in AD brains (Roher et al., 2004). In this study, the Aβ species present in the brains of three FAD patients with the APP mutation V717F (which is a mutation at Aβ residue 46) were examined by mass spectrometry. This mutation leads to early-onset, aggressive dementia and is pathologically characterized by the formation of flocculent plaques without dense cores and an abundance of tangles (Roher et al., 2004). The Aβs from these brains were digested with trypsin and cyanogen bromide, and the expected fragments of long Aβs were identified by mass spectrometry. However, this study did not compare the levels of these long Aβs to those of control brains.

In addition to correlating with AD, the long Aβs should exhibit neurotoxic and synaptotoxic effects or trigger pathological changes in tau if they are indeed a pathogenic entity. Surprisingly, the neurotoxicity of these Aβ species has never been examined.

Although these long Aβs have been shown to be retained in the cell membrane (Lefranc-Jullien et al., 2006, Qi-Takahara et al., 2005), we first rigorously examined the membrane localization of the long Aβs. We next analyzed samples from human AD and transgenic mouse brains for the presence of Aβ45-Aβ49 by immunoprecipitation and western blot. Last, we

established cellular systems for the analysis of the toxicity of these Aβ species, and provide preliminary evidence that these Aβs could exert cytotoxic effects on differentiated human neuroblastoma cells.

Materials and Methods

Cloning. The coding sequences for APP truncated at positions 45, 46, 48, and 49 (Aβ numbering) and harboring the Swedish mutation (K670N/M671L) were inserted into the inducible PiggyBac expression vector (System Bio Sciences) using the Infusion cloning system (Clontech).

Neuro2a stable cell line generation. Monoclonal Neuro2a (N2a) cell lines stably expressing APPε and APPζ were generated. Cells were seeded at a density of 50,000 per well of a 24-well plate, and transfected using Lipofectamine2000 (Invitrogen). Cells were selected by treatment with puromycin, grown until they were confluent, and re-seeded at various densities. Single clones were picked using cloning discs and transferred to 96-well plates. The monoclonal cell lines were screened for APP expression by treatment with cumate and western blot of the cell lysates after 24 h of induction. APP was detected using 22C11 (Millipore).

SH-SY5Y cell differentiation. Cells were seeded at a density of 100,000 cells per well of a fibronectin-coated 24-well plate. Cells were treated with complete growth media (1:1 Eagles Modified Essential Medium (ATCC) and Hamm's F-12 (Sigma-Aldrich) with 10% FBS) supplemented with 10 μM retinoic acid (Sigma-Aldrich) for 7 days. After 7 days, the cells were treated with serum free media (1:1 EMEM and F-12) containing 50 ng/mL brain-derived neurotrophic growth factor (BDNF) (Life Technologies) for 4 days.

Treatment of SH-SY5Y cells with Aβ peptides. Purified, synthetic Aβ peptides (Anaspec) were added to serum-free SY5Y media containing 50 ng/mL BDNF at 0.1, 1, 10 and 100 nM concentrations. Differentiated SY5Y cells were treated with the media containing the Aβ peptides, along with either 10 μM γ-secretase inhibitor DAPT or vehicle alone. The cells were treated for 7 days; the media was changed once on day 4, with fresh Aβ peptide added at this point. Cells were examined for any gross changes in appearance or for visible cell loss by bright field microscopy. Toxicity after the 7 days of Aβ peptide treatment was examined by assaying for lactate dehydrogenase (LDH) in the conditioned media using the LDH kit from Pierce.

Fractionation of brain samples and cells. Brain samples were homogenized in ice-cold TBS containing a protease inhibitor cocktail with 25 strokes of a mechanical Dounce homogenizer and spun at 100,000 X g. The resulting pellet was resuspended in TBS containing 1% TritonX-100 and re-homogenized, again with 25 strokes of a mechanical Dounce homogenizer. The homogenates were then spun at 100,000 X g, and the supernatant containing the Triton-soluble fraction was used for immunoprecipitation. In some cases, RIPA-soluble and formic acid-soluble material was isolated by re-homogenization of the pellet containing Triton-insoluble material in RIPA buffer, spinning at 100,000 X g, collection of the RIPA-soluble supernatant, and solubilization of the RIPA-insoluble fraction in formic acid by nutation overnight at 4 ^{o}C.

For analysis of long Aβ in cells, ten T75 flasks of HEK293 cells overexpressing human APP with the Swedish mutation and ten 15 cm plates of CHO S20 cells (which overexpress all four γ-secretase components) were harvested and homogenized in ice-cold TBS by extrusion through a 27.5 gauge needle. The homogenate was spun at low speed to remove large debris, and the supernatant was spun at 100,000 X g. The pellet was homogenized in Na_2CO_3 pH 11.3, incubated on ice for 20 min, and spun again at 100,000 X g. The resulting pellet was then

homogenized in TBS with 1% TritonX-100, spun again, and the process was repeated with RIPA buffer.

Aβ immunoprecipitation. Samples of the brain and cellular fractions described above were pre-cleared with Protein A sepharose beads, and Aβ was then immunoprecipitated from the samples using AW7 or R1282 (rabbit Aβ antisera, generously provided by Dominic Walsh and Dennis Selkoe) by nutation overnight at 4 ^{o}C. The resin was washed three times in STEN buffer (50 mM Tris, pH 7.6, 150 mM NaCl, 2 mM EDTA, and 1% NP-40), and immunoprecipitated Aβ was eluted from the beads by boiling in sample buffer for 10 min.

Urea gel electrophoresis. Aβs immunoprecipitated from brain samples and cells were analyzed by bicine and tricine urea gel electrophoresis. The bicine gel system has been previously described (Quintero-Monzon et al., 2011), and separates Aβ38-45, while Aβ46-49 run together at the gel front. The tricine gel separates all Aβ species, but CTFβ runs near Aβ40, interfering with its detection. This gel system is composed of a 22-cm separating layer, a 2-cm spacer layer, and a 4-cm comb layer of the following compositions, respectively: 8 M urea, 1 M Tris pH 8.95, 0.1% SDS, and acrylamide (10% T/3% C); 1 M Tris pH 8.95, 0.1% SDS, and acrylamide (10% T/3% C); and 1M Tris pH 8.45, 0.1% SDS, and acrylamide (4% T/ 3.3% C). The tricine gel is run for 1 h at 12 mA and for roughly 5.5 h at 34 W, until the dye front reaches the bottom of the gel. Proteins separated by bicine or tricine gel electrophoresis were transferred to PVDF, and immunoprecipitated Aβ was detected by western blotting with 6E10.

Results

Membrane localization of long Aβs-- Although Aβ45, Aβ46, Aβ48, and Aβ49 have been shown to be membrane-associated (Lefranc-Jullien et al., 2006, Qi-Takahara et al., 2005), we wanted to confirm these results experimentally. Moreover, we wanted to perform a rigorous analysis, including a step in which the membranes are washed with Na_2CO_3 buffer (Figure 4.1A). This step removes adsorbed or membrane-associated proteins that are not inserted into the membrane and which may be found in membrane fractions if this wash step is not performed. We analyzed the Aβs present in the water-soluble, Na_2CO_3-extracted, triton-soluble, and RIPA-soluble fractions from two different cell types (HEK cells overexpressing human APP harboring the Swedish FAD mutation, and S20 cells, CHO cells overexpressing all four γ-secretase components and human APP) by immunoprecipitation followed by urea gel electrophoresis and western blotting with 6E10. The epitope of 6E10 is the Aβ N-terminus, and thus it detects the entire range of C-terminal Aβ species. We found that these long Aβs were primarily in the triton-soluble fraction, and thus are indeed primarily retained within the membrane (Figure 4.1B). Determining the membrane localization of these Aβs could provide some insight into their toxicity (i.e., are the long Aβs toxic despite being retained in the membrane and not secreted from cells and aggregated, or are they non-toxic because they are retained in the membrane?). Such information is particularly important because the toxicity of membrane-inserted, non-secreted Aβ has remained largely unconsidered and has not been previously demonstrated.

Analysis of Aβ45-49 in AD brain samples-- We first analyzed cortical samples from sporadic AD brains for the presence of long Aβs. Aβ was immunoprecipitated from the

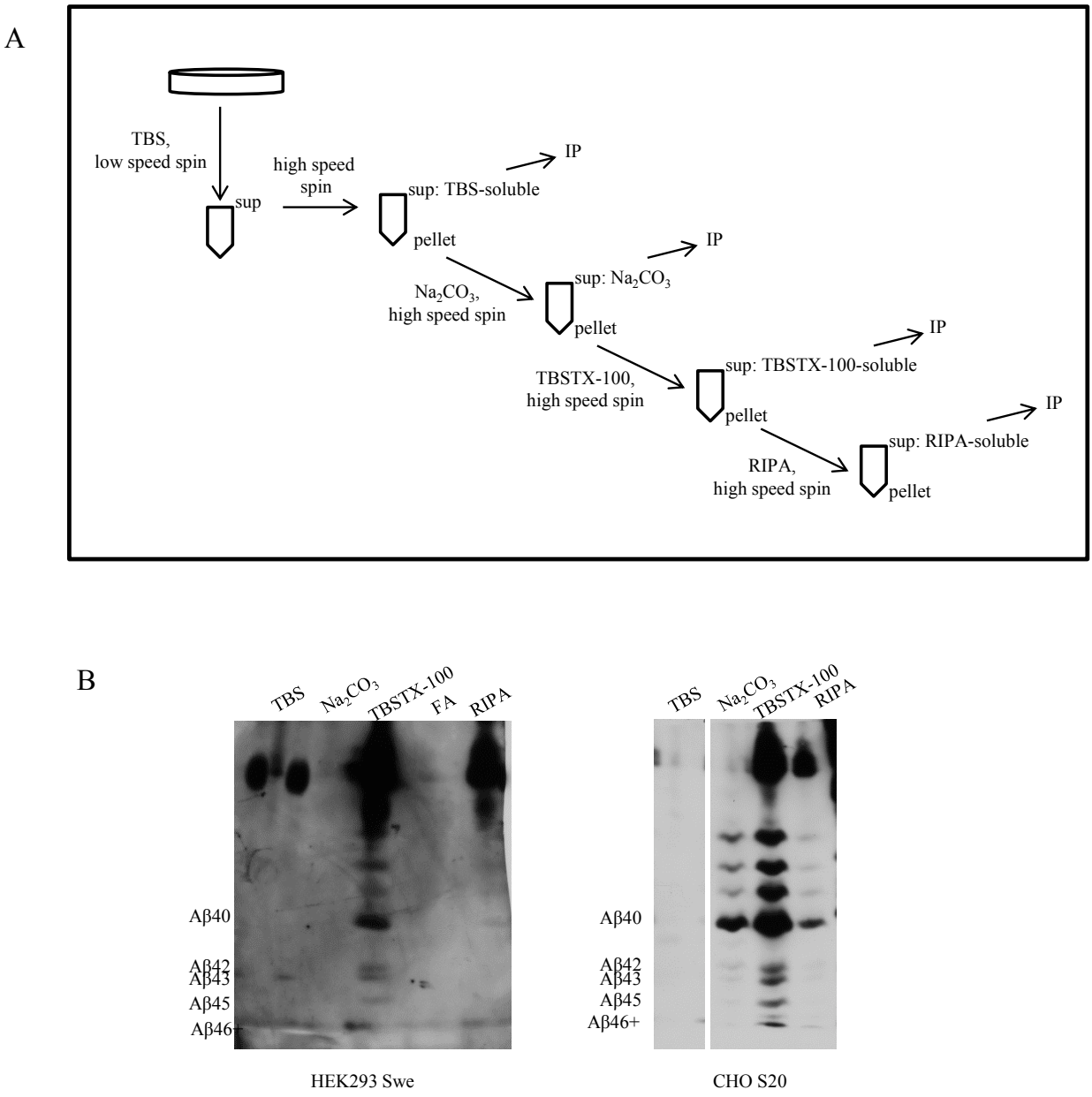

Figure 4.1. Aβ45-49 are primarily in the cell membrane. (A) TBS-soluble, Na_2CO_3-extracted, triton-soluble, and RIPA-soluble fractions were obtained from HEK293 cells overexpressing APP with the Swedish double mutation and from S20 cells, CHO cells overexpressing all four γ-secretase components and human APP. For the HEK cells, the RIPA-insoluble material was re-homogenized in formic acid (FA) for analysis. (B) Aβ was immunoprecipitated from each fraction using AW7 and detected by urea gel electrophoresis followed by western blotting with 6E10.

detergent-soluble fractions of homogenized brain samples (Figure 4.2A) using polyclonal Aβ antibodies. The immunoprecipitated Aβs were separated by urea gel electrophoresis, detected by western blotting with 6E10, and identified by comparing their the migration to that of synthetic Aβ peptides. For the first panel of brain samples we analyzed, which included sporadic AD samples and an age-matched control sample (Figure 4.2B), we observed putative long Aβs specifically in the AD brains; however, these species didn't quite co-migrate with any Aβ standards and were immunoreactive with the Aβ40- and Aβ42-specific antibodies 2G3 and 21F12; thus, their identity is unknown. We speculate that these unidentified Aβs could simply be post-translationally modified shorter Aβ peptides. For example, they may be oxidized, phosphorylated, pyro-glutamylated, or perhaps lipid-associated. We also observed putative long Aβs in a second set of AD brain samples (Figure 4.2C), but, again, these Aβs didn't quite co-migrate with the Aβ standards. We again stripped and re-probed the blot using 2G3 and 21F12, and the bands running near Aβ46 in the formic acid fractions of samples 1 and 2 were clearly immunoreactive with these antibodies. However, the overall signal was lower and the synthetic Aβ40 standard was not detected in the re-probed blot, making it difficult to ascertain if the remaining bands running aberrantly in the gel are modified Aβ40 and Aβ42. For the last group of brain samples we analyzed (Figure 4.2D) we increased the amount of initial starting brain material above the standard amounts used for typical analysis of Aβ40 and Aβ42 (McDonald et al., 2010), as we expect that the long Aβs will be present at much lower levels compared to shorter Aβs (Qi-Takahara et al., 2005). However, as shown in Figure 4.2D, we were still unable to detect long Aβ species; the Aβs that co-migrated with the long Aβ standards were again

Figure 4.2. Analysis of Aβ45-49 in AD brain samples. (A) AD and control brains were fractionated as shown. Triton-soluble, and, in some cases, RIPA-soluble and formic acid-soluble fractions were obtained. Formic acid solubilizes Aβ present in plaques. (B-D) Human AD and control cortical brain samples were analyzed for the presence of Aβ45-49 by immunoprecpitation followed by urea gel electrophoresis and western blotting. For panels (B-D), the blot on the left was probed with 6E10 to detect all Aβ species, and the blot on the right is the same membrane, stripped and re-probed with Aβ40- and Aβ42-specific antibodies (2G3 and 21F12). Asterisks indicate Aβs that did not co-migrate with Aβ standards. Samples analyzed in (B) were TBSTX-100-soluble fractions, and the patients who donated these samples were given a Clinical Dementia Rating (CDR). 2/3 indicates moderate to severe AD and 1 indicates mild AD. The control sample was from an age-matched patient with no clinical AD. For each sample, 200 mg of brain was used, and Aβs were separated by tricine urea gel. CTFβ interferes with Aβ40 detection in the tricine gel, and therefore some of the signal co-migrating with Aβ40 may be CTFβ in the membrane. For (C), s1, s2, and s3 were all AD brain samples. No clinical data was available for these samples, other than that they were considered to be cases of severe AD. TBSTX-100-soluble, RIPA-soluble, and formic acid-soluble brain fractions were analyzed. 200 mg samples were used, and the Aβs were separated by tricine urea gel. Again, CTFβ and Aβ40 co-migrate. For (D) the first two sample lanes (labeled s1 and s2) are the Aβs from the TBSTX-100-soluble fraction of the hemibrains of 2 month old 5X FAD mice. The next 4 sample lanes (s3-s6) are the Aβs immunoprecipitated from the TBSTX-100-soluble fraction of 1.2 g human AD brain samples. Aβs were immunoprecipitated from these samples using R1282 and separated by bicine urea gel. As with (C), no clinical data was available for the human samples other than that they were considered to be cases of severe AD.

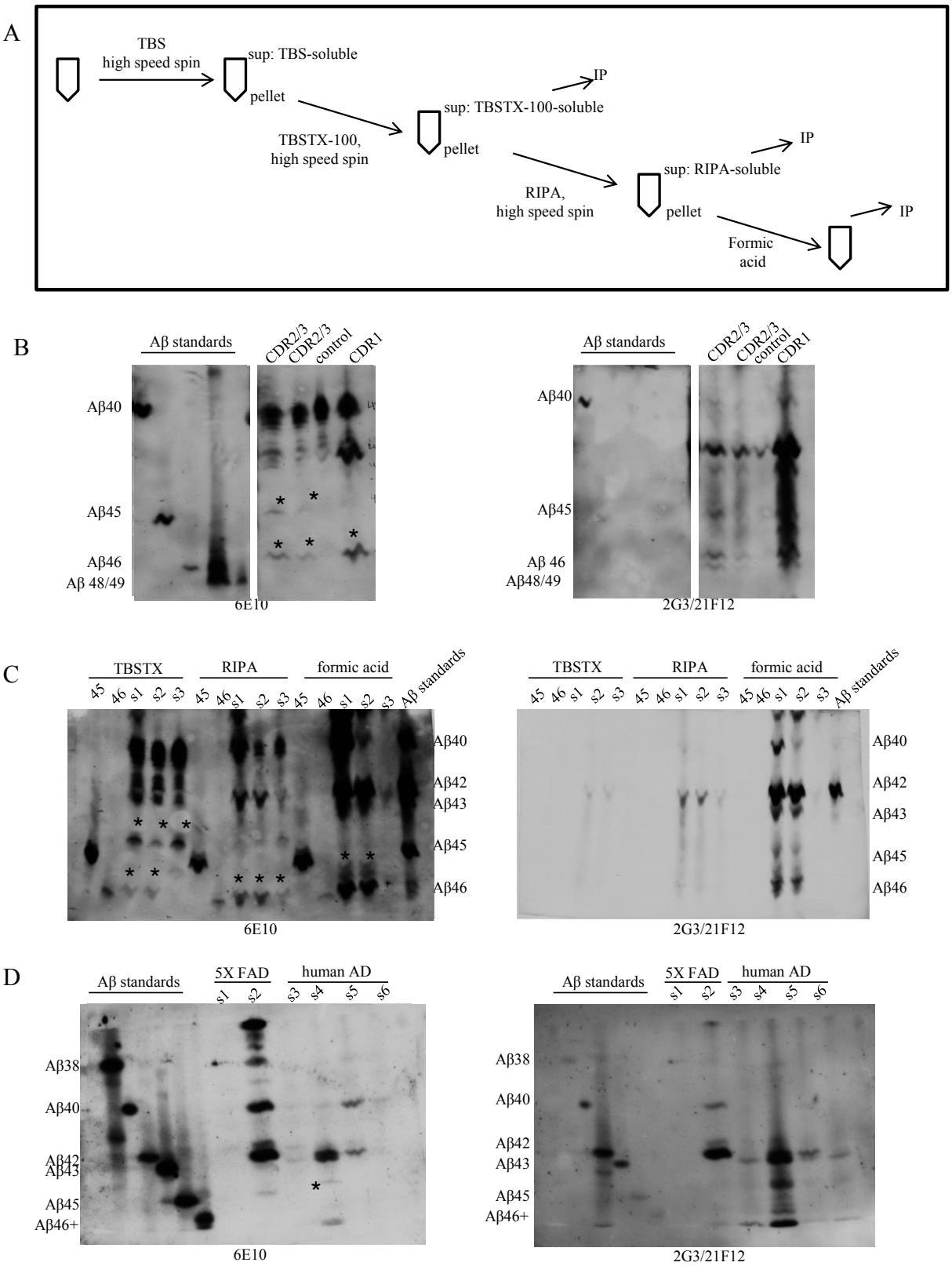

Figure 4.2 continued. Analysis of Aβ45-49 in AD brain samples.

detected by Aβ40- and Aβ42-specific antibodies, and could again simply be modified forms of shorter Aβ.

We also analyzed brains from mice transgenic for human APP and PS1 and harboring five FAD mutations: three within the APP transgene (V717I (the London mutation), I716V (the Florida mutation), and K670N/M671L (the Swedish mutation)) and two within the PS1 transgene (M146L and L286V). These mice exhibit plaque pathology by two months of age, synaptic loss by four months of age, and neuronal loss by nine months of age (Oakley et al., 2006). Synaptic and neuronal loss in these mice is accompanied by memory deficits (Oakley et al., 2006). We immunoprecipitated Aβ from the triton-soluble fraction of the hemibrains of two mice of two months of age. After urea gel electrophoresis and western blotting of the immunoprecipitated Aβ species, we detected a band co-migrating with Aβ45 in one of the samples. Stripping and re-probing the blot with Aβ40- and Aβ42-specific antibodies showed that this band did not cross-react, suggesting that this species could be Aβ45. Oddly, no Aβs (including Aβ40 or Aβ42) were detected in one of the mouse brains.

Development of systems for analysis of long Aβ toxicity-- We developed several systems to investigate the toxicity of Aβ45, Aβ46, Aβ48, and Aβ49. As explained in Chapter 2, attempts at direct expression of these long Aβs along with the APP signal sequence have resulted in very low levels of the Aβs in the membrane (Funamoto et al, 2004). In contrast, the expression of APPε, truncated at Aβ49, has been previously reported (LeFranc-Jullien et al. 2006), and the expression of both APPε49 and APPε48 worked well in our hands (Figure 2.3 and Fernandez et al., 2014); these APPs were not only highly expressed, but their expression resulted in increased

secretion of Aβ40 and Aβ42 in CHO cells, indicating that they are cleaved by β-secretase and subsequently trimmed by γ-secretase (Figure 2.3 and Fernandez et al., 2014). Therefore, we cloned APPζ45, APPζ46, APPε48, and APPε49 into the PiggyBac inducible vector, which places their expression under the control of a cumate-inducible promoter. Expression of these truncated APPs will lead to the production of their respective long Aβs once the APP is cleaved by β-secretase; each construct is harboring the Swedish mutation to boost cleavage by β-secretase (Figure 4.3A). In addition, treatment of the cells with a γ-secretase inhibitor (GSI) will prevent the resulting long Aβs from simply being trimmed to secreted Aβs by γ-secretase (Figure 2.3 and Fernandez et al., 2014) and will instead allow them to accumulate (Figure 4.3A). We first attempted to generate monoclonal SH-SY5Y cell lines stably expressing these APPs. SH-SY5Y is a human neuroblastoma cell line that can be differentiated into a post-mitotic neuronal state characterized by extensive neurites and axonal tau (Encinas et al., 2000). However, these cells are technically challenging to transfect, and we were unable to generate a stable cell line with them despite repeated attempts with various transfection reagents, cell densities, and plasmid concentrations. We were, however, able to generate monoclonal murine N2a cell lines stably expressing APPs truncated at position 48, 46, and 45; the APPε49 clone generated was ruined by bacterial contamination and needs to be repeated. We confirmed that the APPs are indeed expressed upon cumate induction (Figure 4.3B); the truncated APPs run slightly faster than endogenous, full-length APP. These cells have been grown with APP expression induced and with GSI treatment (the conditions under which the long Aβs can accumulate) for up to 10 days, with no obvious differences in cell death, growth, or morphology compared to uninduced cells

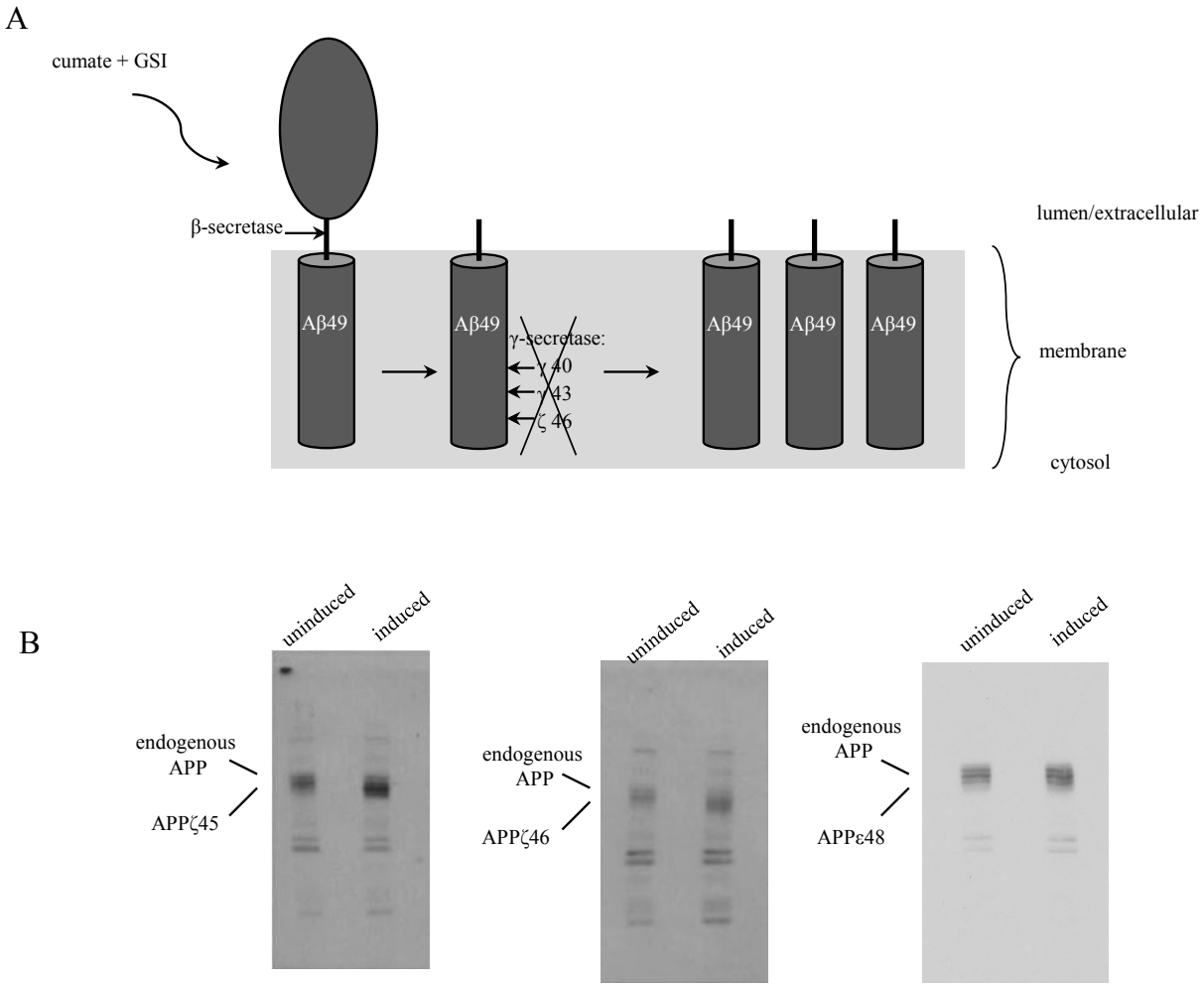

Figure 4.3. Development of inducible APPζ- and APPε-expressing N2a cell lines. (A) The expression of truncated APPs, using the PiggyBac inducible system, will result in APP expression when cumate is added to the media. These APPs will be cleaved by β-secretase to generate the respective long Aβ, and γ-secretase inhibitor (GSI) will prevent their trimming, allowing them to accumulate. (B) The expression of truncated APPs was induced with the addition of cumate to the media of APPε48 and APPζ45, and APPζ46 N2a monoclonal cell lines. Cells were lysed 24 hours post-induction, and APPε and APPζ were detected using 22C11, an antibody that binds the APP ectodomain.

treated with GSI alone. We found that transient expression of the trunctated APPs in N2a cells does not result in an increase in Aβ40 and Aβ42 secretion as measured by ELISA (data not shown). In contrast, transient expression of APPε49 and APPε48 in CHO cells overexpressing γ-secretase did result in increased Aβ40 and Aβ42 secretion (Figure 2.3 and Fernandez et al., 2014). However, unlike the CHO cells used in Chapter 2, the N2a cells express endogenous levels of γ-secretase, and therefore Aβ secretion may have been too low for detection.

As explained in Chapter 1, mice do not develop tau pathology without a human tau transgene (Chin, 2011; Selkoe 2011; Yankner and Lu, 2009). Therefore, testing Aβ45-49 toxicity in a more relevant human neuronal system is still desirable. As attempts to generate stable cell lines using SH-SY5Y cells failed, we decided to obtain preliminary data on long Aβ toxicity using these human cells by simply treating them with the long Aβ peptides. We reasoned that a fraction of the peptides would insert into the membrane due to their extremely hydrophobic C-termini, which would also place them in same orientation that they have when they are generated within cells (Figure 4.4A). We differentiated the SH-SY5Y cells for this experiment, as this differentiated state is more relevant to human neurons, and the resulting neuronal processes could render cells more sensitive to toxic insults. We treated cells with 0, 0.1, 1, 10, and 100 nM Aβ40, Aβ42, Aβ45, and Aβ46. We set 100 nM as the highest concentration to test to avoid extremely high, and physiologically-irrelevant concentrations, and also to prevent aggregation of the peptides in the media, which could interfere with their membrane insertion. Each concentration of each peptide was tested under two conditions: with GSI treatment, which will prevent any inserted Aβ from becoming a γ-secretase substrate, and with vehicle alone. After 7 days of Aβ treatment, the cells were analyzed by bright field microscopy. As shown in

Figure 4.4. Analysis of long Aβ toxicity in differentiated SH-SY5Y cells. (A) Synthetic long Aβ peptides were added to the media of differentiated SH-SY5Y cells at 0.1, 1, 10, and 100 nM concentrations. We hypothesize that this treatment results in the insertion of a small percentage of these long Aβs into the cell membrane. Cells were also treated with 10 μM of the GSI DAPT or vehicle alone. After 7 days of Aβ treatment, cells were examined by microscopy (panel B) and assayed for LDH levels in the conditioned media (panel C). For the positive control LDH samples, lysis buffer was added to the media for 1 hour. n=1. The graph on the right is the same as the graph on the left, but with the positive control data removed.

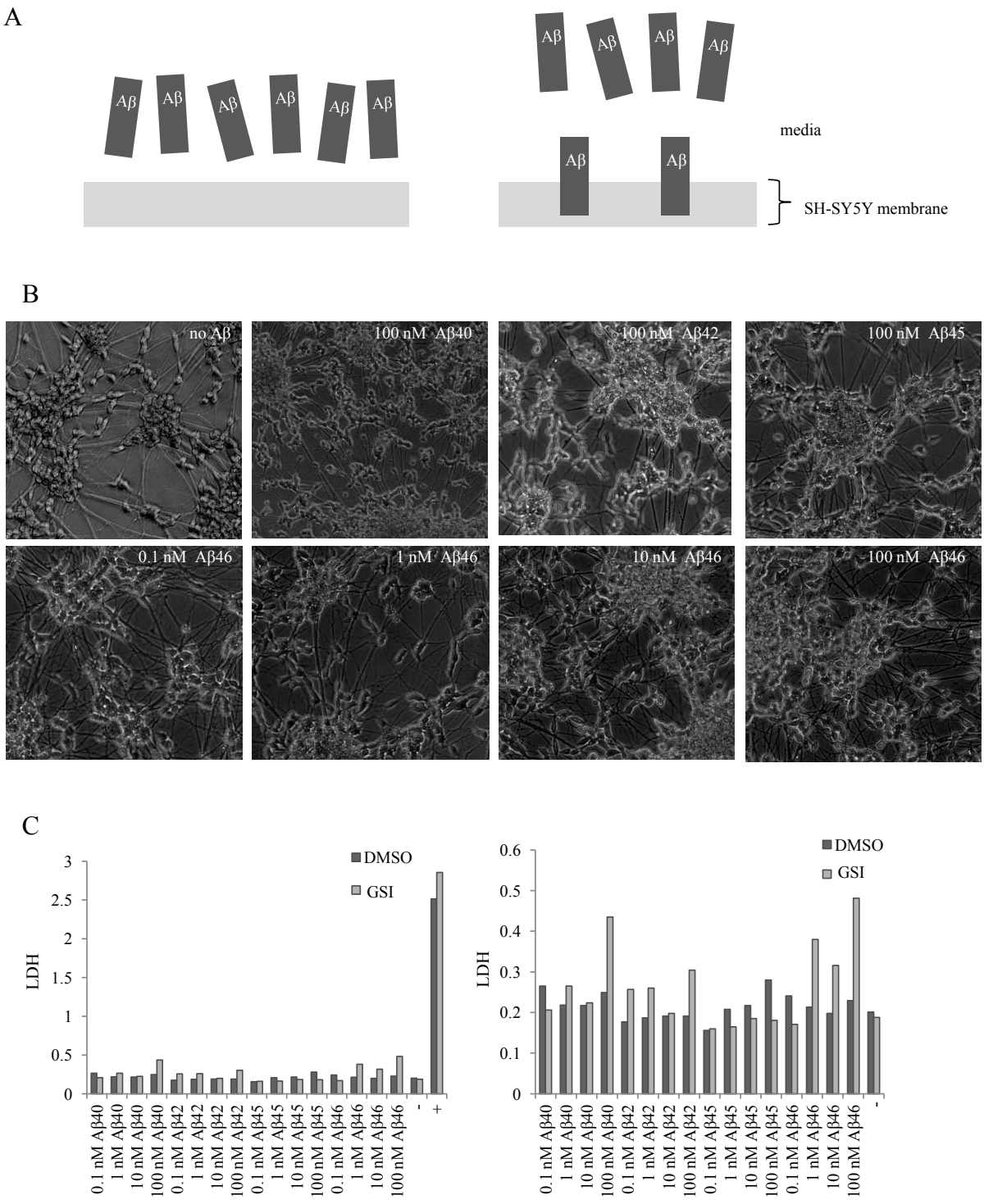

Figure 4.4 continued. Analysis of long Aβ toxicity in differentiated SH-SY5Y cells.

Figure 4.4B, no obvious qualitative changes in the number or condition of cells or neurites could be observed. Next, an LDH assay was performed on the conditioned media of the cells (Figure 4.4C). We found that the 1, 10, and 100 nM Aβ46 treatment resulted in elevated LDH in the conditioned media, although these results need to be repeated for statistical analysis. This increase was dependent on DAPT treatment, suggesting that it could be due to the accumulation of Aβ46 in the membrane, which would otherwise be cleaved by γ-secretase when no inhibitor is present. The lack of a clear dose response may be due to the fact that more aggregation, and therefore less membrane insertion, could occur at higher peptide concentrations. Aβ42 and Aβ40 treatment only elicited increases in LDH levels at 100 nM. However, the toxicity observed with Aβ treatment was subtle compared to the positive control in Figure 4.4C, which represents 100% cell death.

Discussion

The potential role of the long, membrane-associated Aβs 45, 46, 48 and 49 in the pathogenesis of AD should be examined, even if to eliminate these species as potential pathogenic entities. First, the human genetics of AD supports a potential role of these species in AD, as FAD mutations in PS1 not only increase the Aβ42/Aβ40 ratio, but also increase the proportion of these longer Aβs (Chávez-Gutiérrez et al., 2012; Shimojo et al., 2008; Quintero-Monzon et al., 2011). Second, the case of Aβ toxicity is not closed and does not exclude a role for these longer species: the specific Aβ species and the mechanisms by which Aβ exerts its toxic effects and elicits intracellular changes in tau remain unclear (Ittner and Götz, 2011; Selkoe, 2011). If these long Aβs are pathogenic entities in AD, they should be present in FAD and SAD

brains and not in control brains. They should also be neurotoxic and able to elicit AD-relevant pathology such as synaptic damage and tau phosphorylation or tangle formation.

We analyzed brain tissue from an AD mouse model and from human AD and control brain samples. While a putative Aβ45 species was found in a 5X FAD mouse brain, we were unable to detect long Aβ species in human AD brains. These results could indicate that the levels of Aβ45-49 are too low to be detected by immunoprecipitation and western blot, that the modified shorter Aβ species are interfering with Aβ45-49 detection by urea gel electrophoresis, that these species are simply not extracted during our homogenization procedure, that Aβ45-49 are not present in late-stage AD brains, or that they are not present at any stage and therefore are not a causative species in AD. It is clear that the methods we have used here have many drawbacks, such as co-migration of shorter, modified Aβ species, and may not be ideal for analysis of AD brains. Given the limitations of the methods used here, detection of Aβ45-49 by mass spectrometry or using specific antibodies may be necessary. Specific antibodies have been invaluable tools for the analysis of Aβ40, Aβ42, and most recently Aβ43 (Saito et al., 2011), and could be extremely useful for this analysis as well.

We also developed several systems for the analysis of the toxicity of these species. We generated N2a cell lines that express truncated APPs, which are converted to long Aβs once β-secretase cleavage occurs. We will attempt to detect the long Aβs in the membranes of these cells by Aβ immunoprecipitation and western blot, and we will examine the toxicity of these long Aβs by standard toxicity assays, such as measuring LDH release. Controls will include the use of a β-secretase inhibitor, which will ensure that any toxicity is dependent on Aβ production and not simply due to expression of the truncated APPs, and treatment with vehicle alone, as opposed

to with a GSI, as this will allow γ-secretase to trim long Aβs to secreted forms and should attenuate any toxicity.

In addition, we have treated differentiated SH-SY5Y cells with long Aβ peptides. Our results are preliminary so far, yet provide potential evidence of long Aβ toxicity, as Aβ46 increased LDH levels in the conditioned media of these cells at nanomolar concentrations. We will repeat these results and examine the lysates of treated cells for any changes in tau phosphorylation. We will also determine if these long Aβs indeed insert into the membrane when they are added to the media by isolating and solubilizing the membrane from these cells, washing them with Na_2CO_3 buffer, and immunoprecipitating Aβ from the membrane fraction. In addition, we will examine if Aβ40 and Aβ42 are increased upon treatment of cells with long Aβ peptides by performing Aβ40 and Aβ42 ELISAs of the conditioned media; generation of Aβ40 and Aβ42 from the long Aβ peptides will provide evidence that they are inserted into the membrane and in an orientation that allows γ-secretase cleavage. Furthermore, we are planning to examine the effects of these long Aβs in more AD-relevant systems, as explained in Chapter 5.

Abbreviations-- Aβ, amyloid β-peptide; AD, Alzheimer's disease; APP, amyloid β-protein precursor; FAD, familial Alzheimer's disease; GSM, γ-secretase modulator; Bicine, N,N-bis(2-hydroxyethyl)glycine; DAPT, N-[N-(3,5-difluorophenacetyl)-L-alanyl]-S-phenylglycine t-butyl ester; LDH, lactate dehydrogenase; N2a, Neuro2a; SDS, sodium dodecyl sulfate; Tricine, N-(2-Hydroxy-1,1-bis(hydroxymethyl)ethyl)glycine

Acknowledgements-- We thank D. Walsh for providing brain samples and AW7. We thank D. Selkoe for providing R1282.

References

Abramowski D, Rabe S, Upadhaya AR, Reichwald J, Danner S, Staab D, Capetillo-Zarate E, Yamaguchi H, Saido TC, Wiederhold KH, Thal DR, Staufenbiel M. Transgenic expression of intraneuronal Aβ42 but not Aβ40 leads to cellular Aβ lesions, degeneration, and functional impairment without typical Alzheimer's disease pathology. J Neurosci. 2012 Jan 25;32(4): 1273-83

Bentahir M, Nyabi O, Verhamme J, Tolia A, Horré K, Wiltfang J, Esselmann H, De Strooper B. Presenilin clinical mutations can affect gamma-secretase activity by different mechanisms.J Neurochem. 2006 Feb;96(3):732-42. Epub 2006 Jan 9.

Chávez-Gutiérrez L, Bammens L, Benilova I, Vandersteen A, Benurwar M, Borgers M, Lismont S, Zhou L, Van Cleynenbreugel S, Esselmann H, Wiltfang J, Serneels L, Karran E, Gijsen H, Schymkowitz J, Rousseau F, Broersen K, De Strooper B. The mechanism of γ-Secretase dysfunction in familial Alzheimer disease. EMBO J. 2012 May 16;31(10):2261-74.

Chin J. Selecting a mouse model of Alzheimer's disease. Methods Mol Biol. 2011;670:169-89.

Choi SH, Kim YH, Hebisch M, Sliwinski C, Lee S, D'Avanzo C, Chen H, Hooli B, Asselin C, Muffat J, Klee JB, Zhang C, Wainger BJ, Peitz M, Kovacs DM, Woolf CJ, Wagner SL, Tanzi RE, Kim DY. A three-dimensional human neural cell culture model of Alzheimer's disease. Nature. 2014 Nov 13;515(7526):274-8.

Citron M, Westaway D, Xia W, Carlson G, Diehl T, Levesque G, Johnson-Wood K, Lee M, Seubert P, Davis A, Kholodenko D, Motter R, Sherrington R, Perry B, Yao H, Strome R, Lieberburg I, Rommens J, Kim S, Schenk D, Fraser P, St George Hyslop P, Selkoe DJ. Mutant presenilins of Alzheimer's disease increase production of 42-residue amyloid beta-protein in both transfected cells and transgenic mice. Nat Med. 1997 Jan;3(1):67-72.

Duff K, Eckman C, Zehr C, Yu X, Prada CM, Perez-tur J, Hutton M, Buee L, Harigaya Y, Yager D, Morgan D, Gordon MN, Holcomb L, Refolo L, Zenk B, Hardy J, Younkin S.Increased amyloid-beta42(43) in brains of mice expressing mutant presenilin 1.Nature. 1996 Oct 24;383(6602):710-3.

Encinas M, Iglesias M, Liu Y, Wang H, Muhaisen A, Ceña V, Gallego C, Comella JX. Sequential treatment of SH-SY5Y cells with retinoic acid and brain-derived neurotrophic factor gives rise to fully differentiated, neurotrophic factor-dependent, human neuron-like cells. J Neurochem. 2000 Sep;75(3):991-1003.

Fernandez MA, Klutkowski JA, Freret T, Wolfe MS.Alzheimer presenilin-1 mutations dramatically reduce trimming of long amyloid β-peptides (Aβ) by γ-secretase to increase 42-to-40-residue Aβ. J Biol Chem. 2014 Nov 7;289(45):31043-52.

Forny-Germano L, Lyra e Silva NM, Batista AF, Brito-Moreira J, Gralle M, Boehnke SE, Coe BC, Lablans A, Marques SA, Martinez AM, Klein WL, Houzel JC, Ferreira ST, Munoz DP, De Felice FG. Alzheimer's disease-like pathology induced by amyloid-β oligomers in nonhuman primates. J Neurosci. 2014 Oct 8;34(41):13629-43.

Funamoto S, Morishima-Kawashima M, Tanimura Y, Hirotani N, Saido TC, Ihara Y. Biochemistry. 2004 Oct 26;43(42):13532-40.Truncated carboxyl-terminal fragments of beta-amyloid precursor protein are processed to amyloid beta-proteins 40 and 42.Biochemistry. 2004 Oct 26;43(42):13532-40.

Götz J, Chen F, van Dorpe J, Nitsch RM. Formation of neurofibrillary tangles in P301l tau transgenic mice induced by Abeta 42 fibrils. Science. 2001 Aug 24;293(5534):1491-5.

Gu Y, Misonou H, Sato T, Dohmae N, Takio K, Ihara Y.Distinct intramembrane cleavage of the beta-amyloid precursor protein family resembling gamma-secretase-like cleavage of Notch. J Biol Chem. 2001 Sep 21;276(38):35235-8. Epub 2001 Aug 1.

Hardy J, Selkoe DJ..The amyloid hypothesis of Alzheimer's disease: progress and problems on the road to therapeutics. Science. 2002 Jul 19;297(5580):353-6.

Hartley DM, Walsh DM, Ye CP, Diehl T, Vasquez S, Vassilev PM, Teplow DB, Selkoe DJ. Protofibrillar intermediates of amyloid beta-protein induce acute electrophysiological changes and progressive neurotoxicity in cortical neurons. J Neurosci. 1999 Oct 15;19(20):8876-84.

Ittner LM, Ke YD, Delerue F, Bi M, Gladbach A, van Eersel J, Wölfing H, Chieng BC, Christie MJ, Napier IA, Eckert A, Staufenbiel M, Hardeman E, Götz J. Dendritic function of tau mediates amyloid-beta toxicity in Alzheimer's disease mouse models. Cell. 2010 Aug 6;142(3):387-97.

Ittner LM, Götz J. Amyloid-β and tau--a toxic pas de deux in Alzheimer's disease. Nat Rev Neurosci. 2011 Feb;12(2):65-72.

Iwatsubo T, Odaka A, Suzuki N, Mizusawa H, Nukina N, Ihara Y. Visualization of A beta 42(43) and A beta 40 in senile plaques with end-specific A beta monoclonals: evidence that an initially deposited species is A beta 42(43).Neuron. 1994 Jul;13(1):45-53.

Jarrett JT, Berger EP, Lansbury PT Jr. The carboxy terminus of the beta amyloid protein is critical for the seeding of amyloid formation: implications for the pathogenesis of Alzheimer's disease. Biochemistry. 1993 May 11;32(18):4693-7.

Jin M, Shepardson N, Yang T, Chen G, Walsh D, Selkoe DJ. Soluble amyloid beta-protein dimers isolated from Alzheimer cortex directly induce Tau hyperphosphorylation and neuritic degeneration. Proc Natl Acad Sci U S A. 2011 Apr 5;108(14):5819-24.

Lambert MP, Barlow AK, Chromy BA, Edwards C, Freed R, Liosatos M, Morgan TE, Rozovsky I, Trommer B, Viola KL, Wals P, Zhang C, Finch CE, Krafft GA, Klein WL.Diffusible, nonfibrillar ligands derived from Abeta1-42 are potent central nervous system neurotoxins. Proc Natl Acad Sci U S A. 1998 May 26;95(11):6448-53.

Lefranc-Jullien S, Sunyach C, Checler F. APPepsilon, the epsilon-secretase-derived N-terminal product of the beta-amyloid precursor protein, behaves as a type I protein and undergoes alpha-, beta-, and gamma-secretase cleavages. J Neurochem. 2006 May;97(3):807-17.

Lewis J, Dickson DW, Lin WL, Chisholm L, Corral A, Jones G, Yen SH, Sahara N, Skipper L, Yager D, Eckman C, Hardy J, Hutton M, McGowan E. Enhanced neurofibrillary degeneration in transgenic mice expressing mutant tau and APP. Science. 2001 Aug 24;293(5534):1487-91.

Marchesi VT. An alternative interpretation of the amyloid Abeta hypothesis with regard to the pathogenesis of Alzheimer's disease. Proc Natl Acad Sci U S A. 2005 Jun 28;102(26):9093-8.

Mc Donald JM, Savva GM, Brayne C, Welzel AT, Forster G, Shankar GM, Selkoe DJ, Ince PG, Walsh DM; Medical Research Council Cognitive Function and Ageing Study. The presence of sodium dodecyl sulphate-stable Abeta dimers is strongly associated with Alzheimer-type dementia. Brain. 2010 May;133(Pt 5):1328-41. doi: 10.1093/brain/awq065.

Oakley H, Cole SL, Logan S, Maus E, Shao P, Craft J, Guillozet-Bongaarts A, Ohno M, Disterhoft J, Van Eldik L, Berry R, Vassar R. Intraneuronal beta-amyloid aggregates, neurodegeneration, and neuron loss in transgenic mice with five familial Alzheimer's disease mutations: potential factors in amyloid plaque formation. J Neurosci. 2006 Oct 4;26(40): 10129-40.

Okochi M, Tagami S, Yanagida K, Takami M, Kodama TS, Mori K, Nakayama T, Ihara Y, Takeda M.γ-secretase modulators and presenilin 1 mutants act differently on presenilin/γ-secretase function to cleave Aβ42 and Aβ43. Cell Rep. 2013 Jan 31;3(1):42-51.

O'Nuallain B, Freir DB, Nicoll AJ, Risse E, Ferguson N, Herron CE, Collinge J, Walsh DM. Amyloid beta-protein dimers rapidly form stable synaptotoxic protofibrils. J Neurosci. 2010 Oct 27;30(43):14411-9.

Qi-Takahara Y, Morishima-Kawashima M, Tanimura Y, Dolios G, Hirotani N, Horikoshi Y, Kametani F, Maeda M, Saido TC, Wang R, Ihara Y. Longer forms of amyloid beta protein: implications for the mechanism of intramembrane cleavage by gamma-secretase.J Neurosci. 2005 Jan 12;25(2):436-45.

Quintero-Monzon O, Martin MM, Fernandez MA, Cappello CA, Krzysiak AJ, Osenkowski P, Wolfe MS. Dissociation between the processivity and total activity of γ-secretase: implications for the mechanism of Alzheimer's disease-causing presenilin mutations. Biochemistry. 2011 Oct 25;50(42):9023-35.

Roberson ED, Scearce-Levie K, Palop JJ, Yan F, Cheng IH, Wu T, Gerstein H, Yu GQ, Mucke L. Reducing endogenous tau ameliorates amyloid beta-induced deficits in an Alzheimer's disease mouse model. Science. 2007 May 4;316(5825):750-4.

Roher AE, Kokjohn TA, Esh C, Weiss N, Childress J, Kalback W, Luehrs DC, Lopez J, Brune D, Kuo YM, Farlow M, Murrell J, Vidal R, Ghetti B. The human amyloid-beta precursor protein770 mutation V717F generates peptides longer than amyloid-beta-(40-42) and flocculent amyloid aggregates. J Biol Chem. 2004 Feb 13;279(7):5829-36.

Rapoport M, Dawson HN, Binder LI, Vitek MP, Ferreira A. Tau is essential to beta -amyloid-induced neurotoxicity. Proc Natl Acad Sci U S A. 2002 Apr 30;99(9):6364-9.

Saito T, Suemoto T, Brouwers N, Sleegers K, Funamoto S, Mihira N, Matsuba Y, Yamada K, Nilsson P, Takano J, Nishimura M, Iwata N, Van Broeckhoven C, Ihara Y, Saido TC.Potent amyloidogenicity and pathogenicity of Aβ43.Nat Neurosci. 2011 Jul 3;14(8):1023-32. doi: 10.1038/nn.2858.

Sastre M, Steiner H, Fuchs K, Capell A, Multhaup G, Condron MM, Teplow DB, Haass C.Presenilin-dependent gamma-secretase processing of beta-amyloid precursor protein at a site corresponding to the S3 cleavage of Notch.EMBO Rep. 2001 Sep;2(9):835-41. Epub 2001 Aug 23.

Sato T, Dohmae N, Qi Y, Kakuda N, Misonou H, Mitsumori R, Maruyama H, Koo EH, Haass C, Takio K, Morishima-Kawashima M, Ishiura S, Ihara Y.Potential link between amyloid beta-protein 42 and C-terminal fragment gamma 49-99 of beta-amyloid precursor protein.J Biol Chem. 2003 Jul 4;278(27):24294-301. Epub 2003 Apr 21.

Scheuner D, Eckman C, Jensen M, Song X, Citron M, Suzuki N, Bird TD, Hardy J, Hutton M, Kukull W, Larson E, Levy-Lahad E, Viitanen M, Peskind E, Poorkaj P, Schellenberg G, Tanzi R, Wasco W, Lannfelt L, Selkoe D, Younkin S. Secreted amyloid beta-protein similar to that in the senile plaques of Alzheimer's disease is increased in vivo by the presenilin 1 and 2 and APP mutations linked to familial Alzheimer's disease. Nat Med. 1996 Aug;2(8):864-70.

Selkoe DJ. Alzheimer's disease: genes, proteins, and therapy. Physiol Rev. 2001 Apr;81(2): 741-66.

Selkoe DJ. Resolving controversies on the path to Alzheimer's therapeutics. Nat Med. 2011 Sep 7;17(9):1060-5.

Shankar GM, Li S, Mehta TH, Garcia-Munoz A, Shepardson NE, Smith I, Brett FM, Farrell MA, Rowan MJ, Lemere CA, Regan CM, Walsh DM, Sabatini BL, Selkoe DJ. Amyloid-beta protein

dimers isolated directly from Alzheimer's brains impair synaptic plasticity and memory. Nat Med. 2008 Aug;14(8):837-42

Shimojo M, Sahara N, Mizoroki T, Funamoto S, Morishima-Kawashima M, Kudo T, Takeda M, Ihara Y, Ichinose H, Takashima A. Enzymatic characteristics of I213T mutant presenilin-1/ gamma-secretase in cell models and knock-in mouse brains: familial Alzheimer disease-linked mutation impairs gamma-site cleavage of amyloid precursor protein C-terminal fragment beta. J Biol Chem. 2008 Jun 13;283(24):16488-96.

Takami M, Nagashima Y, Sano Y, Ishihara S, Morishima-Kawashima M, Funamoto S, Ihara Y. gamma-Secretase: successive tripeptide and tetrapeptide release from the transmembrane domain of beta-carboxyl terminal fragment.J Neurosci. 2009 Oct 14;29(41):13042-52.

Tanzi RE, Bertram L. Twenty years of the Alzheimer's disease amyloid hypothesis: a genetic perspective.Cell. 2005 Feb 25;120(4):545-55.

Tseng BP, Kitazawa M, LaFerla FM. Amyloid beta-peptide: the inside story. Curr Alzheimer Res. 2004 Nov;1(4):231-9.

Vassar R, Bennett BD, Babu-Khan S, Kahn S, Mendiaz EA, Denis P, Teplow DB, Ross S, Amarante P, Loeloff R, Luo Y, Fisher S, Fuller J, Edenson S, Lile J, Jarosinski MA, Biere AL, Curran E, Burgess T, Louis JC, Collins F, Treanor J, Rogers G, Citron M. Beta-secretase cleavage of Alzheimer's amyloid precursor protein by the transmembrane aspartic protease BACE. Science. 1999 Oct 22;286(5440):735-41.

Walsh DM, Klyubin I, Fadeeva JV, Cullen WK, Anwyl R, Wolfe MS, Rowan MJ, Selkoe DJ. Naturally secreted oligomers of amyloid beta protein potently inhibit hippocampal long-term potentiation in vivo. Nature. 2002 Apr 4;416(6880):535-9.

Walsh DM, Selkoe DJ. A beta oligomers - a decade of discovery. J Neurochem. 2007 Jun; 101(5):1172-84

Weidemann A, Eggert S, Reinhard FB, Vogel M, Paliga K, Baier G, Masters CL, Beyreuther K, Evin G. A novel epsilon-cleavage within the transmembrane domain of the Alzheimer amyloid precursor protein demonstrates homology with Notch processing. Biochemistry. 2002 Feb 26;41(8):2825-35.

Wolfe MS, Xia W, Ostaszewski BL, Diehl TS, Kimberly WT, Selkoe DJ. Two transmembrane aspartates in presenilin-1 required for presenilin endoproteolysis and gamma-secretase activity. Nature. 1999 Apr 8;398(6727):513-7.

Yankner BA, Lu T. Amyloid beta-protein toxicity and the pathogenesis of Alzheimer disease. J Biol Chem. 2009 Feb 20;284(8):4755-9.

Zhang Y, McLaughlin R, Goodyer C, LeBlanc A. Selective cytotoxicity of intracellular amyloid beta peptide1-42 through p53 and Bax in cultured primary human neurons. J Cell Biol. 2002 Feb 4;156(3):519-29.

Zhao G, Mao G, Tan J, Dong Y, Cui MZ, Kim SH, Xu X. Identification of a new presenilin-dependent zeta-cleavage site within the transmembrane domain of amyloid precursor protein. J Biol Chem. 2004 Dec 3;279(49):50647-50. Epub 2004 Oct 13.

Chapter 5:

Conclusions and future directions

Alzheimer's disease (AD) is a devastating malady for which there is no cure or disease-modifying treatment. AD is both a personal tragedy and a looming epidemic, threatening to stress healthcare systems as the number of cases worldwide is predicted to rise. Our understanding of the pathogenesis of AD has advanced immensely since Alois Alzheimer first described a dementia associated with plaques and tangles, from the identification of the protein components of these structures, to the finding that mutations that cause AD alter amyloid β-peptide (Aβ) production, to the discovery of γ-secretase as an intramembrane-cleaving protease that generates Aβ. However, many questions still remain about the pathogenesis of this disorder. Moreover, recent advances showing that γ-secretase generates Aβ peptides by endoproteolysis of APP CTFβ followed by C-terminal trimming of the resulting long Aβ peptides have led to more questions about how these proteolytic functions are carried out by the WT enzyme, how they are affected by FAD mutations, and whether the long Aβs generated by cleavage at the ε and ζ sites could play a role in AD. This dissertation work has addressed these questions, and suggests areas for future exploration.

In the first part of this thesis, we examine the C-terminal trimming of ε- and ζ-cleaved Aβs by γ-secretase using isolated enzyme and substrate. We show that Aβ49, Aβ48, Aβ46, and Aβ45 are indeed trimmed by γ-secretase to Aβ40 and Aβ42 *in vitro*. Moreover, cleavage of Aβ49 and Aβ46 primarily leads to Aβ40, and cleavage of Aβ48 and Aβ45 primarily leads Aβ2, providing direct support for the two pathway model originally proposed by Ihara and colleagues (Takami et al., 2009). We also show that dual-pathway carboxypeptidase cleavage is an intrinsic property of γ-secretase and that the membrane is not needed for the enzyme to trim along these

two pathways, as the ratios of Aβ42/Aβ40 products were similar whether the reactions were carried out in proteoliposomes or in CHAPSO detergent.

We next examined the effects of FAD mutations in presenilin-1 (PS1) on the trimming process. PS1 FAD mutations may cause a decrease in γ-secretase cleavage of substrates, but they also increase the proportion of the more aggregation-prone Aβ42 compared to the major secreted Aβ40. These findings have led to a controversy over whether PS1 mutations cause FAD through a loss or a gain of function (De Strooper, 2007; Shen and Kelleher, 2007; Wolfe, 2007). We demonstrate that five FAD mutations with varying ages of onset and locations within PS all dramatically decrease the efficiency of trimming of Aβ48 and Aβ49 to Aβ40 and Aβ42. We also found that the trimming of Aβ49 to Aβ40 by all of the mutant complexes was significantly more reduced than the trimming of Aβ48 to Aβ42, revealing a novel mechanism by which these mutations lead to the production of an increased proportion of pathogenic Aβ42 compared to Aβ40. Thus, our results provide a potential resolution to the loss-of-function versus gain-of-function controversy. These mutations all cause a specific reduction of the trimming function of γ-secretase, particularly the ability to trim Aβ49 or Aβ46 to Aβ40, that results in a gain of Aβ42/Aβ40, a change that increases the propensity of Aβ to aggregate into neurotoxic forms. Moreover, for some of the mutants, the major Aβ49 to Aβ40 conversion was more reduced than the crossover Aβ49 to Aβ42 conversion, and for some the crossover conversion of Aβ48 to Aβ40 was more reduced than the major Aβ48 to Aβ42 conversion. In addition to our novel observations, previous reports show that some FAD mutations shift ε site cleavage to increase Aβ48 production and subsequently Aβ42 (Chávez-Gutiérrez et al., 2012; Sato et al., 2003), and some mutations reduce the conversion of Aβ42 to Aβ38 (Okochi et al., 2013). Taken together,

these results demonstrate that FAD PS1 mutations alter Aβ production by multiple mechanisms that conspire to increase Aβ42/Aβ40. In addition, we note that the loss of trimming function that we report would also result in the accumulation of Aβs longer than Aβ42.

There are a several future studies that should be undertaken to further investigate the effects of FAD mutations on the various proteolytic functions of γ-secretase. First, it will be important to determine if the effects we observed are a common feature of all PS1 FAD mutations. Therefore, the kinetics of C-terminal trimming of Aβ49 and Aβ48 by more FAD PS1 mutant complexes should be examined in the same way that we have described here.

In particular, future study should focus on the PS1 FAD mutations L435F and C410Y. These mutations have been reported to cause a dramatic reduction in Aβ40 and Aβ42 production (Heilig et al., 2010; Heilig et al., 2013). During the writing of this thesis, a study came out describing knock-in mice harboring these FAD mutations (Xia et al., 2015). L435 heterozygotes exhibit memory and long-term potentiation deficits and neurodegeneration. However, homozygous embryos with either mutation had no detectable Aβ40 or Aβ42. These findings have added more fuel to the loss-of-function/gain-of-function debate (Shugart, 2015). While Aβ40 and Aβ42 production seem to be diminished by these mutants, the production of AICD and Aβs longer than Aβ42 were not examined. It is possible that there is some, albeit reduced, ε site cleavage of CTFβ, with little subsequent trimming to Aβ40 and Aβ42 and thus a higher proportion of Aβ43 or longer products. Therefore, AICD and the entire Aβ spectrum generated by these FAD mutant γ-secretase complexes should be examined *in vitro*. The kinetics of Aβ48 and Aβ49 trimming by these mutants should also be examined.

In addition to FAD mutations in PS, FAD mutations within the APP transmembrane domain (TMD) that increase the Aβ42/Aβ40 ratio should be examined. Both the spectrum of Aβs generated from these mutant substrates and the effects of these mutations on the kinetics of Aβ49 and Aβ48 trimming should be analyzed. This analysis will reveal if a reduction in trimming is not only seen for FAD PS1 mutations, but also for FAD mutations within the γ-secretase substrate.

In the second part of this dissertation, we examined substrate determinants of the specificity and efficiency of ε site cleavage and C-terminal trimming of CTFβ by γ-secretase. According to the sequential cleavage model of CTFβ, as well as our results in Chapter 2, the critical ratio of Aβ42 to Aβ40 is primarily dictated by the upstream ε site that is used to generate either Aβ48 or Aβ49 and subsequent cleavage every three residues at the trimming sites. However, little is known about the determinants of the precise locations of γ-secretase endoproteolysis and trimming along the CTFβ TMD. We found that the C-terminal charge of long Aβ intermediates is not necessary for trimming every three amino acids. We next analyzed whether the site of the initial ε cut is primarily determined by a depth of three residues within the TMD, dictated by the hydrophobic S1', S2', and S3' pockets on the enzyme (Esler et al., 2004). We tested this hypothesis by deleting residues around the ε sites; if ε cleavage occurs three residues within the TMD, then the deletions should have shifted the position of the ε cleavage site. Instead, we found that these deletions did not alter the primary Aβ cleavage products generated by γ-secretase. We conclude that the sequence of amino acids along the CTFβ TMD, and not simply depth within the membrane, dictates the location of ε cleavage.

Future work in this area should identify the upstream sequence elements that dictate the ε cleavage site. This can be accomplished by mutagenesis of the CTFβ TMD and analysis of the AICD and Aβ products generated from these mutants; mutations that shift cleavage to novel product lines will indicate key residues.

We examined the role of helical instability in endoproteolysis and trimming of CTFβ by γ-secretase. A requirement for helix-destabilizing residues in substrates has been shown for other intramembrane-cleaving proteases, but has never been demonstrated for γ-secretase (Lemberg and Martoglio, 2002; Urban and Freeman, 2003; Ye et al., 2000). We generated mutant CTFβ substrates with helix-promoting and helix-destabilizing motifs inserted between the ε, ζ, and γ cleavage sites. We measured the effects of these mutations on endoproteolysis at the ε site by analyzing the levels of AICD generated from the mutant substrates in *in vitro* γ-secretase reactions, and the effects on trimming were monitored by analyzing the spectrum of Aβ products. We found that helix destabilization near the ε site significantly increases endoproteolysis by γ-secretase. In addition, insertion of a helix-promoting mutation between each cleavage site resulted in a reduction in trimming past the mutation site and the accumulation of longer Aβ species. These results suggest that flexibility of the transmembrane helix is necessary for efficient trimming by γ-secretase.

A similar analysis should be carried out for other substrates of γ-secretase, as well as for non-substrates, such as integrinβ1 (Hemming et al., 2008). Although there is no defining motif or consensus sequence within the primary sequences of γ-secretase substrates, perhaps conformational flexibility is a requirement for all γ-secretase substrates and provides a basis for γ-secretase substrate selectivity.

Last, we considered the potential role of Aβ45-49 in AD pathogenesis. Work on Aβ neurotoxicity has focused almost exclusively on secreted forms of Aβ, with the current focus being on soluble Aβ aggregates, such as dimers, trimers, or protofibrils (Walsh and Selkoe, 2007). Despite the many advances in our understanding of AD pathogenesis, the toxic forms of Aβ and pathways by which Aβ elicits intracellular changes in tau, whether by interaction with specific protein receptors or with the neuronal membrane, remain unclear (Ittner and Götz, 2011).

As summarized above, our results in Chapter 2 demonstrate that the efficiency of γ-secretase trimming of both Aβ49 and Aβ48 to Aβ40 and Aβ42 is dramatically decreased by FAD mutations in PS1; however, the trimming of Aβ49 to Aβ40 was more reduced than that of Aβ48 to Aβ42, thus resulting in an increase in the Aβ42/Aβ40 ratio (Fernandez, et al. 2014). In addition, we and others have demonstrated that FAD mutations in PS not only increase the Aβ42/Aβ40 ratio, but also increase the proportion of Aβ45-49 (Chávez-Gutiérrez et al., 2012; Shimojo et al., 2008; Quintero-Monzon et al., 2011). Thus, an increase in Aβ42/Aβ40 coincides with an increase in the relative proportion of the longer, membrane-anchored Aβ species. The most provocative interpretation of these results is that the increased proportion of the longer Aβ species is in fact the pathogenic initiator of AD, and that increases in Aβ42/Aβ40 and the formation of Aβ oligomers and plaques are epiphenomena. By analogy, it has been demonstrated that extracellular plaques of prion protein (PrP), formed by PrP lacking its glycosylphosphatidylinositol membrane anchor, are insufficient to cause disease in mice, and that membrane-anchored PrP is necessary for the development of clinical scrapie (Chesebro, et al., 2005). However, it is also possible that a role of Aβ45-49 and secreted Aβ42 are not

mutually exclusive. It has been proposed that soluble Aβ assemblies interact with and disrupt the neuronal membrane to exert toxicity (Jin et al., 2011; Marchesi, 2005; Selkoe, 2011); the long Aβs within the membrane may therefore be ideally located to elicit neurotoxic effects and intracellular changes in tau alongside membrane-associated Aβ42 oligomers. In addition, it is possible that an interaction between soluble Aβ oligomers and membrane-anchored Aβ is important for toxicity, although there is no experimental evidence for such an interaction. Last, it is possible that these longer species do not play a role in AD pathogenesis. Nevertheless, it is important that the question of the pathogenicity of these Aβs is examined, as the focus of the AD field on oligomers of secreted Aβ species would need to be expanded if these longer species are indeed pathogenic. Most notably, drug discovery efforts would need to shift from γ-secretase modulators that stimulate trimming to reduce Aβ42 levels to compounds that also decrease the levels of Aβ45-49.

If Aβ45-59 are pathogenic entities in AD, they should correlate with AD, exhibit neurotoxic and synaptotoxic effects, and trigger pathological changes in tau. Despite numerous attempts, we were unable to detect long Aβs in human sporadic AD (SAD) brain samples by immunoprecipitation and western blot. This could indicate that these Aβ species are in fact not present in SAD brains, that they are not extracted during our fractionation procedure or are otherwise degraded in the brain samples, that they are present at too low a level to detect via immunoprecipitation and western blot, or that modified shorter species are interfering with their detection by western blot. While the identification of these species by mass spectrometry has been previously reported from one APP FAD-mutant brain, these long Aβs are extremely hydrophobic and therefore mass spectrometric analysis is technically challenging. Specific

antibodies could be invaluable for analyzing their presence in AD brains, and development of these antibodies should be a priority for future analysis of brain samples. In addition, we have only analyzed brains from patients with a clinical diagnosis of AD. Brain samples from patients with mild cognitive impairment should also be analyzed for long Aβs, as it is possible that they are present at this earlier stage of pathogenesis.

We also analyzed hemibrains from 2-month-old 5X FAD mice (Oakley et al., 2006) for the presence of Aβ45-49 by immunoprecipitation and western blot, and we did detect putative Aβ45. While we will examine more mice of this age, one advantage of examining samples from mouse models is that they can be analyzed at specific stages of pathogenesis. The 5X FAD mice exhibit plaque pathology by two months of age (Oakley et al., 2006). One-month-old mice that have not yet developed plaques should also be analyzed to determine if long Aβs are present at this earlier stage. Older mice that exhibit synaptic and neuronal loss, which occurs at 4 and 9 months of age, respectively, should also be examined (Oakley et al., 2006).

Last, the Aβ species present in the recently described 3-dimensional culture system of differentiated human neural progenitor cells should be examined (Choi et al., 2014). These cells were transfected with FAD-mutant PS1 and APP and grown in a 3D matrix. These conditions led to the formation of Aβ plaques and neurofibrillary tangles (NFTs). Notably, these NFTs were formed from endogenous tau. While NFT formation depended on β- and γ-secretase, indicating that Aβ elicited these effects, the Aβ species or assembly responsible for these changes in tau were not identified, and the Aβ species present in these cultures were not characterized; therefore, the presence of Aβ45-49 in this system should be examined.

We also developed cell-based systems to analyze long Aβ toxicity. We first developed Neuro2a (N2a) cell lines that inducibly express APPs truncated at the ε and ζ sites; cleavage of these APPs by β-secretase will result in the generation of long Aβs, and treatment with a γ-secretase inhibitor (GSI) will prevent them from being trimmed by γ-secretase and will instead allow them to accumulate. Thus far, we have not observed any differences in the overall appearance of the cells or an increase in cell death when truncated APP expression is induced along with GSI treatment compared to GSI treatment alone. However, analysis of the toxicity of truncated APP expression in this system should continue by measuring LDH release from these cells, along with important controls, as outlined in Chapter 4. These include the use of a β-secretase inhibitor (to ensure that any effects are due to Aβ generation, and not truncated APP expression) and treatment with vehicle as opposed to GSI (which should attenuate any toxic effects if they are indeed the result of long Aβ accumulation).

We attempted to generate stable SH-SY5Y cell lines expressing these same truncated APPs, but these attempts were unsuccessful. However, a system using human cells was still desirable, as murine cells lack the tau isoforms of humans and do not develop tau pathology (Chin, 2011; Selkoe 2011; Yankner and Lu, 2009). Instead, we differentiated these cells into a post-mitotic neuronal state and treated them with long Aβ peptides; we reasoned that these Aβs will insert into the membrane via their hydrophobic C-termini. While we did not see any gross qualitative changes in the amount or appearance of cells and neurites with Aβ peptide treatment, LDH was elevated in the media of these cells, suggesting that Aβ46 treatment may be toxic. An important control used here was treatment with vehicle as opposed to GSI: the increase in LDH release from the Aβ46-treated cells was dependent on GSI treatment, suggesting that it could be

due to the accumulation of Aβ46 in the membrane, which may otherwise be trimmed by γ-secretase when no GSI is present. These results need to be repeated; we will also determine if the long Aβs are indeed inserted in the membrane and if they can be trimmed by γ-secretase to Aβ40 and Aβ42 (which would demonstrate that the peptides are inserted into the membrane in an orientation that allows for γ-secretase cleavage). In addition to the LDH assay, the lysates of these Aβ-treated cells should be examined for changes in tau phosphorylation and in the levels of synaptic markers. Thioflavin S staining and sarkosyl extraction should also be performed to detect aggregated tau. In addition, it will be important to corroborate the results obtained by using truncated APP expression. Because our previous attempts at generating stable SH-SY5Y cell lines by transfection failed, we will introduce these genes by lentiviral transduction. In addition to using the systems we have established in this thesis, both the expression of truncated APPs and the treatment of cells with Aβ peptides should be performed with rat primary neurons. Unlike mice, rats have the six isoforms of tau present in humans (Hanes et al., 2009); treatment of rat primary neurons with Aβ oligomers has been shown to lead to tau phosphorylation (Jin et al., 2011), and NFTs have been detected in the brains of rats with FAD-mutant APP and PS1 transgenes (Cohen et al., 2013). We will also use neuronal cells derived from human IPS cells (Muratore et al., 2013) and the 3-dimensional culture system described above. The use of all of these systems in parallel will strengthen any conclusions concerning the neurotoxicity of Aβ45-49, and the results obtained will inform the necessity of further work, including *in vivo* modeling.

References

Chávez-Gutiérrez L, Bammens L, Benilova I, Vandersteen A, Benurwar M, Borgers M, Lismont S, Zhou L, Van Cleynenbreugel S, Esselmann H, Wiltfang J, Serneels L, Karran E, Gijsen H, Schymkowitz J, Rousseau F, Broersen K, De Strooper B. The mechanism of γ-Secretase dysfunction in familial Alzheimer disease. EMBO J. 2012 May 16;31(10):2261-74.

Chesebro B, Trifilo M, Race R, Meade-White K, Teng C, LaCasse R, Raymond L, Favara C, Baron G, Priola S, Caughey B, Masliah E, Oldstone M. Anchorless prion protein results in infectious amyloid disease without clinical scrapie. Science. 2005 Jun 3;308(5727):1435-9.

Chin J. Selecting a mouse model of Alzheimer's disease. Methods Mol Biol. 2011;670:169-89.

Choi SH, Kim YH, Hebisch M, Sliwinski C, Lee S, D'Avanzo C, Chen H, Hooli B, Asselin C, Muffat J, Klee JB, Zhang C, Wainger BJ, Peitz M, Kovacs DM, Woolf CJ, Wagner SL, Tanzi RE, Kim DY. A three-dimensional human neural cell culture model of Alzheimer's disease. Nature. 2014 Nov 13;515(7526):274-8.

Cohen RM, Rezai-Zadeh K, Weitz TM, Rentsendorj A, Gate D, Spivak I, Bholat Y, Vasilevko V, Glabe CG, Breunig JJ, Rakic P, Davtyan H, Agadjanyan MG, Kepe V, Barrio JR, Bannykh S, Szekely CA, Pechnick RN, Town T. A transgenic Alzheimer rat with plaques, tau pathology, behavioral impairment, oligomeric aβ, and frank neuronal loss. J Neurosci. 2013 Apr 10;33(15): 6245-56.

De Strooper, B. Loss-of-function presenilin mutations in Alzheimer disease. Talking Point on the role of presenilin mutations in Alzheimer disease. 2007; EMBO Rep 8, 141-146.

Esler WP, Das C, Wolfe MS. Probing pockets S2-S4' of the gamma-secretase active site with (hydroxyethyl)urea peptidomimetics.Bioorg Med Chem Lett. 2004 Apr 19;14(8):1935-8.

Fernandez MA, Klutkowski JA, Freret T, Wolfe MS.Alzheimer presenilin-1 mutations dramatically reduce trimming of long amyloid β-peptides (Aβ) by γ-secretase to increase 42-to-40-residue Aβ. J Biol Chem. 2014 Nov 7;289(45):31043-52.

Hanes J, Zilka N, Bartkova M, Caletkova M, Dobrota D, Novak M. Rat tau proteome consists of six tau isoforms: implication for animal models of human tauopathies. J Neurochem. 2009 Mar; 108(5):1167-76.

Heilig EA, Xia W, Shen J, Kelleher RJ 3rd. A presenilin-1 mutation identified in familial Alzheimer disease with cotton wool plaques causes a nearly complete loss of gamma-secretase activity. J Biol Chem. 2010 Jul 16;285(29):22350-9.

Heilig EA, Gutti U, Tai T, Shen J, Kelleher RJ 3rd. Trans-dominant negative effects of pathogenic PSEN1 mutations on γ-secretase activity and Aβ production. J Neurosci. 2013 Jul 10;33(28):11606-17

Hemming ML, Elias JE, Gygi SP, Selkoe DJ. Proteomic profiling of gamma-secretase substrates and mapping of substrate requirements. PLoS Biol. 2008 Oct 21;6(10):e257

Ittner LM, Götz J. Amyloid-β and tau--a toxic pas de deux in Alzheimer's disease. Nat Rev Neurosci. 2011 Feb;12(2):65-72

Jin M, Shepardson N, Yang T, Chen G, Walsh D, Selkoe DJ. Soluble amyloid beta-protein dimers isolated from Alzheimer cortex directly induce Tau hyperphosphorylation and neuritic degeneration. Proc Natl Acad Sci U S A. 2011 Apr 5;108(14):5819-24.

Lemberg MK, Martoglio B. Requirements for signal peptide peptidase-catalyzed intramembrane proteolysis.Mol Cell. 2002 Oct;10(4):735-44.

Marchesi VT. An alternative interpretation of the amyloid Abeta hypothesis with regard to the pathogenesis of Alzheimer's disease. Proc Natl Acad Sci U S A. 2005 Jun 28;102(26):9093-8.

Muratore CR, Rice HC, Srikanth P, Callahan DG, Shin T, Benjamin LN, Walsh DM, Selkoe DJ, Young-Pearse TL. The familial Alzheimer's disease APPV717I mutation alters APP processing and Tau expression in iPSC-derived neurons. Hum Mol Genet. 2014 Jul 1;23(13):3523-36.

Oakley H, Cole SL, Logan S, Maus E, Shao P, Craft J, Guillozet-Bongaarts A, Ohno M, Disterhoft J, Van Eldik L, Berry R, Vassar R. Intraneuronal beta-amyloid aggregates, neurodegeneration, and neuron loss in transgenic mice with five familial Alzheimer's disease mutations: potential factors in amyloid plaque formation. J Neurosci. 2006 Oct 4;26(40): 10129-40

Okochi M, Tagami S, Yanagida K, Takami M, Kodama TS, Mori K, Nakayama T, Ihara Y, Takeda M.γ-secretase modulators and presenilin 1 mutants act differently on presenilin/γ-secretase function to cleave Aβ42 and Aβ43. Cell Rep. 2013 Jan 31;3(1):42-51.

Quintero-Monzon O, Martin MM, Fernandez MA, Cappello CA, Krzysiak AJ, Osenkowski P, Wolfe MS. Dissociation between the processivity and total activity of γ-secretase: implications for the mechanism of Alzheimer's disease-causing presenilin mutations. Biochemistry. 2011 Oct 25;50(42):9023-35.

Sato T, Dohmae N, Qi Y, Kakuda N, Misonou H, Mitsumori R, Maruyama H, Koo EH, Haass C, Takio K, Morishima-Kawashima M, Ishiura S, Ihara Y.Potential link between amyloid beta-protein 42 and C-terminal fragment gamma 49-99 of beta-amyloid precursor protein.J Biol Chem. 2003 Jul 4;278(27):24294-301. Epub 2003 Apr 21.
Selkoe DJ. Resolving controversies on the path to Alzheimer's therapeutics. Nat Med. 2011 Sep 7;17(9):1060-5.

Selkoe DJ. Resolving controversies on the path to Alzheimer's therapeutics. Nat Med. 2011 Sep 7;17(9):1060-5.

Shen, J., and Kelleher, R. J., 3rd. (2007) The presenilin hypothesis of Alzheimer's disease: evidence for a loss-of-function pathogenic mechanism. Proc Natl Acad Sci U S A 104, 403-409

Shimojo M, Sahara N, Mizoroki T, Funamoto S, Morishima-Kawashima M, Kudo T, Takeda M, Ihara Y, Ichinose H, Takashima A. Enzymatic characteristics of I213T mutant presenilin-1/ gamma-secretase in cell models and knock-in mouse brains: familial Alzheimer disease-linked mutation impairs gamma-site cleavage of amyloid precursor protein C-terminal fragment beta. J Biol Chem. 2008 Jun 13;283(24):16488-96.

Shugart J. Mutant Presenilin Knock-in Mice Mimic Knockouts, Stir Old Debate. www.alzforum.org. 2015 Mar 10.

Takami M, Nagashima Y, Sano Y, Ishihara S, Morishima-Kawashima M, Funamoto S, Ihara Y. gamma-Secretase: successive tripeptide and tetrapeptide release from the transmembrane domain of beta-carboxyl terminal fragment. J Neurosci. 2009 Oct 14;29(41):13042-52.

Urban S, Freeman M.Substrate specificity of rhomboid intramembrane proteases is governed by helix-breaking residues in the substrate transmembrane domain.Mol Cell. 2003 Jun;11(6): 1425-34.

Walsh DM, Selkoe DJ. A beta oligomers - a decade of discovery. J Neurochem. 2007 Jun; 101(5):1172-84

Wolfe, M. S. When loss is gain: reduced presenilin proteolytic function leads to increased Abeta42/Abeta40. Talking Point on the role of presenilin mutations in Alzheimer disease. EMBO Rep 2007;8, 136-140

Xia D, Watanabe H, Wu B, Lee SH, Li Y, Tsvetkov E, Bolshakov VY, Shen J, Kelleher RJ 3rd. Presenilin-1 Knockin Mice Reveal Loss-of-Function Mechanism for Familial Alzheimer's Disease. Neuron. 2015 Mar 4;85(5):967-81.

Yankner BA, Lu T. Amyloid beta-protein toxicity and the pathogenesis of Alzheimer disease. J Biol Chem. 2009 Feb 20;284(8):4755-9.

Ye J, Davé UP, Grishin NV, Goldstein JL, Brown MS.Asparagine-proline sequence within membrane-spanning segment of SREBP triggers intramembrane cleavage by site-2 protease.Proc Natl Acad Sci U S A. 2000 May 9;97(10):5123-8.

Appendix:

Supplementary figures

Figure S1. Mass spectrometric analysis of the Aβs generated from CTFβ deletion mutants. Reactions were run as described in Figure 3.3. Aβ was immunoprecipitated from the reaction mixture using 4G8. The peaks are labeled with the molecular masses and the identity of the Aβ peptide. Each Aβ has an additional N-terminal methionine derived from the C100-FLAG substrate.

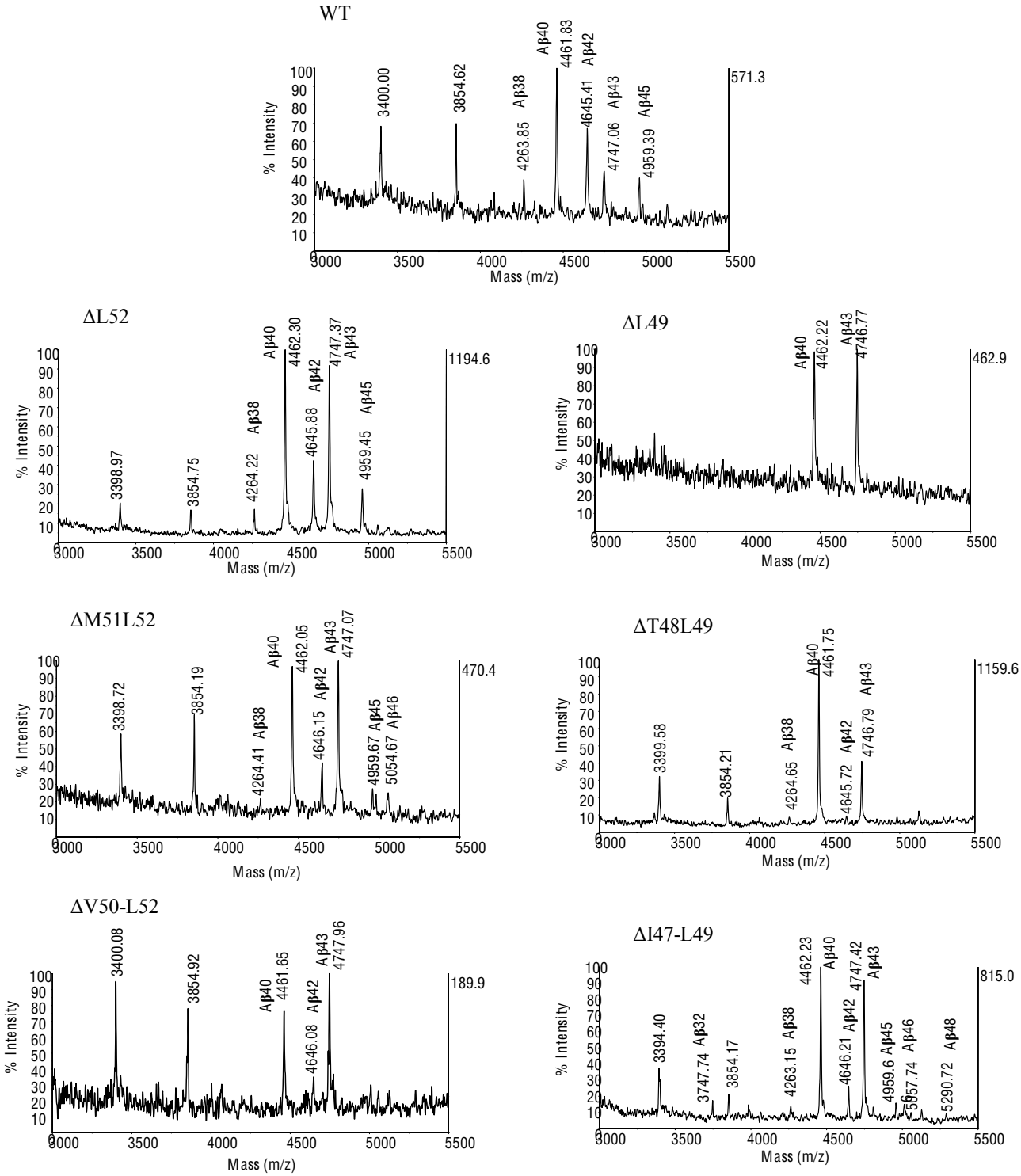

Figure S1 continued. Mass spectrometric analysis of the Aβs generated from CTFβ deletion mutants.

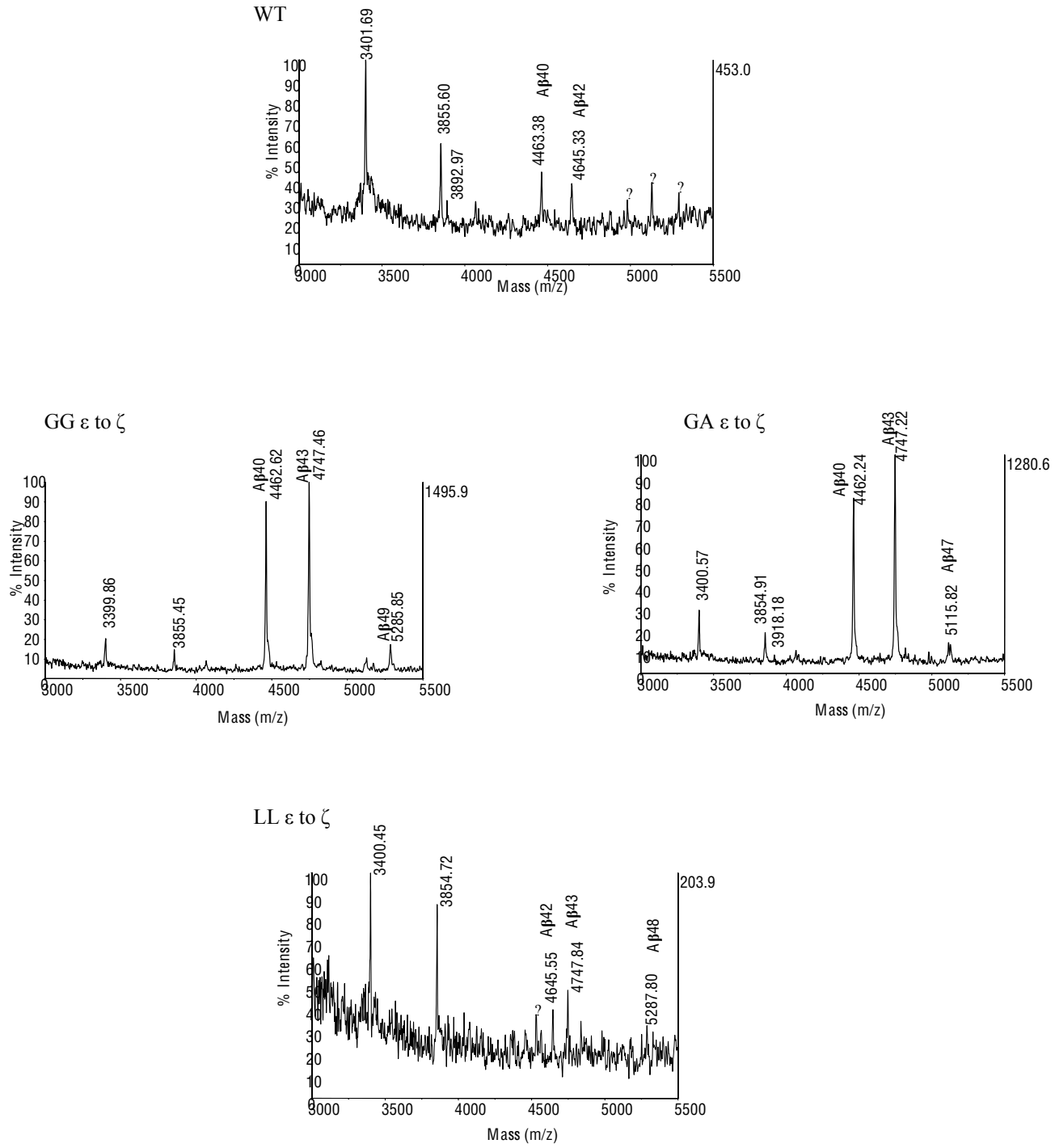

Figure S2. Mass spectrometric analysis of the Aβs generated from ε to ζ site helical stability mutant CTFβs. Reactions were run as described in Figure 3.5. Aβ was analyzed as in S1.

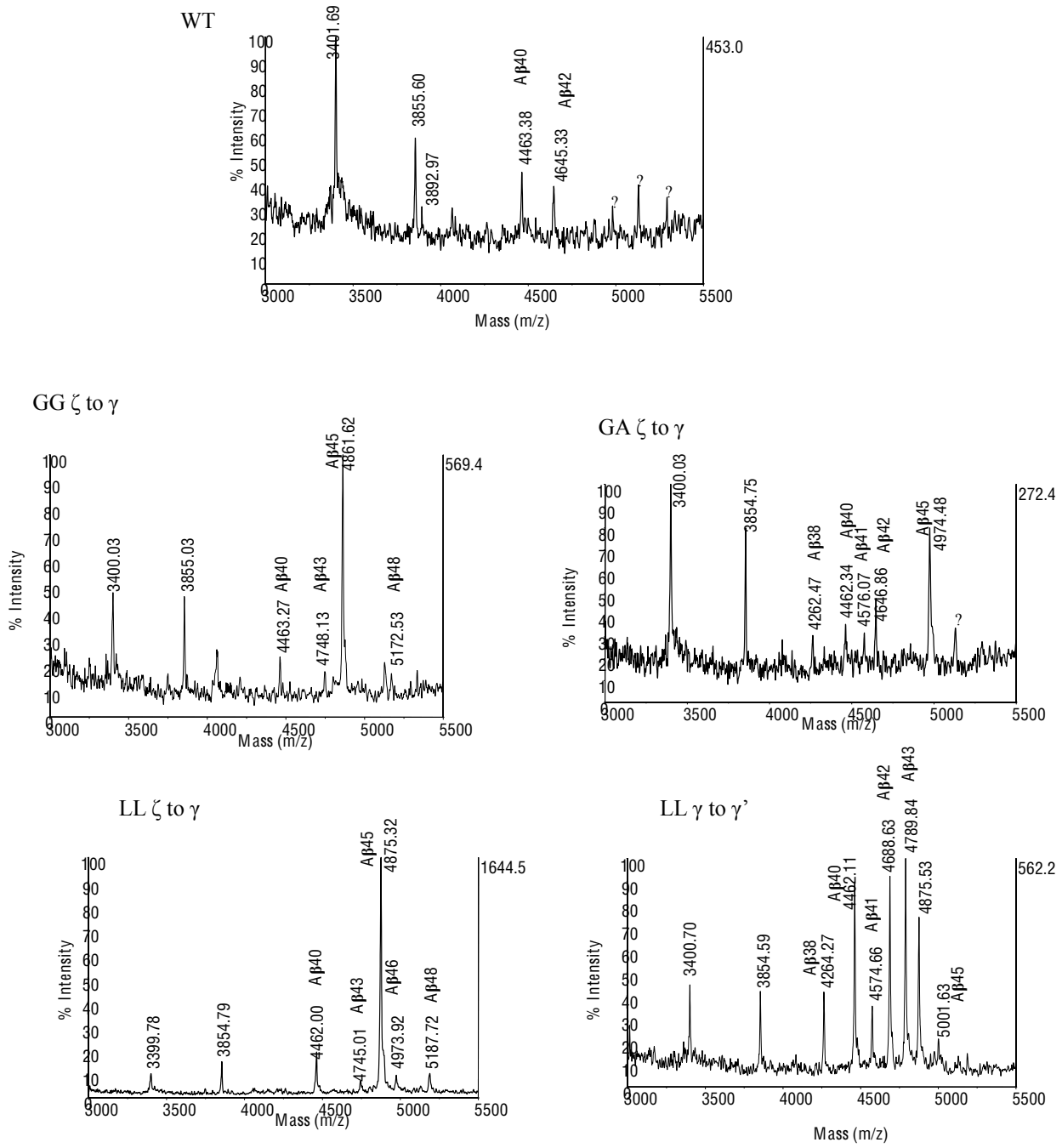

Figure S3. Mass spectrometric analysis of the Aβs generated from ζ to γ site and γ to γ' site helical stability mutant CTFβs. Reactions were carried out as described in Figure 3.7. Aβ was analyzed as in S1.